

**SYNTHESIS AND ELECTROCHEMISTRY OF  
TETRAPYRROLE DERIVATIVES SUBSTITUTED WITH  
FERROCENYL MOIETIES**

**By**

**Ka-Wo POON**

**(潘家和)**

**A thesis submitted in partial fulfillment of**

**the requirements for the degree of**

**Master of Philosophy**

**in**

**Chemistry**

**The Chinese University of Hong Kong**

**1999**

**Thesis Committee :**

**Prof. Kevin W. P. Leung, Chairman**

**Prof. Clifford C. Leznoff, External Examiner**

**Prof. Dennis K. P. Ng**

**Prof. Z. Xie**



## ABSTRACT

A series of phthalocyanines containing four, eight, and sixteen 2-ferrocenylethoxy moieties on the periphery have been prepared and spectroscopically characterized. The UV-Vis spectrum of the tetraferrocenyl phthalocyanine **55** shows an unusual long-wavelength band at ca. 760 nm in non-polar solvents. By studying the spectral changes of this compound and its analog 1,8,15,22-tetrakis(3-pentyloxy)phthalocyaninatozinc(II) (**70**) in different solvents and concentrations, and their fluorescence spectra, it can be concluded that this band is not likely due to a slipped cofacial dimer as reported previously. Compound **55** is not emissive which can be explained by the efficient quenching due to electron transfer from ferrocene to the excited phthalocyanine. The value of  $\Delta G^\circ$  for this photoinduced electron transfer has been estimated to be  $-0.48$  eV. Electrochemical studies of these phthalocyanine-ferrocene conjugates by cyclic voltammetry have revealed that all the ferrocenyl redox centers attached to the macrocyclic core are electrochemically independent and undergo an oxidation at the same potential.

Another series of ferrocenyl tetrapyrrole derivatives based on nickel(II) 5,15-diphenylporphyrin (**90**), zinc(II) phthalocyanine (**83**) and 2,3-naphthalocyanine (**87**) have also been prepared in which up to eight ferrocenyl groups are connected on the periphery via ethynyl linkers. Compound **87** represents the first example of ferrocene-containing 2,3-naphthalocyanine. Due to the more extended conjugated  $\pi$  system, all the  $\pi-\pi^*$  transitions are significantly shifted to the red compared with the parent tetrapyrroles. The electrochemical response of these compounds depends largely on the electrode used. By using a platinum microsphere working electrode, the oxidation couple due to the ferrocenyl units in these compounds is slightly split showing that these redox-active units are weakly coupled.



## 摘要

我們合成了一系列含有四，八和十六個 2-二茂鐵乙氧基取代的新型酞菁化合物，並用各種光譜手段對其進行了鑒定。四二茂鐵取代的酞菁 **55** 在非極性的溶劑中的紫外可見吸收光譜在 760nm 除出現一個反常的吸收峰。通過對其及其類似物 1, 8, 15, 22-四(3-戊氧基) 酞菁鋅(II) (**70**) 在不同溶劑中不同濃度時的吸收光譜和熒光光譜的研究，我們斷定該吸收峰不是象以前報道的那樣屬於酞菁錯開的面對面二聚體。化合物 **55** 分子內存在高效率的由二茂鐵到酞菁的電子轉移反應，因此酞菁的熒光被猝滅，整個分子沒有熒光發射。我們估算了這種分子內電子轉移反應的自由能變化 ( $\Delta G^0$ ) 為 -0.48eV。我們還運用循環伏安法研究了這類酞菁-二茂鐵體系的氧化還原性質，結果顯示這類化合物中所有的二茂鐵均為獨立的氧化還原中心，都在相同的電位下被氧化。

此外，我們通過共軛三鍵將二茂鐵和 5, 15-二苯基卟啉鎳(II) **90**，酞菁鋅(II) **83** 和 2, 3-萘酞菁 **87** 連接在一起，合成了一系列具有更大共軛體系的化合物。在這些化合物中，最多連有八個二茂鐵。其中化合物 **87** 是第一個二茂鐵萘酞菁化合物。由于在此類化合物中，共軛體系得到擴展，所有的  $\pi - \pi^*$  躍遷和相應的卟啉或酞菁相比均有明顯的紅移。這些化合物的電化學相應受電機的影響很大，當用鉑微相電極為工作電極時，化合物 **83**, **87** 和 **90** 中的二茂鐵的氧化峰有少許的分裂。說明在此體系中，二茂鐵之間有弱的相互作用。



## ACKNOWLEDGMENT

I am especially grateful to my supervisor, Prof. Dennis K. P. Ng, for his invaluable advice and guidance during the course of my research and the preparation of this thesis.

Particular thanks are due to Dr. Y. Yan and Prof. K. Y Wong for their technical support in electrochemical measurements, and Dr. X.-Y. Li for his assistance in recording the fluorescent spectra.

Thanks are also due to Anthony C. H. Ng, M. W. Woo, and K. L. Cheng for their encouragement and helpful discussions.

I would also like to thank Prof. Dominic T. W. Chan, Leo Y. C. Lee and P. K. Chan for recording the MALDI-TOF mass spectra, and K. W. Kwong and W. P. Chung for the FAB, EI and LSI mass spectral service.

Finally, this research work was made possible by the generous financial support from the Hong Kong Research Grants Council and The Chinese University of Hong Kong.

Ka-Wo Poon

Department of Chemistry

The Chinese University of Hong Kong

June 1999

## CONTENTS

	PAGE
<b>ABSTRACT</b>	i
<b>ACKNOWLEDGMENT</b>	iii
<b>CONTENTS</b>	iv
<b>LIST OF FIGURES</b>	vi
<b>LIST OF TABLES</b>	x
<b>ABBREVIATIONS</b>	xi
<b>1. INTRODUCTION</b>	1
1.1 General Background of Tetrapyrrole Derivatives	1
1.2 Electronic Interactions in Systems with Multiple Redox Sites	8
1.2.1 Electronic Interactions in One-dimensional Systems	9
1.2.2 Electronic Interactions in Three-dimensional Systems	12
1.3 Ferrocene-containing Tetrapyrrole Derivatives	22
1.3.1 Ferrocene-containing Porphyrins	22
1.3.2 Ferrocene-containing Porphyrazines	29
1.3.3 Ferrocene-containing Phthalocyanines	30
<b>2. RESULTS AND DISCUSSION</b>	38
2.1 Ferrocenylphthalocyanines with Oxyethylene Linkers	38
2.1.1 Synthesis and Characterization	38
2.1.1.1 Preparation of Tetrakis(2-ferrocenylethoxy)- phthalocyaninatozinc(II) ( <b>55</b> )	38
2.1.1.2 Preparation of Octakis(2-ferrocenylethoxy)- phthalocyaninatozinc(II) ( <b>62</b> )	43
2.1.1.3 Preparation of Metal Free Hexadecakis(2- ferrocenylethoxy)phthalocyanine ( <b>65</b> )	49

2.1.2	Electronic Absorption Spectra	52
2.1.3	Electrochemical Studies	60
2.2	Ferrocenyl Tetrapyrroles with Ethynyl Linkers	68
2.2.1	Synthesis and Characterization	68
2.2.1.1	Preparation of Octakis(ferrocenylethynyl)- phthalocyaninatozinc(II) ( <b>83</b> )	71
2.2.1.2	Preparation of Octakis(ferrocenylethynyl)- Naphthalocyaninatozinc(II) ( <b>87</b> )	76
2.2.1.3	Preparation of 5,15-bis(ferrocenylethynyl)- 10,20-diphenylporphyrinatonicel(II) ( <b>90</b> )	81
2.2.2	Electrochemical Studies	84
2.3	Conclusion	92
<b>3.</b>	<b>EXPERIMENTAL SECTION</b>	93
3.1	General Methods	93
3.2	Physical Measurements	93
3.3	Synthesis of Ferrocenylphthalocyanines with Oxyethylene Linkers	95
3.4	Synthesis of Ferrocenyl Tetrapyrrole Derivatives with Ethynyl Linkers	105
<b>4.</b>	<b>REFERENCES</b>	113
APPENDIX A	$^1\text{H}$ NMR spectra of dinitriles	121
APPENDIX B	$^{13}\text{C}\{^1\text{H}\}$ NMR spectra of dinitriles	126



## LIST OF FIGURES

	PAGE
<b>Figure 1.</b> Energy level diagrams of macrocycles 2-5.	3
<b>Figure 2.</b> General UV-Vis spectra of (a) metallophthalocyanines and (b) metalloporphyrins.	4
<b>Figure 3.</b> Cyclic voltammogram of zinc(II) phthalocyanine (6) (0.4 mM) in DMA containing 0.1 M [NBu <sub>4</sub> ][ClO <sub>4</sub> ] at a scan rate of 50 mV S <sup>-1</sup> .	6
<b>Figure 4.</b> Cyclic voltammograms of nickel(II) tetraphenylporphyrin (7) (0.5 mM) in CH <sub>2</sub> Cl <sub>2</sub> containing 0.1 M [NBu <sub>4</sub> ][ClO <sub>4</sub> ] (—) or [NBu <sub>4</sub> ][PF <sub>6</sub> ] (---) at a scan rate of 100 mV S <sup>-1</sup> .	7
<b>Figure 5.</b> Model for the electronic interactions between two redox sites.	8
<b>Figure 6.</b> Cyclic voltammogram of 8 in CH <sub>2</sub> Cl <sub>2</sub> containing 0.1 M [NBu <sub>4</sub> ][PF <sub>6</sub> ] at a scan rate of 100 mV s <sup>-1</sup> .	10
<b>Figure 7.</b> Cyclic voltammograms of compound 13 in (a) CH <sub>2</sub> Cl <sub>2</sub> or (b) CH <sub>2</sub> Cl <sub>2</sub> /MeCN (v/v 5 : 1) containing 0.1 M [NBu <sub>4</sub> ][PF <sub>6</sub> ] at a scan rate of 100 mV s <sup>-1</sup> .	15
<b>Figure 8.</b> Cyclic voltammograms of (a) 15, (b) 16, and (c) 17 (1.0 mM) in CH <sub>2</sub> Cl <sub>2</sub> containing 0.1 M [NBu <sub>4</sub> ][PF <sub>6</sub> ] at a scan rate of 100 mV s <sup>-1</sup> .	17
<b>Figure 9.</b> Cyclic voltammogram of 24 in DMF containing 0.1 M [NBu <sub>4</sub> ][BF <sub>4</sub> ] at a scan rate of 400 mV s <sup>-1</sup> .	20
<b>Figure 10.</b> Cyclic voltammogram of 25 (1.0 mM) in DMF containing 0.1 M [NBu <sub>4</sub> ][BF <sub>4</sub> ] at a scan rate of 400 mV s <sup>-1</sup> .	21

<b>Figure 11.</b>	Cyclic voltammogram of <b>28</b> in CH <sub>2</sub> Cl <sub>2</sub> solution.	24
<b>Figure 12.</b>	Spectro-electrochemical UV-Vis spectra of (a) <b>27</b> and (b) <b>28</b> .	25
<b>Figure 13.</b>	(a) Cyclic voltammogram ( $\nu = 100 \text{ mV s}^{-1}$ ) and (b) differential pulse voltammogram ( $\nu = 400 \text{ mV s}^{-1}$ ) of <b>29</b> (1.4 mM) in CH <sub>2</sub> Cl <sub>2</sub> solution containing 0.1 M [NBu <sub>4</sub> ][ClO <sub>4</sub> ].	26
<b>Figure 14.</b>	Cyclic voltammogram of <b>31</b> (0.5 mM) in CH <sub>2</sub> Cl <sub>2</sub> /MeCN (v/v 3 : 2) containing 0.2 M [NBu <sub>4</sub> ][BF <sub>4</sub> ].	29
<b>Figure 15.</b>	(a) Cyclic voltammogram ( $\nu = 200 \text{ mV s}^{-1}$ ) and (b) differential pulse voltammogram ( $\nu = 5 \text{ mV s}^{-1}$ ) of <b>42</b> (0.05 mM) in CH <sub>2</sub> Cl <sub>2</sub> containing 0.1 M [NBu <sub>4</sub> ][PF <sub>6</sub> ].	33
<b>Figure 16.</b>	<sup>1</sup> H NMR spectrum of <b>55</b> in CDCl <sub>3</sub> .	42
<b>Figure 17.</b>	<sup>1</sup> H NMR spectrum of <b>62</b> in C <sub>6</sub> D <sub>6</sub> .	47
<b>Figure 18.</b>	(a) Experimental and (b) simulated pattern for the molecular ion of <b>62</b> .	48
<b>Figure 19.</b>	<sup>1</sup> H NMR spectrum of <b>65</b> in CDCl <sub>3</sub> .	51
<b>Figure 20.</b>	UV-Vis spectra of <b>55</b> (a) in diethyl ether, THF and DMF (b) in toluene, CH <sub>2</sub> Cl <sub>2</sub> and CHCl <sub>3</sub> .	54
<b>Figure 21.</b>	UV-Vis spectra of <b>55</b> in toluene with different concentration.	56
<b>Figure 22.</b>	UV-Vis spectra of <b>55</b> in CH <sub>2</sub> Cl <sub>2</sub> with different concentration.	56
<b>Figure 23.</b>	UV-Vis spectra of <b>70</b> in CH <sub>2</sub> Cl <sub>2</sub> with different concentration.	57
<b>Figure 24.</b>	Fluorescence spectrum of <b>70</b> in CH <sub>2</sub> Cl <sub>2</sub> upon excitation at 630 nm.	58
<b>Figure 25.</b>	UV-Vis spectrum of <b>62</b> in THF.	59
<b>Figure 26.</b>	UV-Vis spectrum of <b>65</b> in THF.	60

<b>Figure 27.</b>	Cyclic voltammogram of <b>55</b> in DMF containing 0.1 M [NBu <sub>4</sub> ][ClO <sub>4</sub> ] at a scan rate of 100 mV s <sup>-1</sup> .	64
<b>Figure 28.</b>	Cyclic voltammogram of <b>62</b> in DMF containing 0.1 M [NBu <sub>4</sub> ][ClO <sub>4</sub> ] at a scan rate of 20 mV s <sup>-1</sup> .	65
<b>Figure 29.</b>	Cyclic voltammogram of <b>65</b> in CH <sub>2</sub> Cl <sub>2</sub> containing 0.1 M [NBu <sub>4</sub> ][ClO <sub>4</sub> ] at a scan rate of 100 mV s <sup>-1</sup> .	65
<b>Figure 30.</b>	Absorption spectra of a mixture of ferrocene and <b>70</b> (4:1) (···) and <b>55</b> (—) in CHCl <sub>3</sub> .	67
<b>Figure 31.</b>	UV-Vis spectrum of <b>83</b> in THF.	73
<b>Figure 32.</b>	UV-Vis spectrum of <b>87</b> in THF.	78
<b>Figure 33.</b>	UV-Vis spectrum of <b>88</b> in THF.	78
<b>Figure 34.</b>	<sup>1</sup> H NMR spectrum of <b>90</b> in CDCl <sub>3</sub> .	82
<b>Figure 35.</b>	UV-Vis spectrum of <b>90</b> in THF.	83
<b>Figure 36.</b>	Cyclic voltammogram of <b>83</b> in THF containing 0.1 M [NBu <sub>4</sub> ][ClO <sub>4</sub> ] at a scan rate of 20 mV s <sup>-1</sup> (using a platinum disc working electrode).	88
<b>Figure 37.</b>	Cyclic voltammogram of <b>87</b> in THF containing 0.1 M [NBu <sub>4</sub> ][ClO <sub>4</sub> ] at a scan rate of 20 mV s <sup>-1</sup> (using a platinum disc working electrode).	88
<b>Figure 38.</b>	Cyclic voltammogram of <b>90</b> in CH <sub>2</sub> Cl <sub>2</sub> containing 0.1 M [NBu <sub>4</sub> ][ClO <sub>4</sub> ] at a scan rate of 100 mV s <sup>-1</sup> (using a platinum disc working electrode).	89



- Figure 39.** Cyclic voltammogram of **83** in THF containing 0.1 M  $[\text{NBu}_4][\text{ClO}_4]$  at a scan rate of  $20 \text{ mV s}^{-1}$  (using a platinum microsphere as working electrode). 89
- Figure 40.** Cyclic voltammogram of **87** in THF containing 0.1 M  $[\text{NBu}_4][\text{ClO}_4]$  at a scan rate of  $20 \text{ mV s}^{-1}$  (using a platinum microsphere as working electrode). 90
- Figure 41.** Cyclic voltammogram of **90** in  $\text{CH}_2\text{Cl}_2$  containing 0.1 M  $[\text{NBu}_4][\text{ClO}_4]$  at a scan rate of  $10 \text{ mV s}^{-1}$  (using a platinum microsphere working electrode). 90

## LIST OF TABLES

	PAGE
<b>Table 1.</b> Electrochemical data (vs. Fc/Fc <sup>+</sup> ) of <b>9</b> (n = 1-5) ( $7 - 9 \times 10^{-5}$ M) in CH <sub>2</sub> Cl <sub>2</sub> containing 0.1 M [NBu <sub>4</sub> ][PF <sub>6</sub> ] at a scan rate of 100 mV s <sup>-1</sup> .	11
<b>Table 2.</b> Electrochemical data (vs. SCE) of <b>10</b> (n = 1-6) containing 0.1 M [NBu <sub>4</sub> ][BF <sub>4</sub> ] at a scan rate of 100 mV s <sup>-1</sup> .	12
<b>Table 3.</b> Electrochemical data (vs. Fc/Fc <sup>+</sup> ) of <b>27</b> and <b>28</b> in CH <sub>2</sub> Cl <sub>2</sub> solution.	24
<b>Table 4.</b> Electrochemical data (vs. Ag/Ag <sup>+</sup> ) of <b>30 – 33</b> (0.5 mM) in CH <sub>2</sub> Cl <sub>2</sub> /MeCN (v/v 3 : 2) containing 0.2 M [NBu <sub>4</sub> ][BF <sub>4</sub> ].	28
<b>Table 5.</b> UV-Vis spectral data of <b>55</b> in different solvents (in nm).	53
<b>Table 6.</b> UV-Vis spectral data of <b>55</b> , <b>62</b> , and <b>65</b> in THF (in nm).	60
<b>Table 7.</b> Electrochemical data of the dinitriles <b>34</b> , <b>54</b> , <b>60</b> , and <b>64</b> , and the phthalocyanines <b>55</b> , <b>62</b> , and <b>65</b> .	62
<b>Table 8.</b> Electrochemical data of the dinitriles <b>82</b> and <b>86</b> and the tetrapyrroles <b>83</b> , <b>87</b> , and <b>90</b> , using a platinum disc working electrode.	87
<b>Table 9.</b> Electrochemical data of ferrocenyl couples of <b>83</b> , <b>87</b> and <b>90</b> using a platinum microsphere working electrode.	91

## Abbreviations

### General:

Ar	Aryl group
Bu	<i>n</i> -Butyl
<sup>t</sup> Bu	<i>tert</i> -Butyl
Cp	Cyclopentadienyl
DMA	<i>N,N</i> -dimethylacetamide
DMF	<i>N,N</i> -dimethylformamide
equiv.	Equivalent
Et	Ethyl
Fc	Ferrocene
FT	Fourier transform
h	hour(s)
HOMO	Highest occupied molecular orbital
LUMO	Lowest unoccupied molecular orbital
Me	Methyl
min	minute(s)
NBS	<i>N</i> -Bromosuccinimide
OAc	Acetate
Ph	Phenyl
py	Pyrrolic
r.t.	Room temperature
THF	Tetrahydrofuran
UV-Vis	Ultraviolet-visible

### Nuclear Magnetic Resonance (NMR) data:

{ <sup>1</sup> H}	Proton decouple
δ	Chemical shift
br. s	Broad signal
d	Doublet
dd	Doublet of doublet
<i>J</i>	Coupling constant
m	Multiplet



q	Quartet
s	Singlet
t	Triplet

**Mass Spectrometry (MS) data:**

$m/z$	Mass / charge
$M^+$	Molecular ion
MALDI-TOF	Matrix-assisted laser desorption/ionization time-of-flight
EI	Electron impact
FAB	Fast atom bombardment
ICR	Ion cyclotron resonance
LSI	Liquid secondary ion

**Infra-red (IR) data:**

vs	Very strong
sh	Shoulder
s	Strong
m	Medium
w	Weak

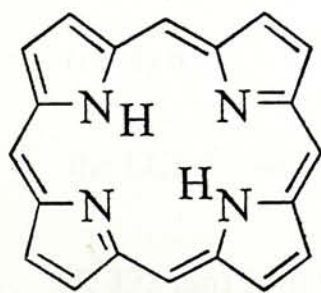
**Cyclic Voltammetric (CV) data:**

$E_{1/2}$	Half-wave potential
$\Delta E$	Peak to peak separation
$i_{pa}$	Anodic peak current
$i_{pc}$	Cathodic peak current
SCE	Saturated calomel electrode

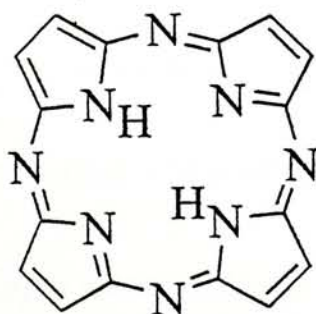
# 1. INTRODUCTION

## 1.1 General Background of Tetrapyrrole Derivatives

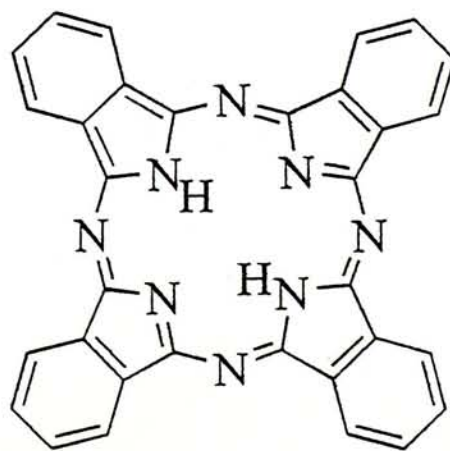
Tetrapyrrole derivatives are macrocyclic compounds containing four pyrrole units. Classical examples include porphyrins (e.g. 1), porphyrazines (or tetraazaporphyrins, e.g. 2), phthalocyanines (e.g. 3), 2,3-naphthalocyanines (e.g. 4), and 2,3-anthracocyanines (e.g. 5). Having a highly delocalized  $\pi$  system, these compounds are highly colored and exhibit a range of intriguing properties which render them useful in various disciplines.<sup>1,2</sup> Porphyrins, for example, are biomolecules which play a key role in respiration and photosynthesis.<sup>3</sup> Phthalocyanines are usually robust and are widely used in the field of materials science.<sup>1</sup> Their potential applications in electrochromic materials,<sup>4</sup> conducting materials,<sup>5</sup> sensors,<sup>6</sup> and photosensitizers<sup>7</sup> have been studied extensively.



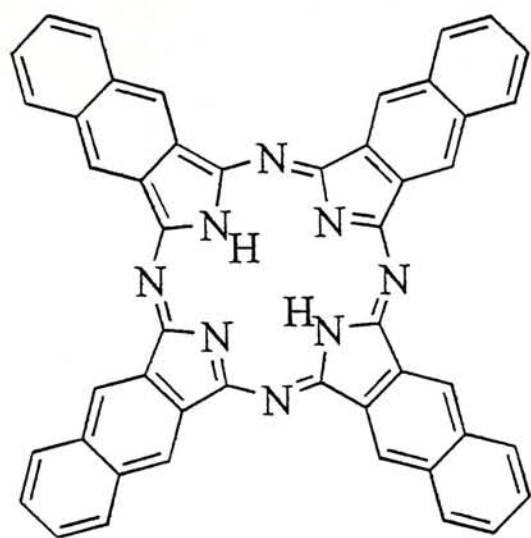
1



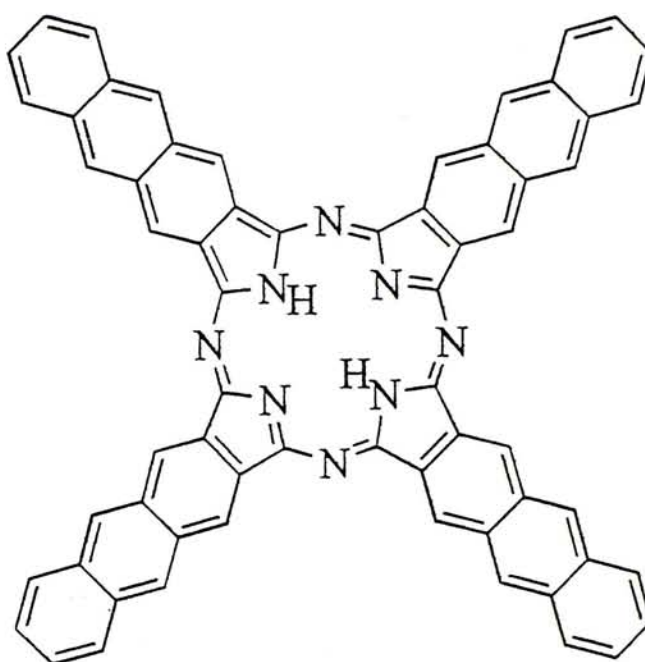
2



3



4



5

Due to the highly conjugated  $\pi$ -systems, these macrocyclic compounds have high absorptivity in the red spectral region. Figure 1 shows the energy level diagrams of 2-5.<sup>8</sup> The Q band, which is ascribed to the transition from HOMO to LUMO, shifts to longer wavelength ( $\lambda_{\text{max}}$  : 2, 592; 3, 662; 4, 725; 5, 760 nm) and intensifies with expansion of the  $\pi$  - systems showing that the energy gap between the HOMO and the LUMO decreases as the size of the  $\pi$  - system increases. The Soret (or B) band is associated with the transition from the next to highest occupied MO to the LUMO, which also experiences a bathochromic shift ( $\lambda_{\text{max}}$  : 2, 317; 3, 332; 4, 352; 5, 393 nm) with enlargement of the  $\pi$ -systems.



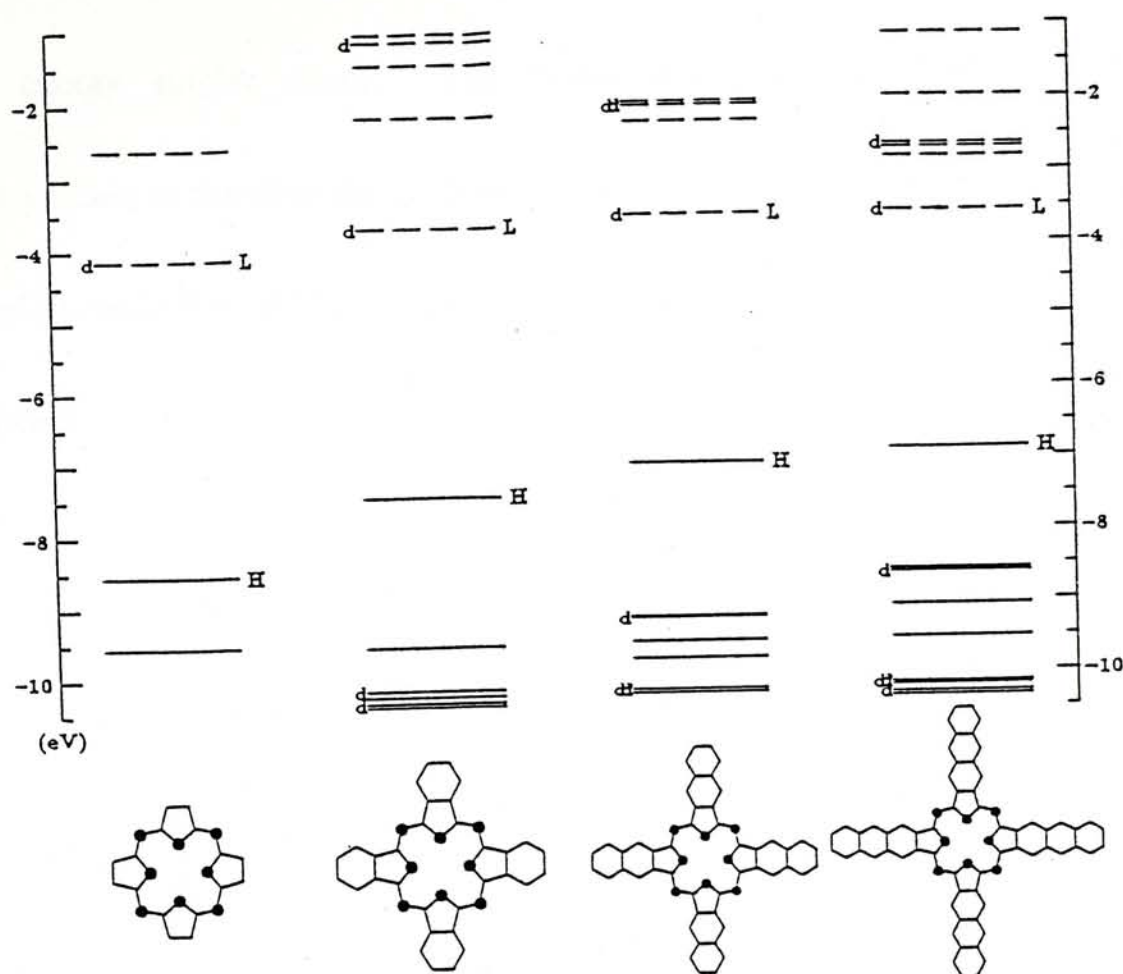


**Figure 1.** Energy level diagrams of macrocycles 2-5. (H = HOMO; L = LUMO; d = degenerate).

The spectral properties of phthalocyanines are significantly different from those of porphyrins. Because of the aza-bridges in phthalocyanines, the Q band transition, which is designated to an  $a_{1u}$  to  $e_g$  transition, is distinguishable from that of porphyrins which is an  $a_{2u}$  to  $e_g$  transition. As a result of the significant energy separation between the  $a_{1u}$  and the  $a_{2u}$ , the two top filled molecular orbitals, the Q state of phthalocyanines is considerably less coupled to the second singlet excited state.

But in porphyrins, an extensive configuration interaction occurs between the two lowest energy singlet states. The molar absorptivity of the Q band in phthalocyanines is therefore up to 10 times higher than that of porphyrins. Figures 2 (a) and (b) show typical UV-Vis spectra of metallo-phthalocyanines and porphyrins, respectively.

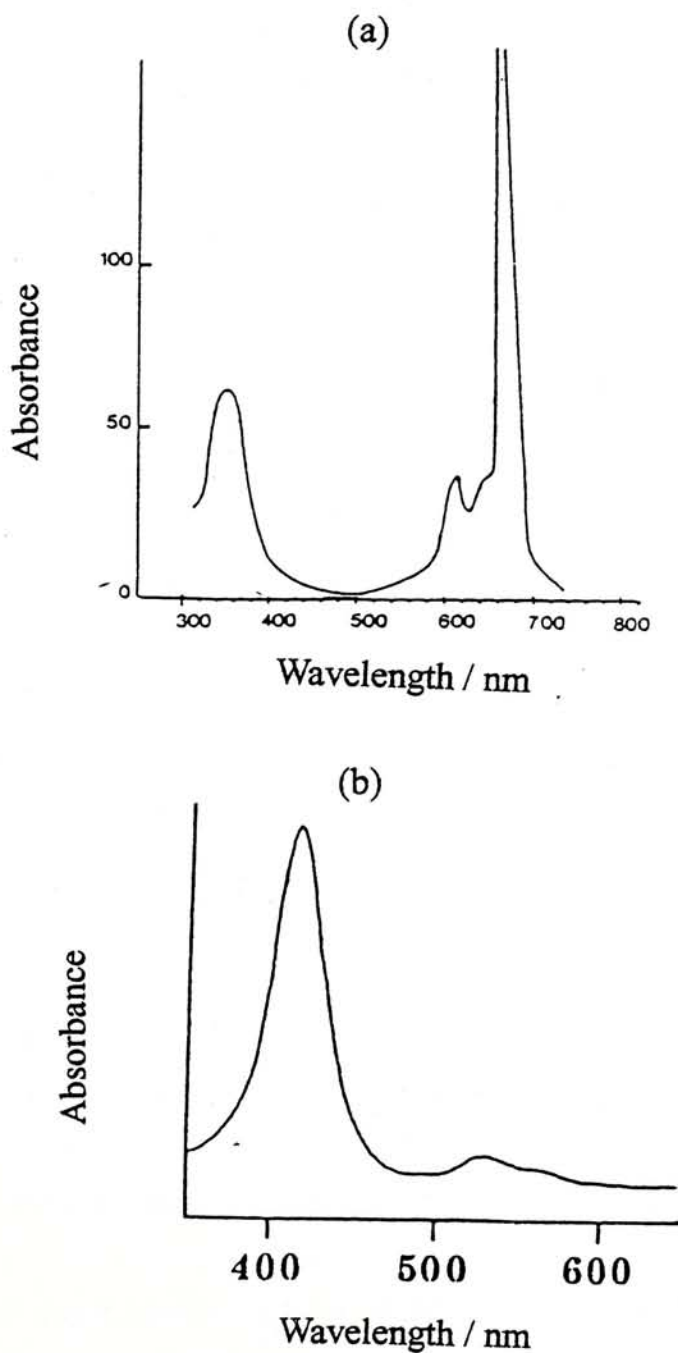


**Figure 2.** General UV-Vis spectra of (a) metallophthalocyanines and (b) metalloporphyrins.

These tetrapyrrole derivatives also exhibit rich electrochemistry. For main group phthalocyanines the first ring oxidation is separated from the first ring reduction by ca. 1.5 V which corresponds approximately to the magnitude of energy separation between the HOMO and LUMO.<sup>9</sup> The individual potentials, however, vary remarkably. Generally, the more polarizing the central metal ions, the easier it is to reduce the ring and the more difficult to oxidize the ring. A linear relationship has been revealed and is shown as equations (1) and (2).<sup>10</sup>

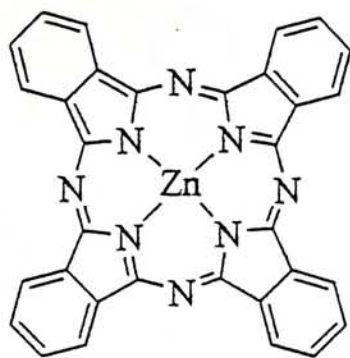
$$E^{\circ}_{\text{ox1}} = 1170 - 11.7 (r/ze) \dots\dots\dots (1)$$

$$E^{\circ}_{\text{red1}} = -385 - 12 (r/ze) \dots\dots\dots (2)$$

where  $E^{\circ}_{\text{ox1}}$  and  $E^{\circ}_{\text{red1}}$  are the first oxidation potential and the first reduction potential versus SCE (in mV), respectively,  $r$  is the radius of the central metal ion (in pm), and  $ze$  is the charge of the central metal ion.<sup>11</sup> As expected, different substituents on the phthalocyanine core will also induce changes in the redox potentials.

The electrochemistry of zinc phthalocyanines has been well documented.<sup>9,12</sup>

As zinc(II) is a closed shell ion which is redox inactive, all the redox processes are attributed to the macrocycles. Figure 3 shows a typical cyclic voltammogram of zinc(II) phthalocyanine (6).<sup>12d</sup>



6

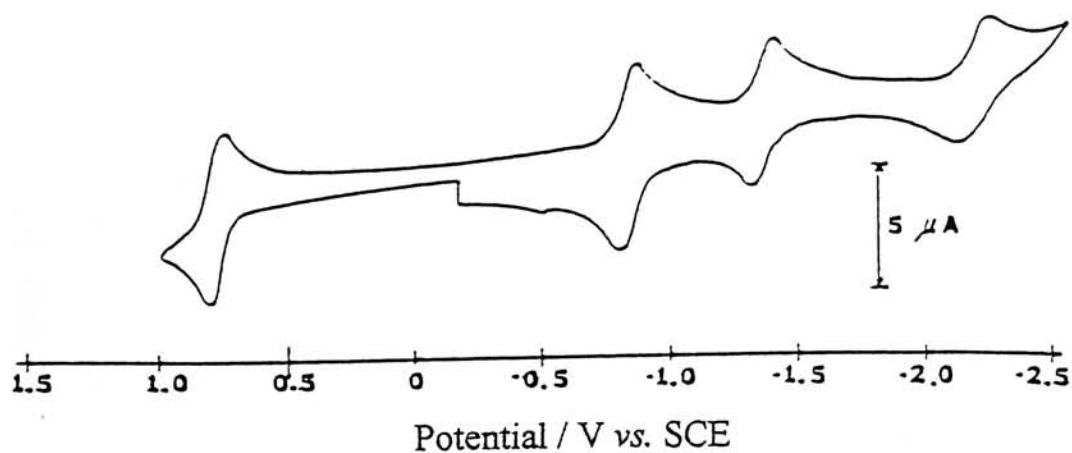
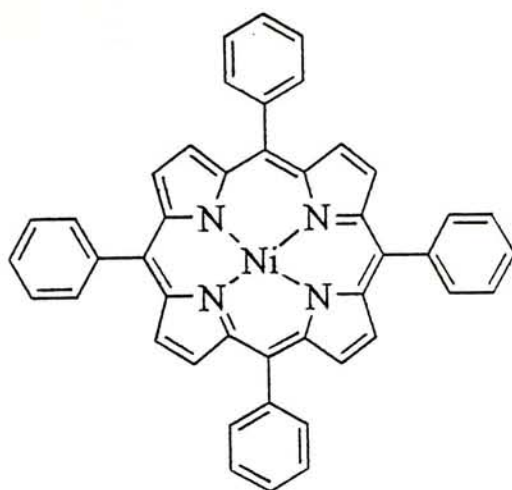


**Figure 3.** Cyclic voltammogram of zinc(II) phthalocyanine (6) (0.4 mM) in DMA containing 0.1 M  $[\text{NBu}_4][\text{ClO}_4]$  at a scan rate of  $50 \text{ mV s}^{-1}$ .

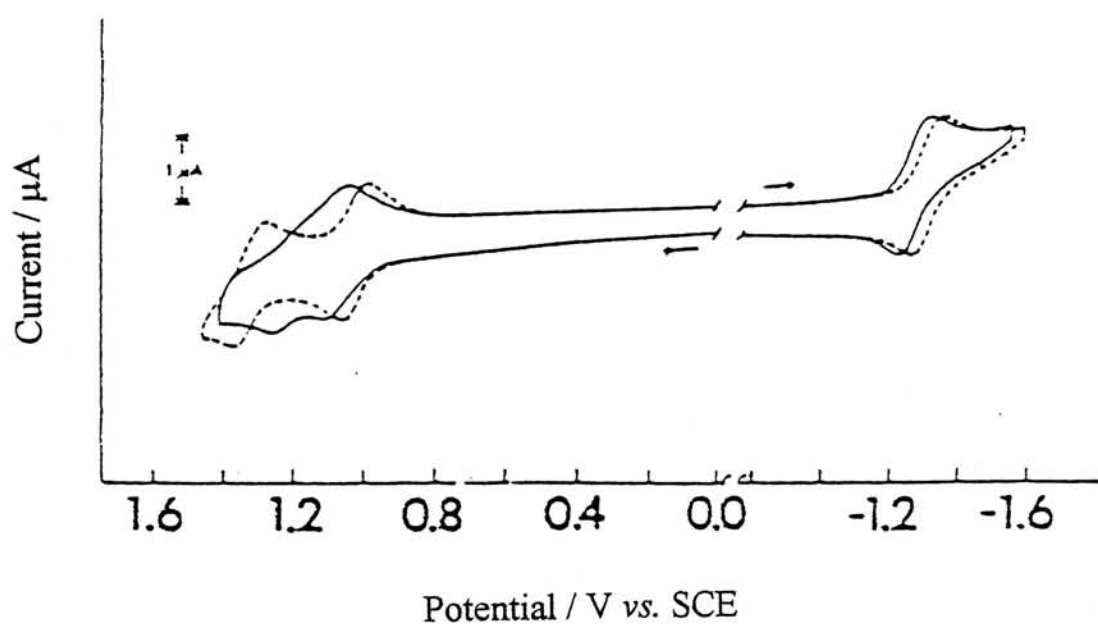
The electrochemistry of porphyrins has also been studied extensively.<sup>13</sup>

Figure 4 gives typical cyclic voltammograms of nickel(II) tetraphenylporphyrin (7) reported by Kadish et al. In contrast to the  $\text{Zn(II)}$  ion, the  $\text{Ni(II)}$  ion can undergo an oxidation to  $\text{Ni(III)}$  and this process is revealed by the couple at 1.0 V using  $[\text{NBu}_4][\text{PF}_6]$  as the electrolyte.<sup>14</sup>





7



**Figure 4.** Cyclic voltammograms of nickel(II) tetraphenylporphyrin (**7**) (0.5 mM) in  $\text{CH}_2\text{Cl}_2$  containing 0.1 M  $[\text{NBu}_4][\text{ClO}_4]$  (—) or  $[\text{NBu}_4][\text{PF}_6]$  (---) at a scan rate of  $100 \text{ mV s}^{-1}$ .

## 1.2 Electronic Interactions in Systems with Multiple Redox Sites

In the past few years, there has been a growing interest in molecular systems containing multiple redox-active centers.<sup>15-17</sup> These molecules can act as potential candidates for multi-electron redox catalysts<sup>16</sup> and serve as models for the studies of light-initiated intramolecular electron transfer that may shed light on the complex but practically useful processes such as solar energy conversion and artificial photosynthesis.<sup>15a,17</sup> Ferrocene, owing to its chemical stability and well-defined electrochemistry, has been widely used in the construction of such multi-component systems. It can also act as an electron relay group because the electron transfer of this group is known to be very fast.<sup>18</sup> Studies of the electronic interactions between the redox sites in a molecule are a subject of great fundamental importance, particularly in the field of molecular electronics.<sup>19</sup> The interactions may be in general through chemical bonds or space (Figure 5) and can be studied with a range of physical methods such as electrochemical techniques, electron spin resonance spectroscopy, magnetic measurements, and electronic spectroscopy.<sup>20</sup>

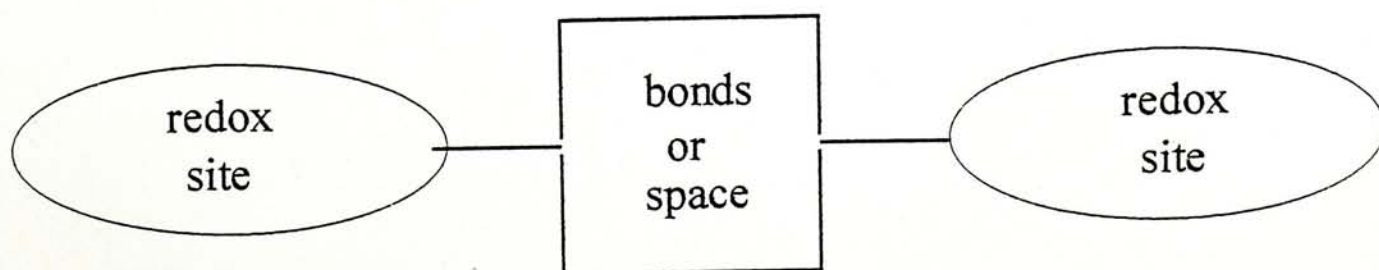
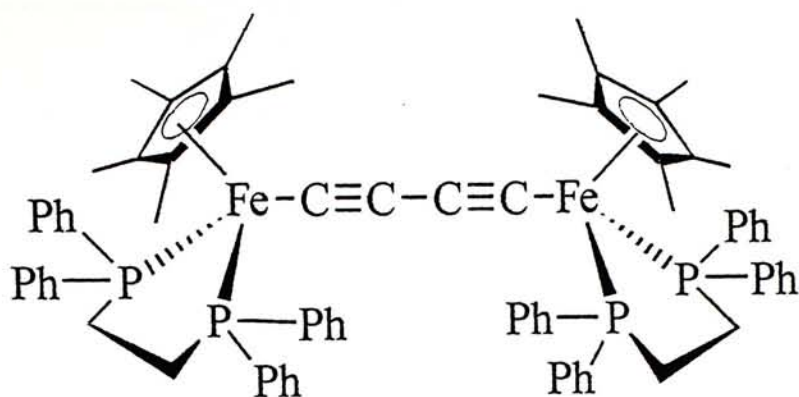


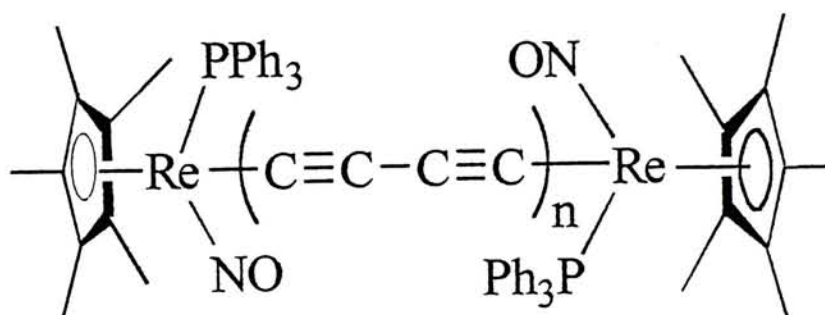
**Figure 5.** Model for the electronic interactions between two redox sites.

### 1.2.1 Electronic Interactions in One-dimensional Systems

Molecular wires such as compounds **8**<sup>21</sup> and **9**<sup>21c,22</sup> are typical examples of one-dimensional systems. As the two redox sites are linked with a conjugated system, electronic interaction may occur through the chemical bonds. Figure 6 shows the cyclic voltammogram of compound **8** which exhibits two reversible couples assignable to the oxidation of the two iron centers. Similarly, the voltammograms of **9** ( $n = 1-4$ ) also show two oxidation couples for the metal centers and the results are listed in Table 1. The separation of the two couples ( $\Delta E$ ) decreases when the two redox sites are farther apart. Only one couple at 0.74 V appears when the two Re centers are separated by 10 triple bonds [i.e. **9** ( $n = 5$ )]. The appearance of two oxidation couples suggests that the redox sites are oxidized in sequence and electronic interactions exist between the two metal centers. For systems in which the two redox sites are independent to each other, they should be oxidized simultaneously at the same potential so that only one couple will be seen.



8



$n = 1-5$

9

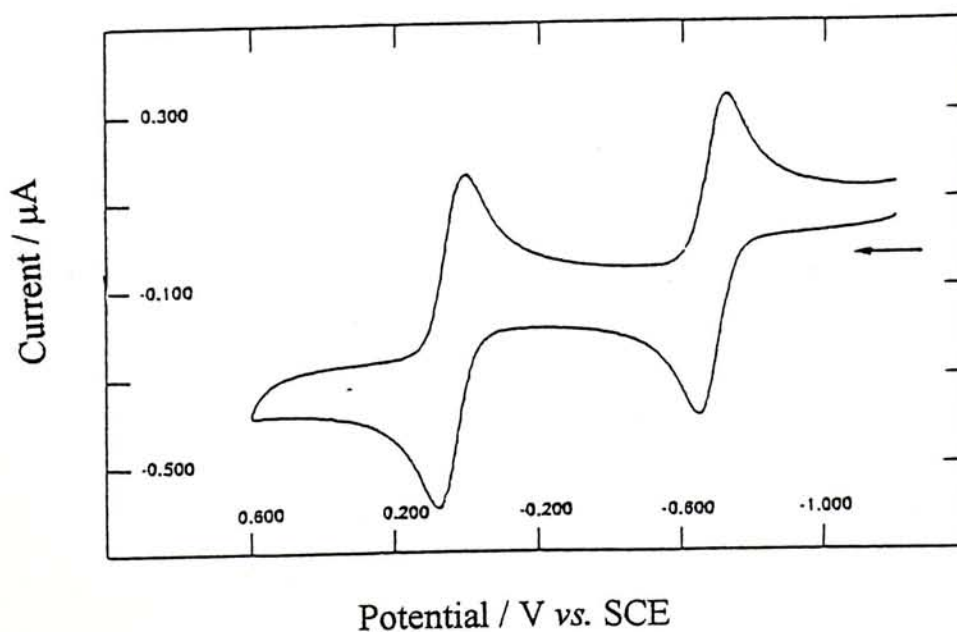


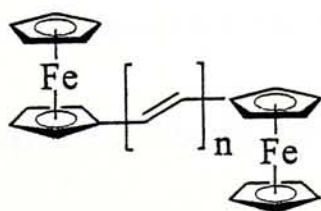
**Figure 6.** Cyclic voltammogram of **8** in  $\text{CH}_2\text{Cl}_2$  containing 0.1 M  $[\text{NBu}_4][\text{PF}_6]$  at a scan rate of  $100 \text{ mV s}^{-1}$ .



n	$E^{\circ}_1$ (V)	$E^{\circ}_2$ (V)	$\Delta E$ (V)
1	0.11	0.64	0.53
2	0.34	0.62	0.28
3	0.56	0.75	0.19
4	0.67	0.76	0.09
5	0.74 (2 e process)		-----

**Table 1.** Electrochemical data (vs.  $\text{Fc}/\text{Fc}^+$ ) of **9** ( $n = 1-5$ ) ( $7 - 9 \times 10^{-5}$  M) in  $\text{CH}_2\text{Cl}_2$  containing 0.1 M  $[\text{NBu}_4][\text{PF}_6]$  at a scan rate of  $100 \text{ mV s}^{-1}$ .

Diferrocenylpolyenes of the general formula  $\text{Fc}(\text{CH}=\text{CH})_n\text{Fc}$  (**10**) ( $n = 1-6$ ) are the other well-studied one-dimensional systems.<sup>23</sup> As shown in Table 2, the electronic communication between the redox-active ferrocenyl groups is also quite sensitive to the separation between the redox sites. Again, only one ferrocenyl couple appears when the ferrocenyl groups are separated by more than three double bonds.



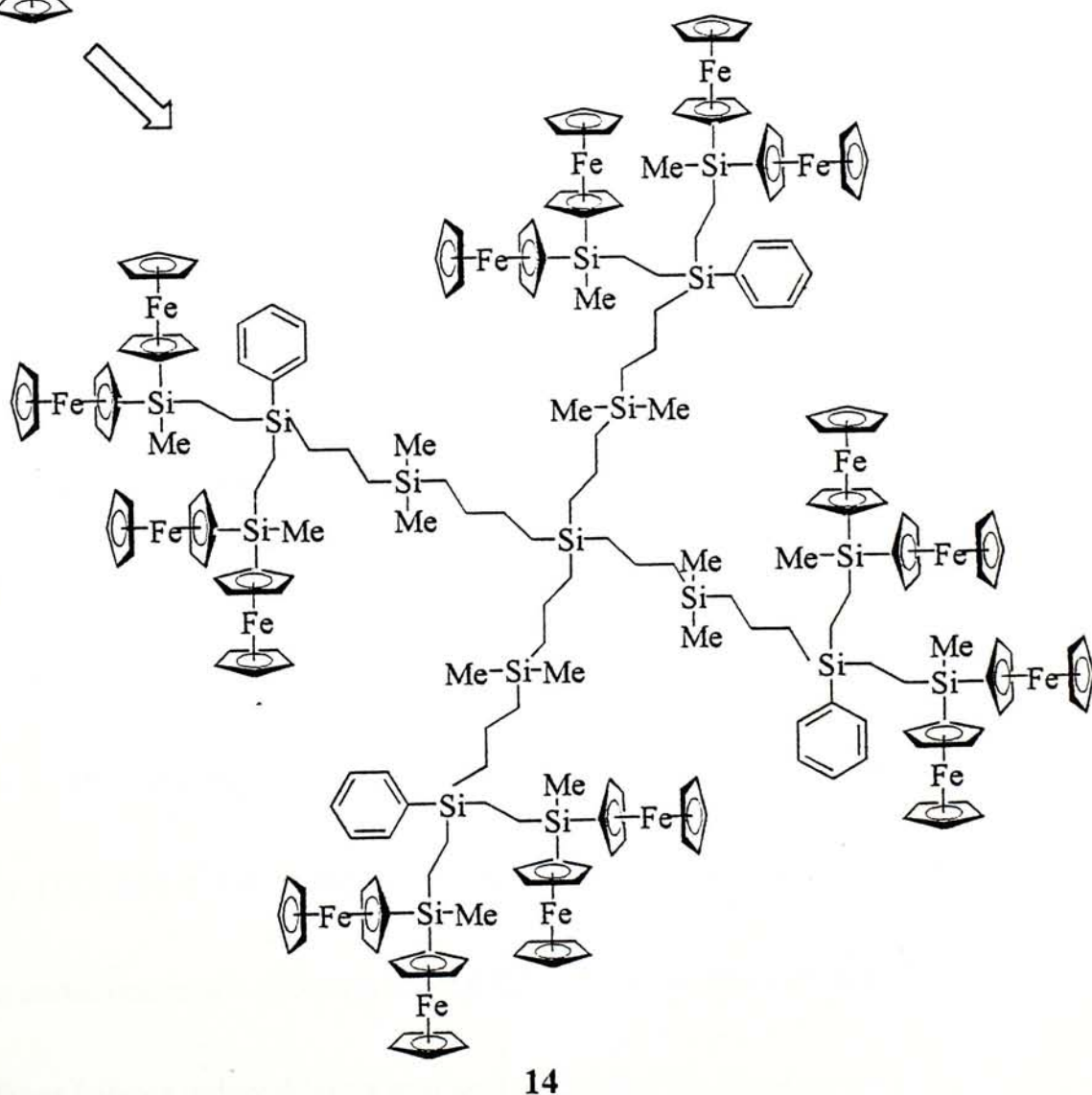
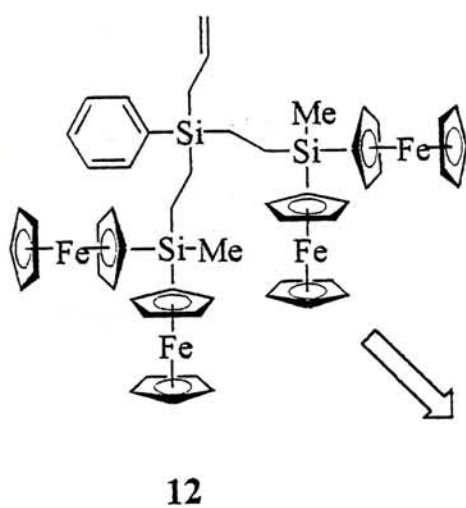
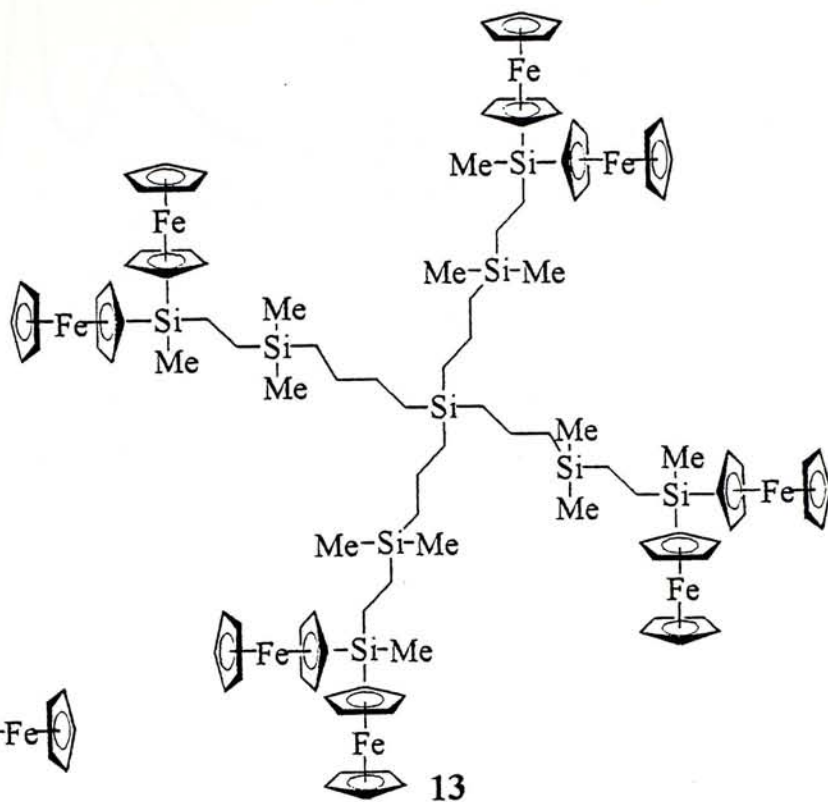
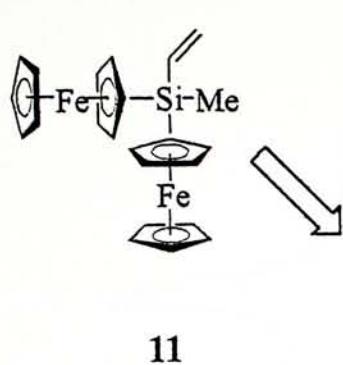
n	$E^{\circ}_1$ (mV)	$E^{\circ}_2$ (mV)	$\Delta E$ (mV)
1	290	460	170
2	294	423	129
3	366	460	94
4	405 (2 e process)		-----
5	400 (2 e process)		-----
6	402 (2 e process)		-----

**Table 2.** Electrochemical data (vs. SCE) of **10** ( $n = 1-6$ ) containing 0.1 M  $[\text{NBu}_4][\text{BF}_4]$  at a scan rate of  $100 \text{ mV s}^{-1}$ .

### 1.2.2 Electronic Interactions in Three-dimensional Systems

Compared with one-dimensional systems, electronic interactions in three-dimensional systems are relatively rare; most of them are based on dendritic framework with redox-active sites as the surface groups. Because of the globular structure of dendrimers, the electronic interactions may occur through space. The organometallic dendrimers **13** and **14** containing eight and sixteen ferrocenyl groups respectively have been synthesized by hydrosilylation of the dendrons **11** and **12** with  $\text{Si}[(\text{CH}_2)_3\text{SiMe}_2\text{H}]_4$ , which acts as the core.<sup>24</sup> Both compounds **11** and **12** exhibit two well-separated and reversible oxidation waves of equal intensity in the cyclic

voltammograms. Dendrimers **13** (Figure 7) and **14** also show a similar cyclic voltammetric response. This suggests that the ferrocenyl units in these compounds are electronically coupled. It is worth to note that the redox behavior of the dendrimers **13** and **14** is solvent dependent. A sharp cathodic stripping peak and a typical diffusional shape of anodic peak are observed in  $\text{CH}_2\text{Cl}_2$  (Figure 7a). This indicates the precipitation of the dendrimers onto the electrode upon oxidation. Besides, upon continuous scanning in  $\text{CH}_2\text{Cl}_2$ , there is an increase in the peak current with successive scans, which indicates that the formation of an electroactive film on the electrode surface. The cathodic stripping peak disappears (Figure 7b) when a small amount of MeCN is added to the  $\text{CH}_2\text{Cl}_2$  electrolyte medium. These are the first organometallic dendritic molecules displaying electronic interactions between transition metal atoms in the dendritic structure.





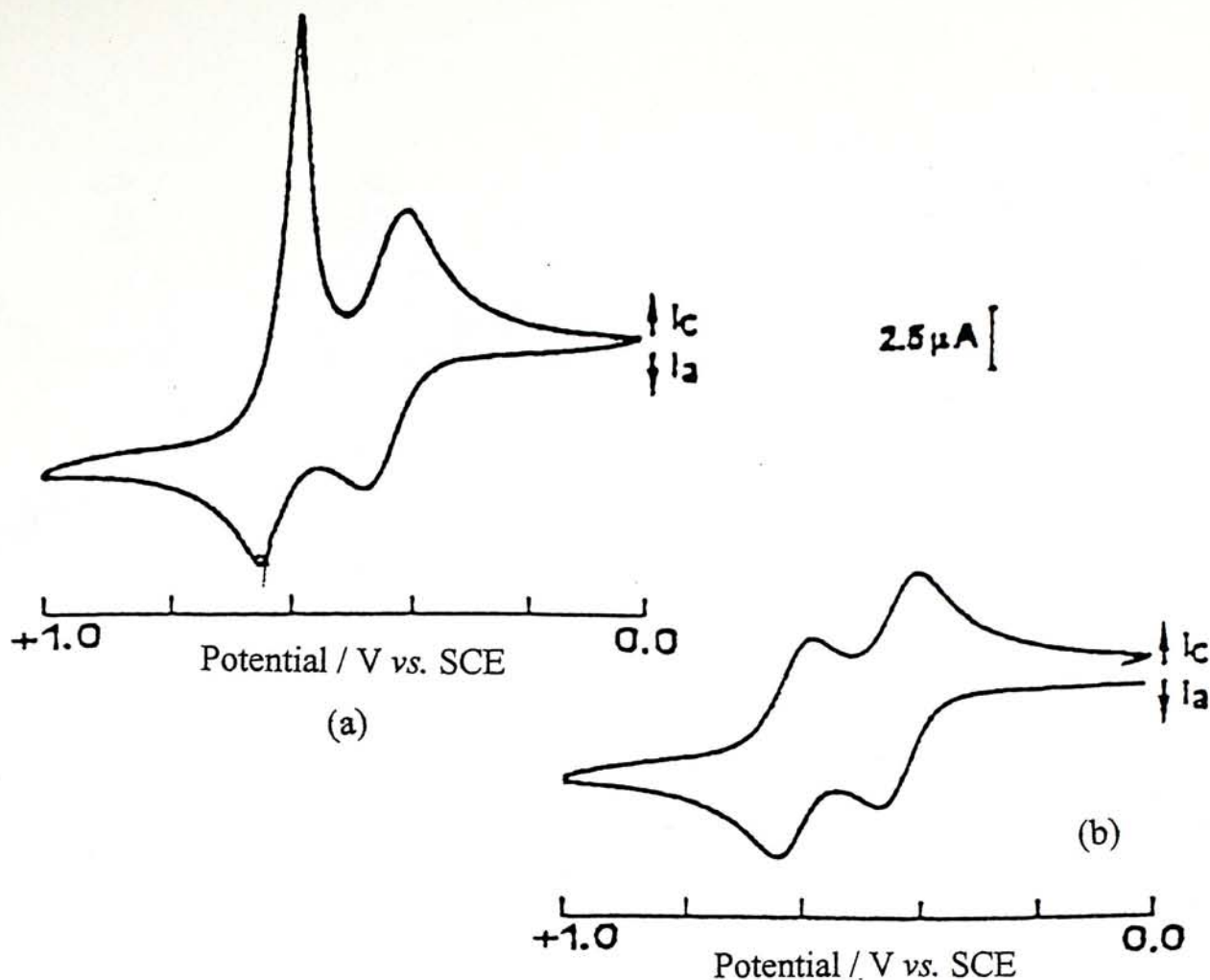
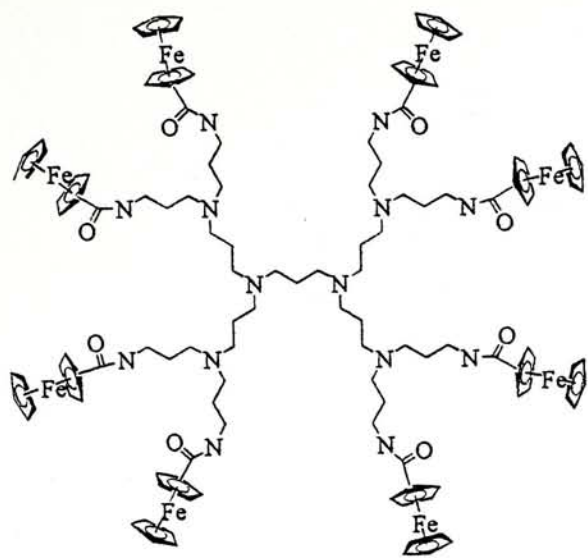
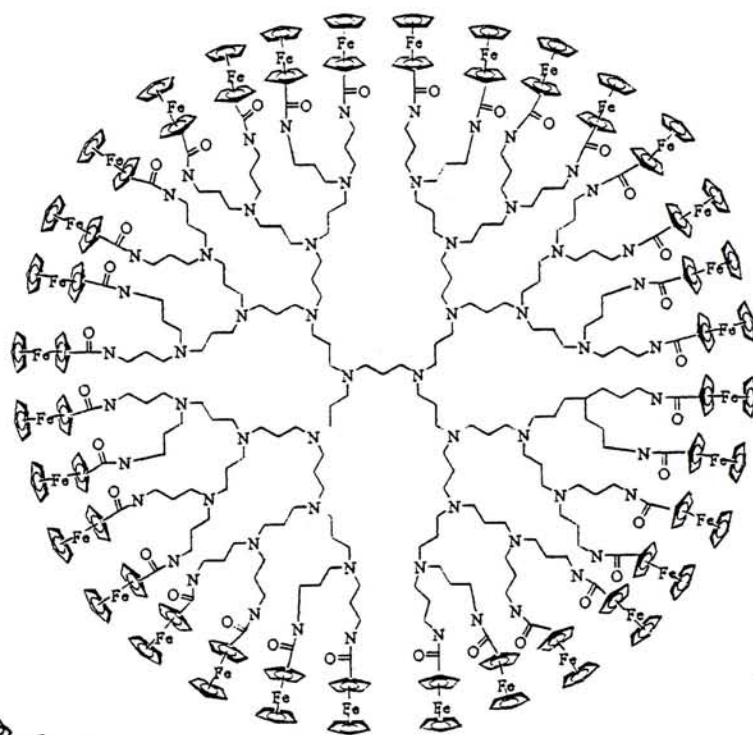


**Figure 7.** Cyclic voltammograms of compound 13 in (a)  $\text{CH}_2\text{Cl}_2$  or (b)  $\text{CH}_2\text{Cl}_2/\text{MeCN}$  (v/v 5 : 1) containing 0.1 M  $[\text{NBu}_4][\text{PF}_6]$  at a scan rate of  $100 \text{ mV s}^{-1}$ .

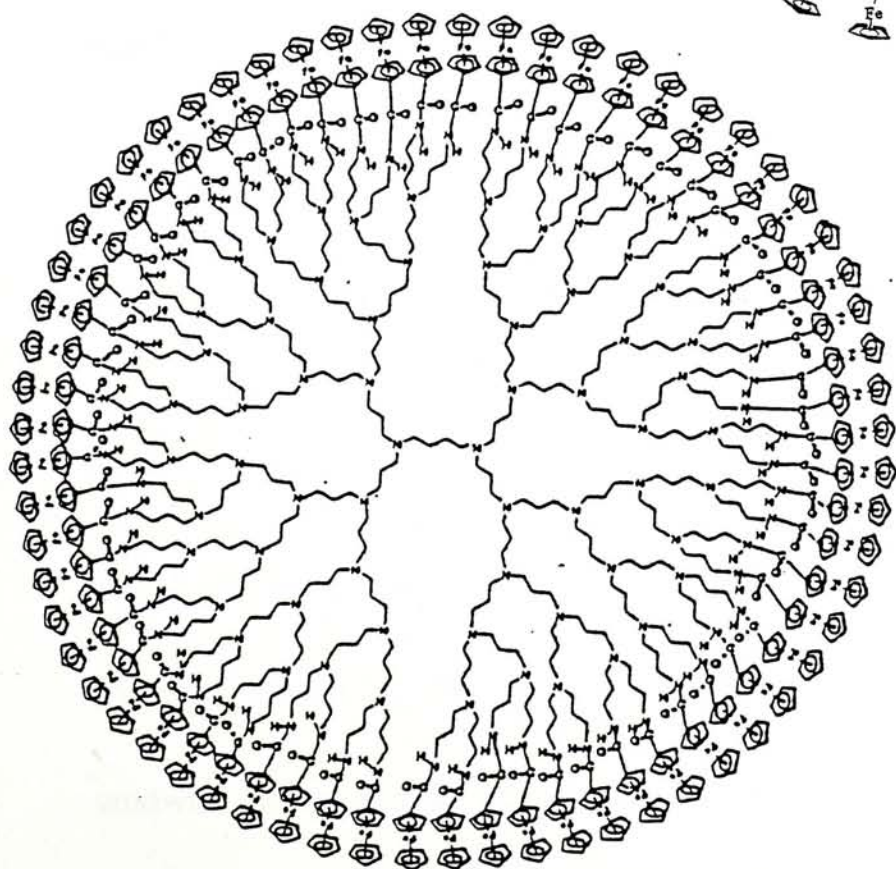
Cuadrado et al. also reported another series of ferrocenyl dendrimers in 1996 (15-17).<sup>25</sup> The organometallic dendrimers containing up to 64 peripheral ferrocenyl moieties (G5) have been prepared by coupling an excess of ferrocene carbonyl chloride to amino-terminated poly(propyleneimine) dendrimers. Figure 8 shows the cyclic voltammograms of the dendrimers with eight (15), thirty-two (16) and sixty-four (17) ferrocenyl groups. It can be seen that one oxidation wave appears in the voltammograms showing that all the ferrocenyl moieties attached to the dendritic surfaces behave independently and are oxidized at the same potential.



15



16



17

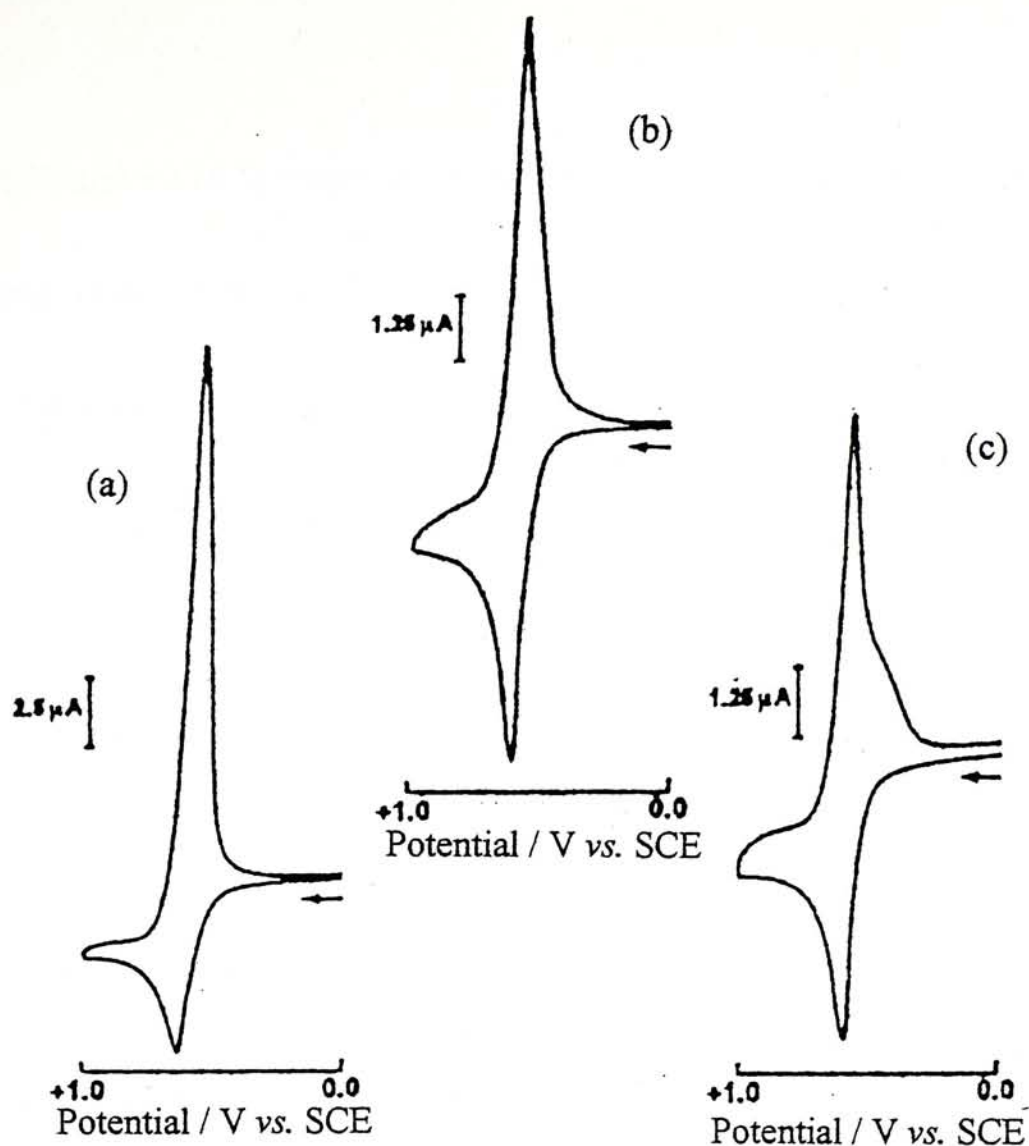


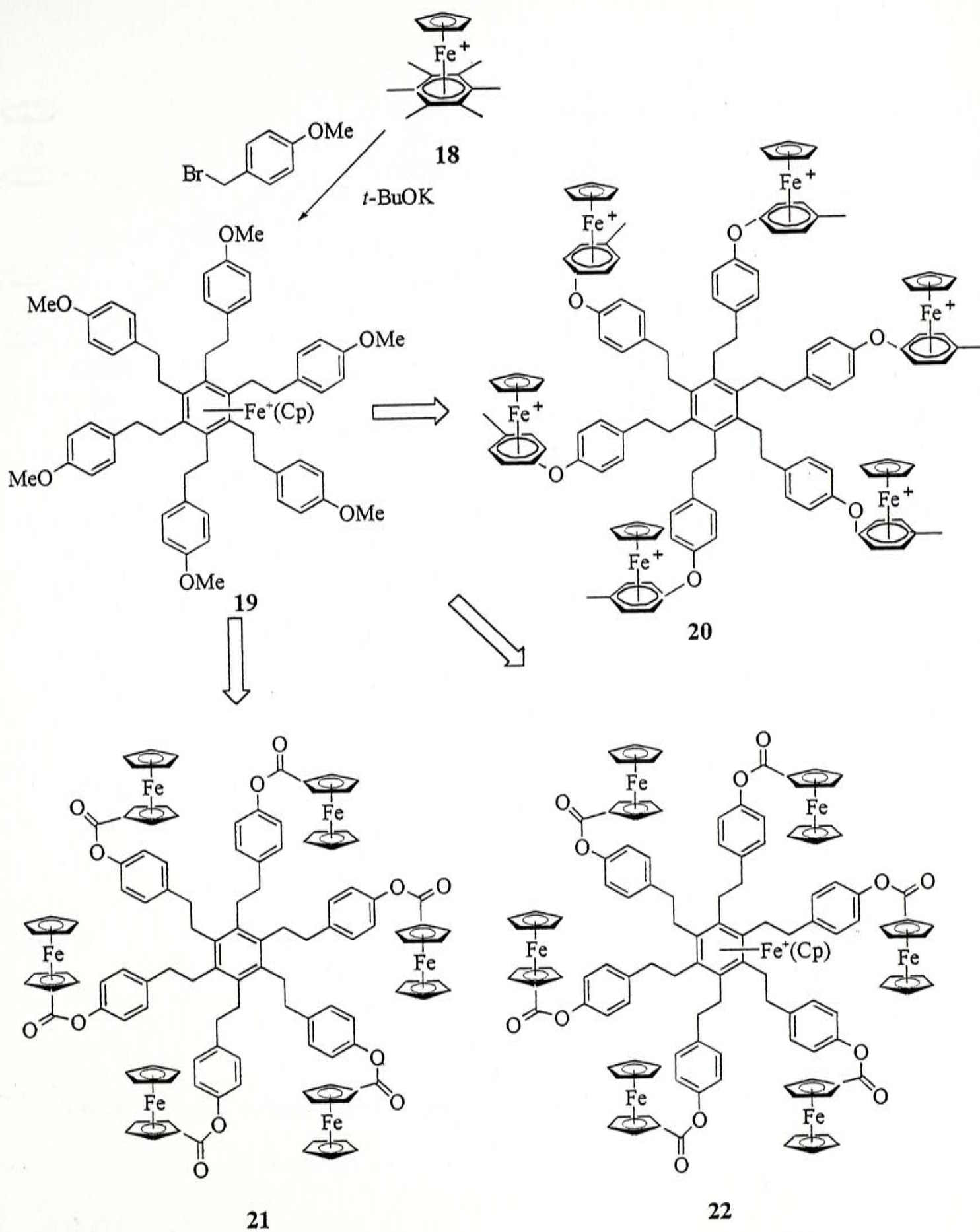
**Figure 8.** Cyclic voltammograms of (a) 15, (b) 16, and (c) 17 (1.0 mM) in  $\text{CH}_2\text{Cl}_2$  containing 0.1 M  $[\text{NBu}_4][\text{PF}_6]$  at a scan rate of  $100 \text{ mV s}^{-1}$ .

Astruc et al. have also reported a number of multi-ferrocenyl systems based on a polyphenyl core.<sup>26</sup> The key intermediate 19 has been synthesized by polyalkylation of the  $\text{Fe}(\text{Cp})^+$  complex of hexamethylbenzene 18. The methoxy groups of 19 can then be converted to other  $\text{Fe}(\text{Cp})$  derivatives giving the hexa-iron sandwich complexes 20 and 21, and the hepta-iron derivative 22. As shown by cyclic voltammetry, the hexa-iron complexes 20 and 21 exhibit a single reversible



wave at -1.30 and +0.78 V, respectively, which is due to the simultaneous transfer of six electrons. For compound **22**, a reversible couple at -1.34 V also appears which can be assigned to the one-electron reduction of the central cationic iron unit. The peripheral ferrocenyl moieties undergo a simultaneous oxidation at +0.88 V, which is shifted by 0.1 V by comparing with **21**. This may suggest that an interaction between the central and surface iron centers exists. To clarify this point, Astruc et al. have also prepared compounds **23** and **24**.<sup>27</sup> The oxidation potentials of the peripheral ferrocenyl units in both compounds have a similar value at about +0.44 V (Figure 9), despite the presence of an additional  $[\text{FeCp}]^+$  moiety in **24**. This observation indicates that the redox potentials are largely dependent on the structural environment around the metal vicinities.





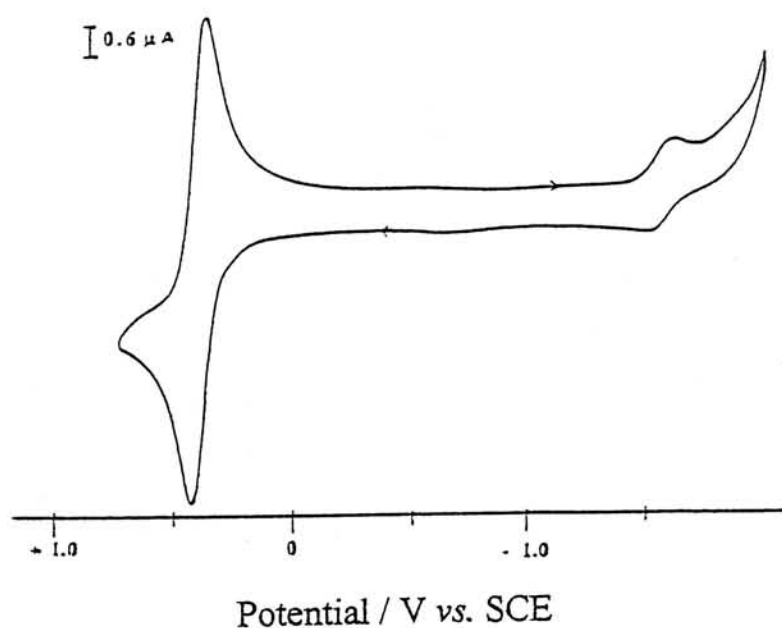
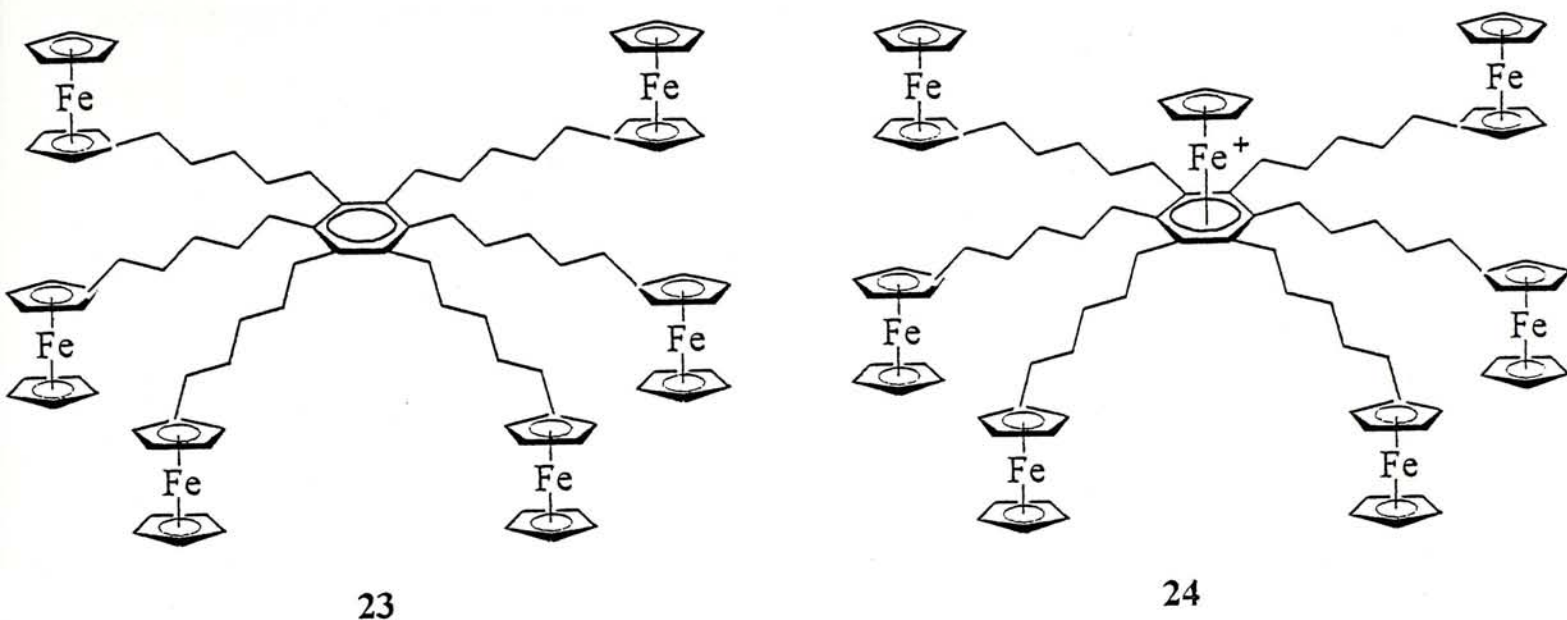
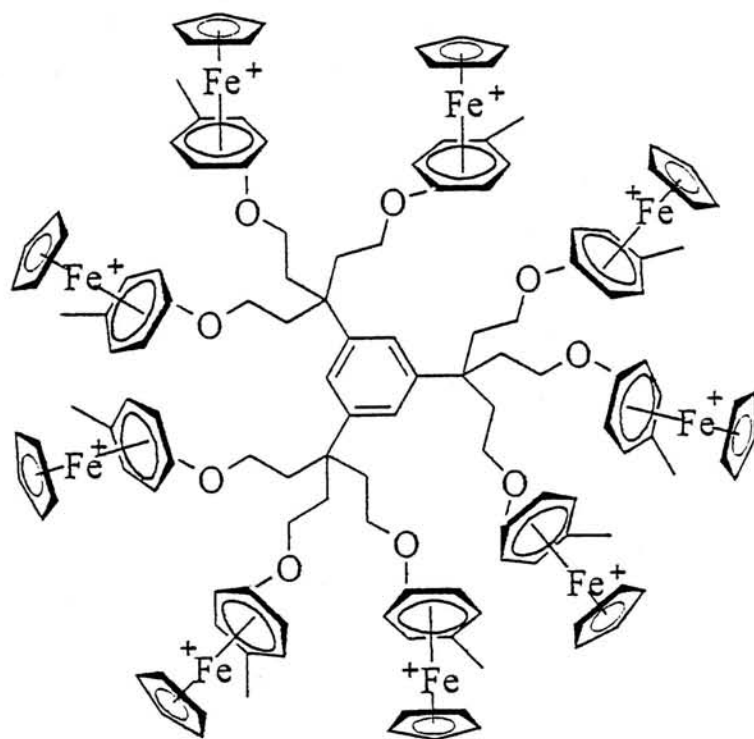


**Figure 9.** Cyclic voltammogram of **24** in DMF containing 0.1 M  $[\text{NBu}_4][\text{BF}_4]$  at a scan rate of  $400 \text{ mV s}^{-1}$ .

The nona-iron complex **25** has also been prepared and its electrochemistry studied by cyclic voltammetry.<sup>28</sup> As shown in Figure 10, this complex exhibits a

single reduction wave at  $-1.37$  V, indicating that all nine peripheral  $[\text{FeCp}(\text{arene})]^+$  moieties appear to be electrochemically independent to each other.



25

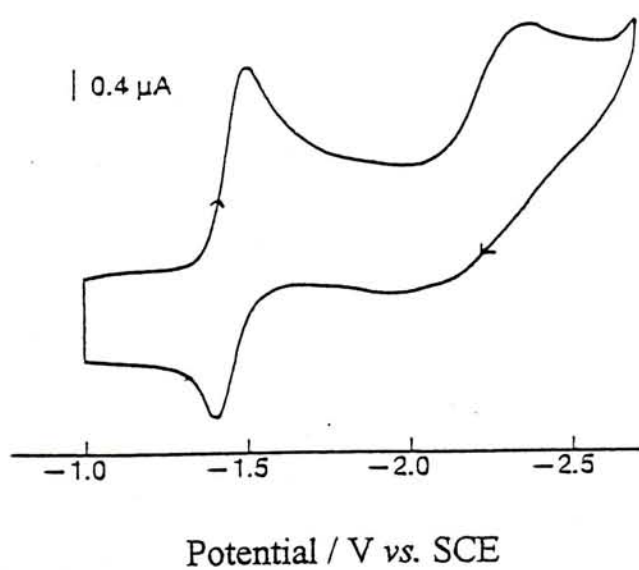


**Figure 10.** Cyclic voltammogram of **25** ( $1.0$  mM) in DMF containing  $0.1$  M  $[\text{NBu}_4][\text{BF}_4]$  at a scan rate of  $400 \text{ mV s}^{-1}$ .

Although studies of electronic interactions in one- and three-dimensional systems have been well-documented, a related investigation on two-dimensional analogs has been relatively rare. The main objective of this work is to examine the electronic coupling between the redox-active ferrocenyl moieties connected to a two-dimensional tetrapyrrole platform. Ferrocene-containing tetrapyrroles have only been reported sporadically and are summarized in the following section.

### 1.3 Ferrocene-containing Tetrapyrrole Derivatives

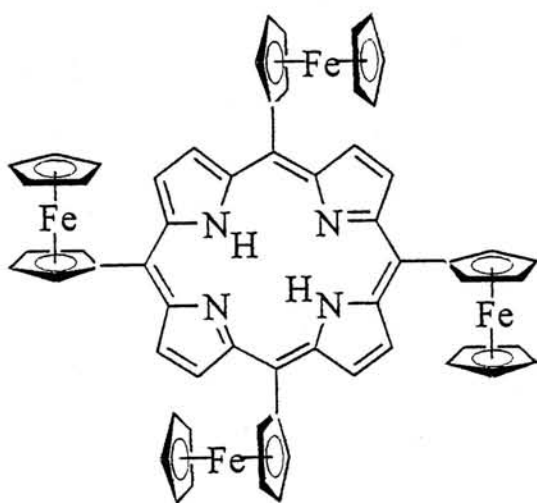
Ferrocene-containing porphyrins, porphyrazines and phthalocyanines have been known in which the porphyrin systems have received much attention. On the other hand, 2,3-naphthalocyanines with ferrocenyl substituents have not been reported previously.

#### *1.3.1 Ferrocene-containing Porphyrins*

The first example of ferrocene-containing porphyrin was reported in 1977.<sup>29</sup> *meso*-Tetraferrocenylporphyrin **26** was synthesized by typical condensation of ferrocenecarboxaldehyde and pyrrole. Its electrochemistry was studied very briefly

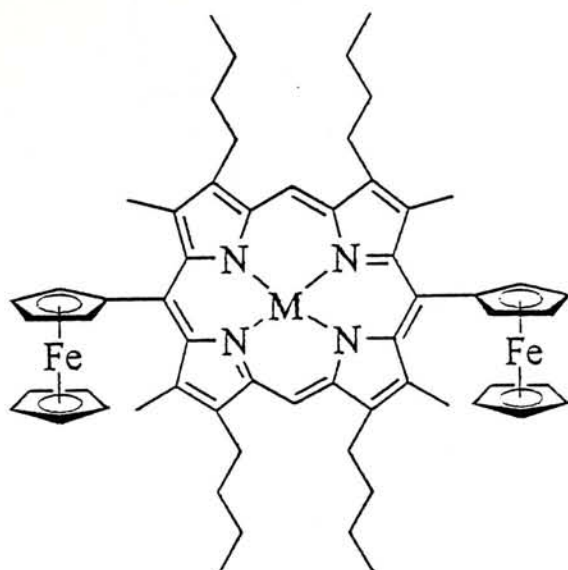


by differential-pulse polarography. The polarogram showed only a broad oxidation wave indicating that electronic coupling between ferrocenyl groups is insignificant.



26

Very recently, Burrell et al. have synthesized a related bis(ferrocenyl)porphyrin **27** and its nickel derivative **28**.<sup>30</sup> The metal-free porphyrin **27** is formed in a classical condensation reaction between ferrocenecarboxaldehyde and a tetraalkyl dipyrromethane. Metalation of **27** gives nickel(II) complex **28**. Figure 11 shows the cyclic voltammogram of compound **28** and Table 3 gives the electrochemical data for the ferrocene oxidation couples. It can be seen that the ferrocenyl units in both porphyrins, in particular **28**, exhibit a strong electronic coupling. This has been supported by the UV-Vis spectra of **27** (Figure 12a) and **28** (Figure 12b) which show a growth of an absorption peak at 1080 and 946 nm, respectively, with single electron oxidation. These are assigned as intravalence charge-transfer bands. Further oxidation leads to the depletion of these features.



27 M = H<sub>2</sub>

28 M = Ni

Compound	E <sup>o</sup> <sub>1</sub> (V)	E <sup>o</sup> <sub>2</sub> (V)	ΔE (V)
27	-0.24	-0.08	0.16
28	-0.24	0.17	0.41

**Table 3.** Electrochemical data (vs. Fc/Fc<sup>+</sup>) of **27** and **28** in CH<sub>2</sub>Cl<sub>2</sub> solution.

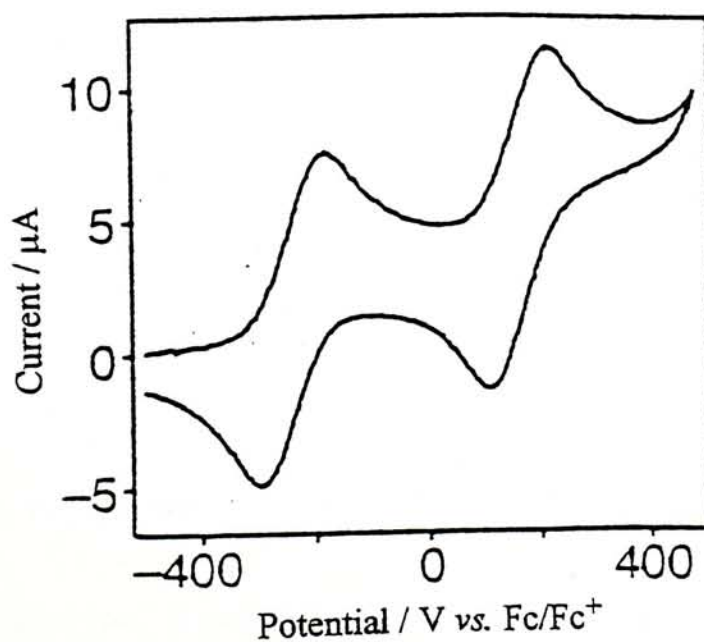


**Figure 11.** Cyclic voltammogram of **28** in CH<sub>2</sub>Cl<sub>2</sub> solution.

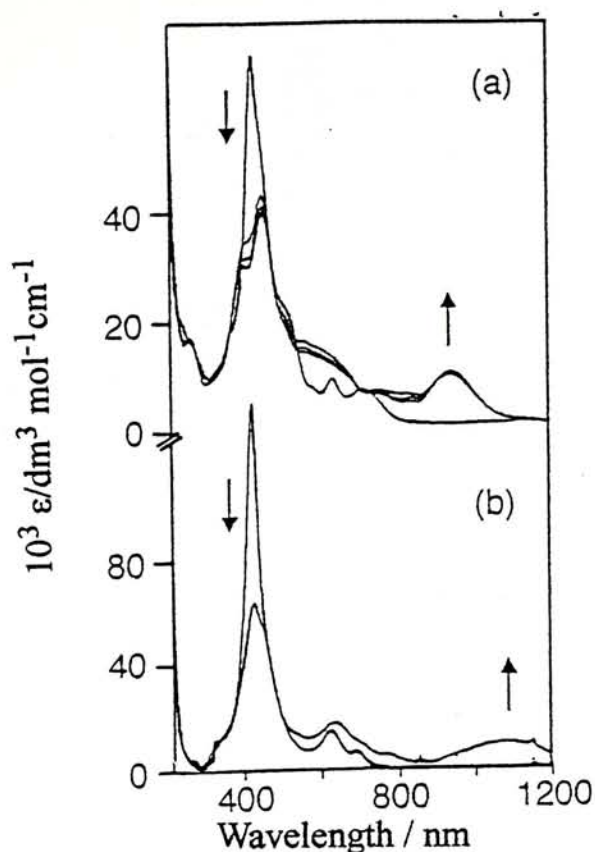
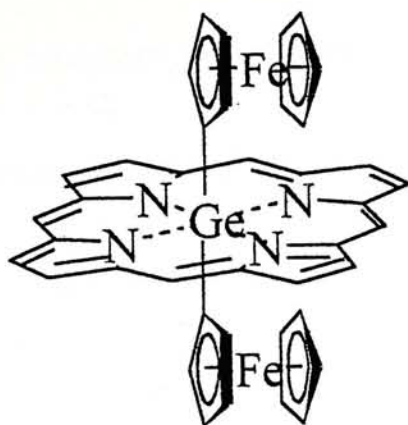


**Figure 12.** Spectro-electrochemical UV-Vis spectra of (a) **27** and (b) **28**; arrows indicate direction of change in peaks during oxidation.

Axial coordination of ferrocenyl units to metalloporphyrins has also been reported by Kadish et al.<sup>31</sup> The germanium porphyrin-bridged biferrocene complex **29** exhibits four reversible oxidations at 0.14, 0.32, 1.32, and 1.57 V as revealed by the cyclic (Figure 13a) and differential pulse voltammogram (Figure 13b). The third and fourth oxidation waves correspond to the oxidation of the porphyrin  $\pi$  system, while the first two couples are due to the ferrocene oxidation. As the ferrocenyl wave is split into two, it suggests that the two ferrocenyl units are electronically coupled.



29

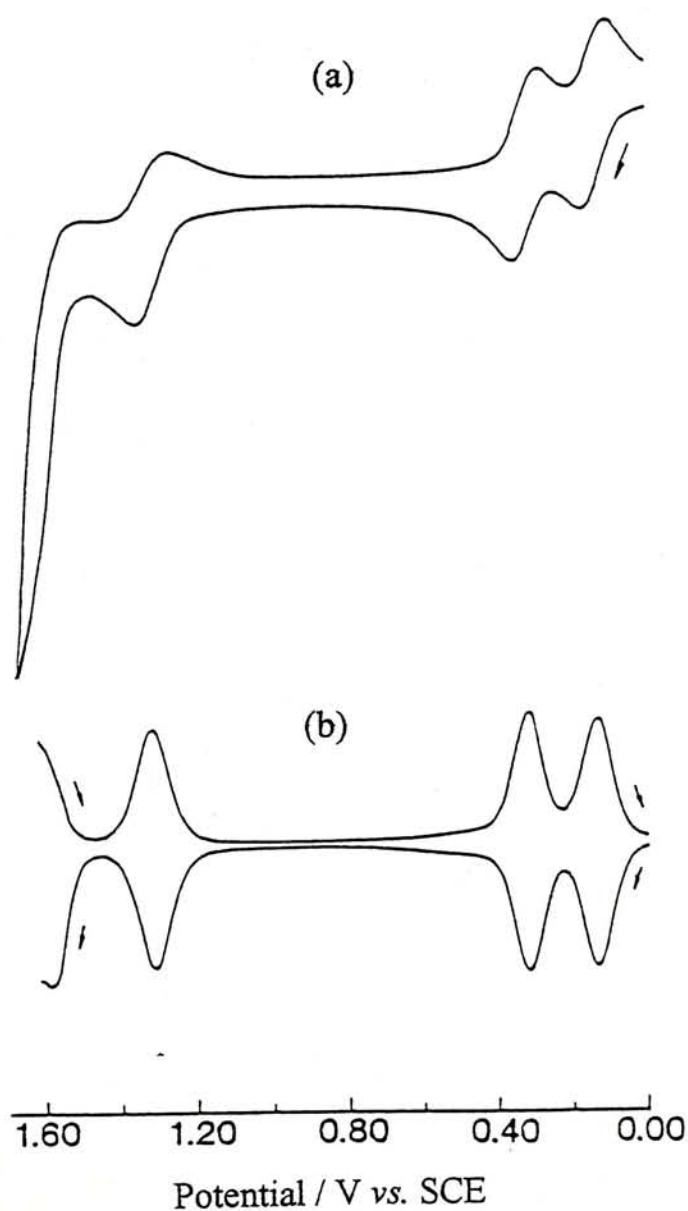
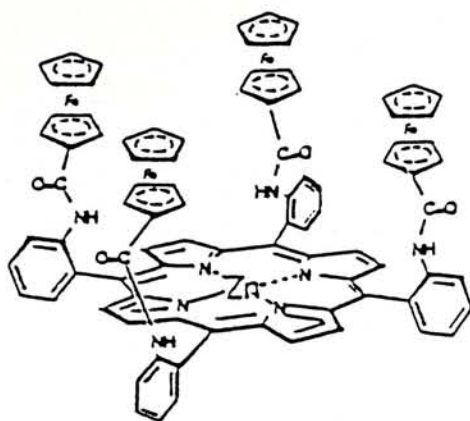


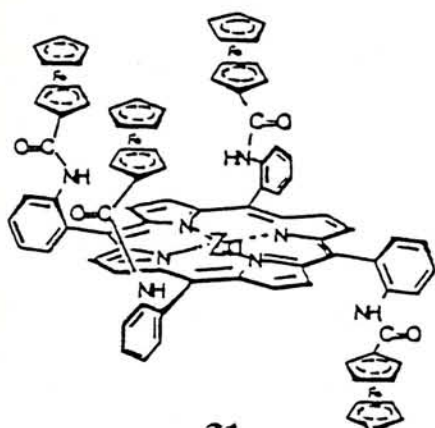
**Figure 13.** (a) Cyclic voltammogram ( $\nu = 100 \text{ mV s}^{-1}$ ) and (b) differential pulse voltammogram ( $\nu = 400 \text{ mV s}^{-1}$ ) of **29** (1.4 mM) in  $\text{CH}_2\text{Cl}_2$  solution containing 0.1 M  $[\text{NBu}_4][\text{ClO}_4]$ .



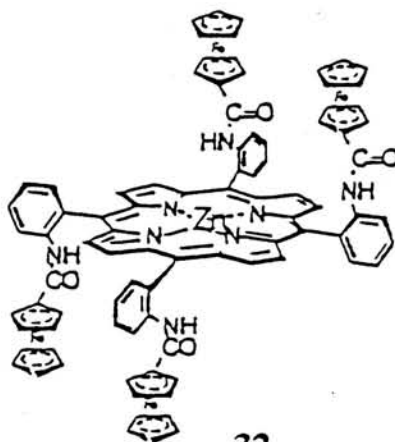
The metalloporphyrin receptors **30** - **33** have been described by Beer et al<sup>32</sup> which are able to sense anions selectively. Compounds **30** - **33** are atropisomers formed by condensation reactions of ferrocene carbonyl chloride and the appropriate 5,10,15,20-tetrakis(2-aminophenyl)porphyrin atropisomers, which can be prepared by the established procedure.<sup>33</sup> All these compounds exhibit a single two-electron porphyrin-based oxidation wave in the range of 0.67 to 0.71 V and two one-electron porphyrin-based reduction waves in -1.08 to -1.37 V and -1.49 to -1.79 V (Table 4). For compounds **30**, **32** and **33**, the four ferrocenyl units exhibit a single four-electron oxidation wave, indicating that these redox sites are electrochemically equivalent and undergo independent one-electron transfer at the same potential. However, compound **31** shows two oxidation waves (Figure 14) for the ferrocenyl units with a peak-current ratio of 3 : 1 which suggests that one of the ferrocene amide groups is electrochemically inequivalent with the other three ferrocenyl units.



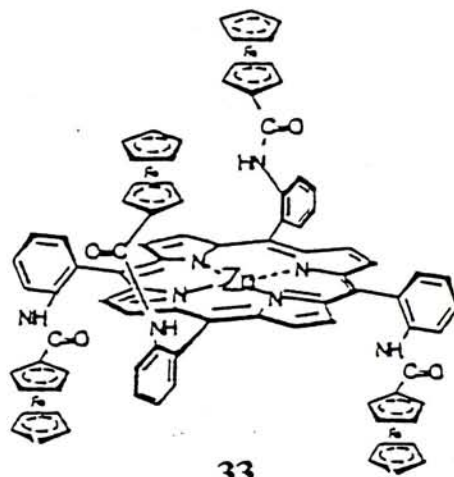
30



31



32



33

Compound	$E^0$ (V) Porphyrin	$E^0$ (V) Ferrocene	$E^0$ (V) Porphyrin	$E^0$ (V) Porphyrin
	oxidation	oxidation	reduction (1)	reduction (2)
30	0.71 (2 e)	0.43 (4 e)	-1.26	-1.68
31	0.69 (2 e)	0.48 (3 e), 0.43 (1 e)	-1.08	-1.49
32	0.67 (2 e)	0.43 (4 e)	-1.37	-1.78
33	0.71 (2 e)	0.44 (4 e)	-1.18	-1.79

Table 4. Electrochemical data (vs.  $\text{Ag}/\text{Ag}^+$ ) of 30 – 33 (0.5 mM) in  $\text{CH}_2\text{Cl}_2/\text{MeCN}$  (v/v 3 : 2) containing 0.2 M  $[\text{NBu}_4][\text{BF}_4]$ .

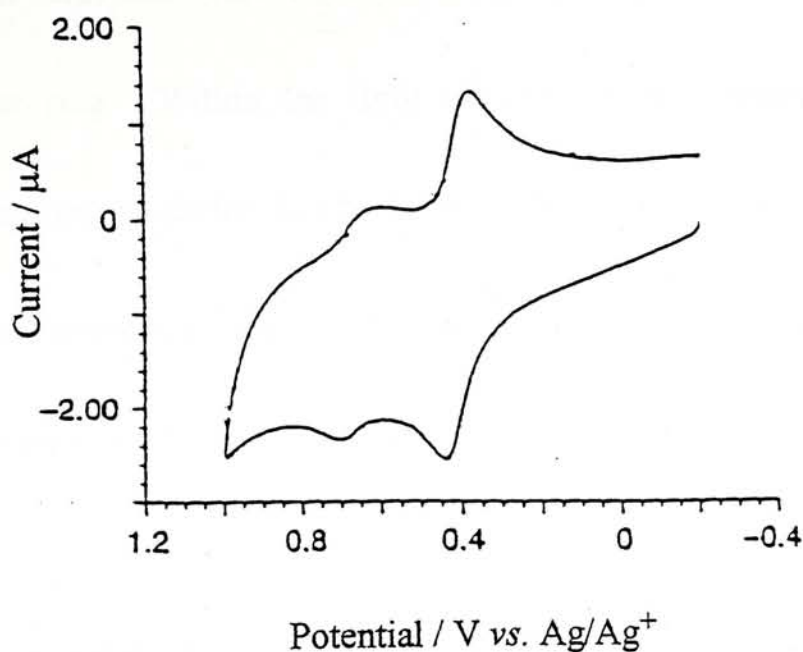


**Figure 14.** Cyclic voltammogram of **31** (0.5 mM) in  $\text{CH}_2\text{Cl}_2/\text{MeCN}$  (v/v 3 : 2) containing 0.2 M  $[\text{NBu}_4][\text{BF}_4]$ .

### 1.3.2 Ferrocene-containing Porphyrazines

The first ferrocene-containing porphyrazine was prepared by Hoffman et al. in 1994.<sup>34</sup> Mixed condensation of 1,2-dicyanobenzene (**34**) with dithiomaleonitrile derivative **35** in the presence of  $\text{Mg}(\text{OBu})_2$  and BuOH gives the unsymmetrical porphyrazine **36**, which undergoes demetalation with trifluoroacetic acid to give compound **37**. Reductive debenzoylation with sodium in liquid ammonia produces the norphthalocyanine dithiolate, which is then capped *in situ* with [1,1'-bis(diphenylphosphino)ferrocene]palladium(II) dichloride to afford the solitary porphyrazine **38** (Scheme 1). This macrocycle exhibits two reversible one-electron



reductions at  $-1.27$  and  $-1.51$  V (vs.  $\text{Fc}^+/\text{Fc}$ ), which are attributed to reductions of the porphyrazine ring. Within the limit of  $+150$  V as determined by the solvent ( $\text{CH}_2\text{Cl}_2$ ), no ring oxidation can be observed but a reversible one-electron couple at  $0.18$  V and an irreversible wave at  $0.63$  mV appear which are due to the  $\text{Fe(II/III)}$  and  $\text{Pd(II/III)}$  oxidation respectively.

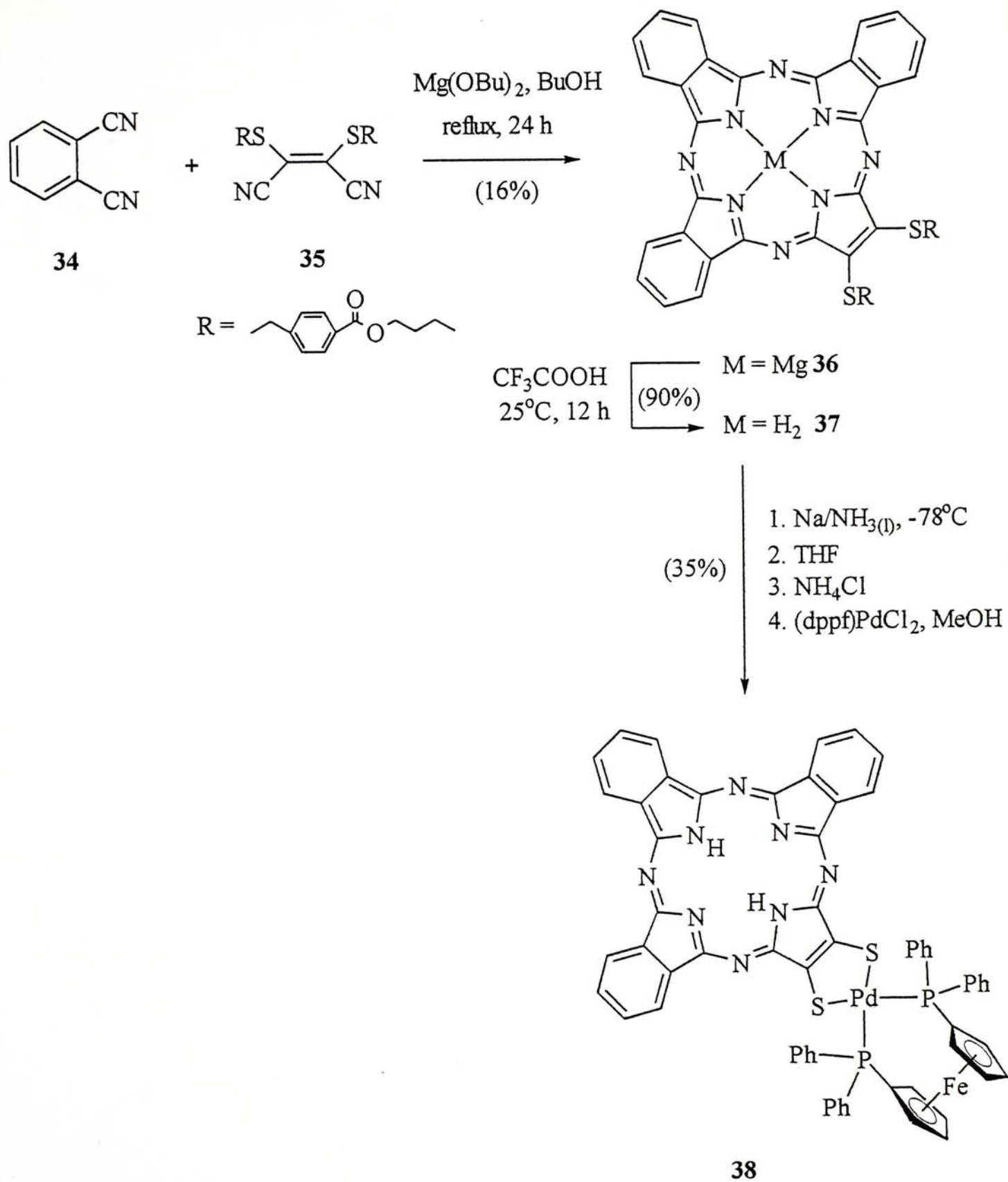
### 1.3.3 *Ferrocene-containing Phthalocyanines*

The tetraferrocenyl phthalocyanine **42** was prepared by Leznoff et al. using the method shown in Scheme 2.<sup>35</sup> Treatment of the ferrocenium chloride (**39**) with 4-diazoniumphthalonitrile bisulfate (**40**) gives the dinitrile **41**, which undergoes base-promoted cyclization to give **42**.

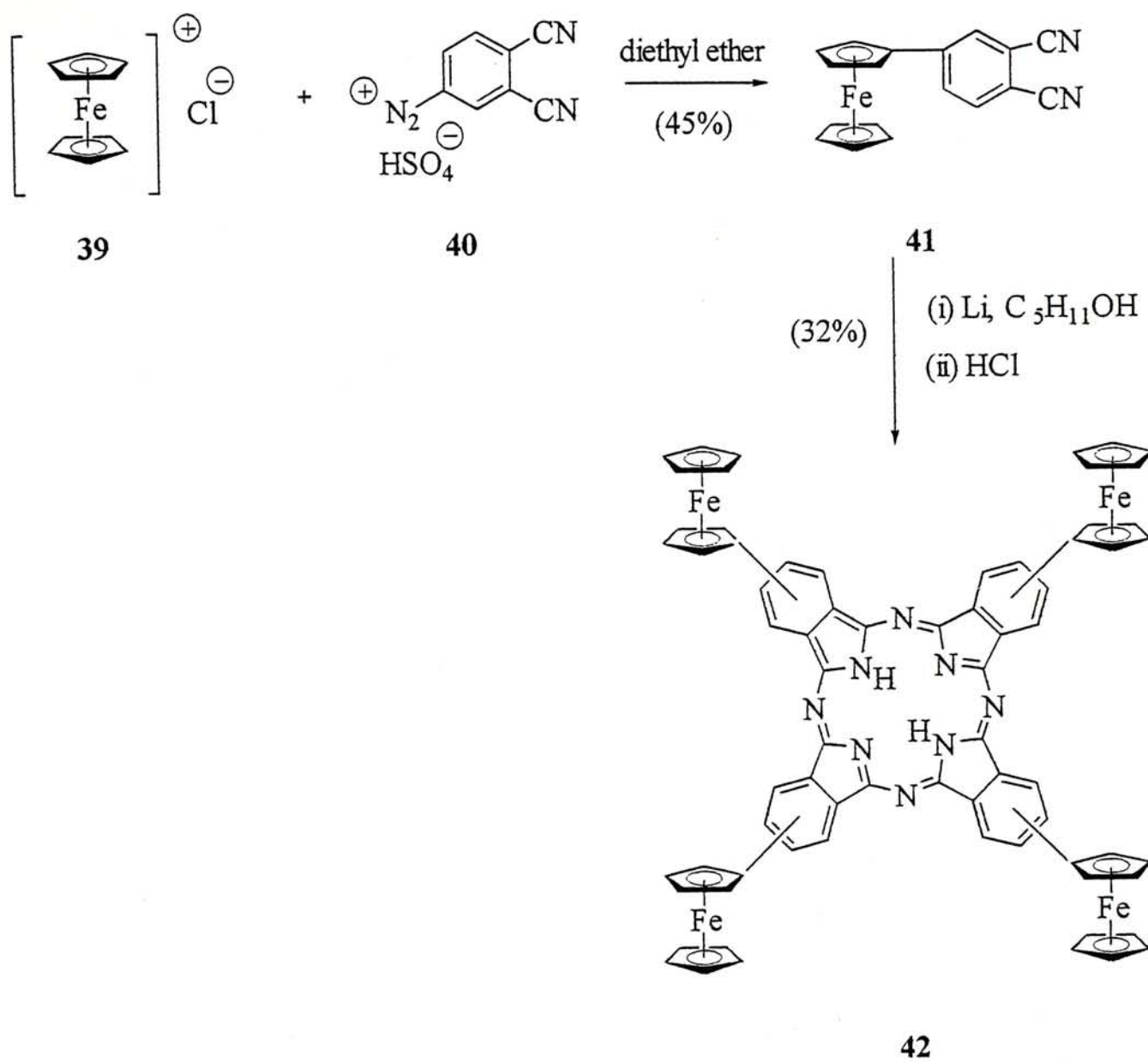
Figures 15 (a) and (b) show the cyclic and differential pulse voltammograms of **42**, respectively. Similarly, only one ferrocenyl couple is observed at  $0.52$  V, indicating that the four ferrocenyl units are electrochemically independent to each other. Compound **42** also exhibits two reversible reductions at  $-1.14$  and  $-0.79$  V and two oxidations at  $1.05$  and  $1.12$  V, all are attributed to the phthalocyanine ring. The ferrocenyl cathodic peak has a much higher current which indicates an adsorption phenomenon on the working electrode.



Scheme 1



Scheme 2



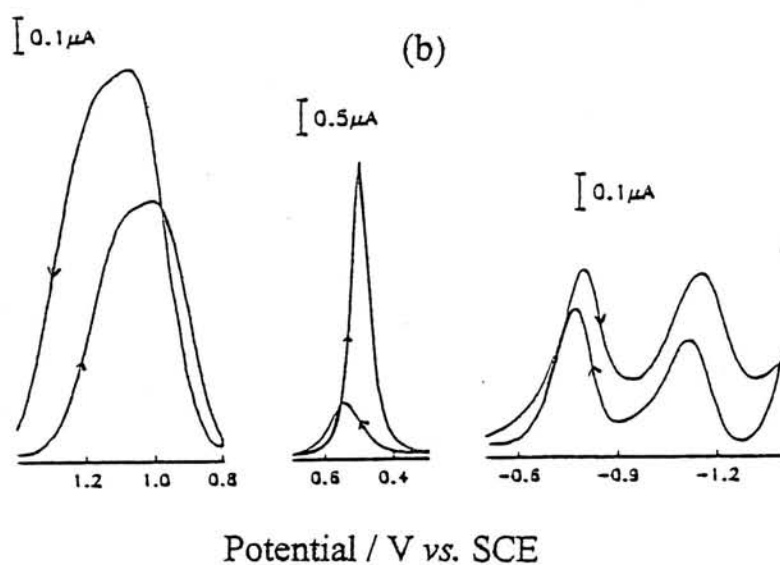
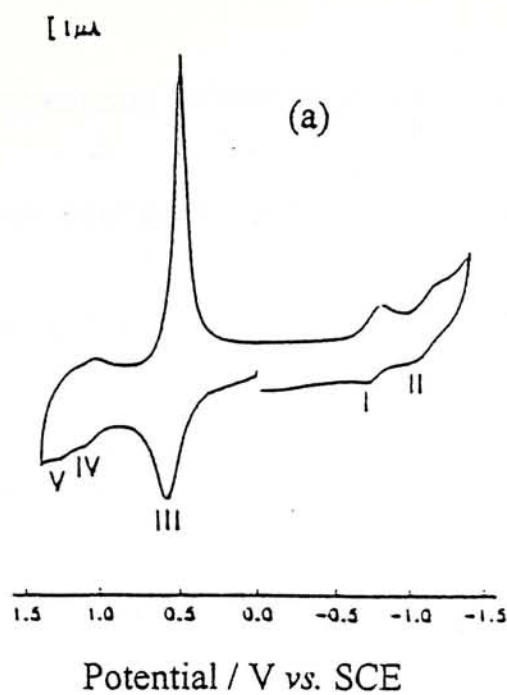
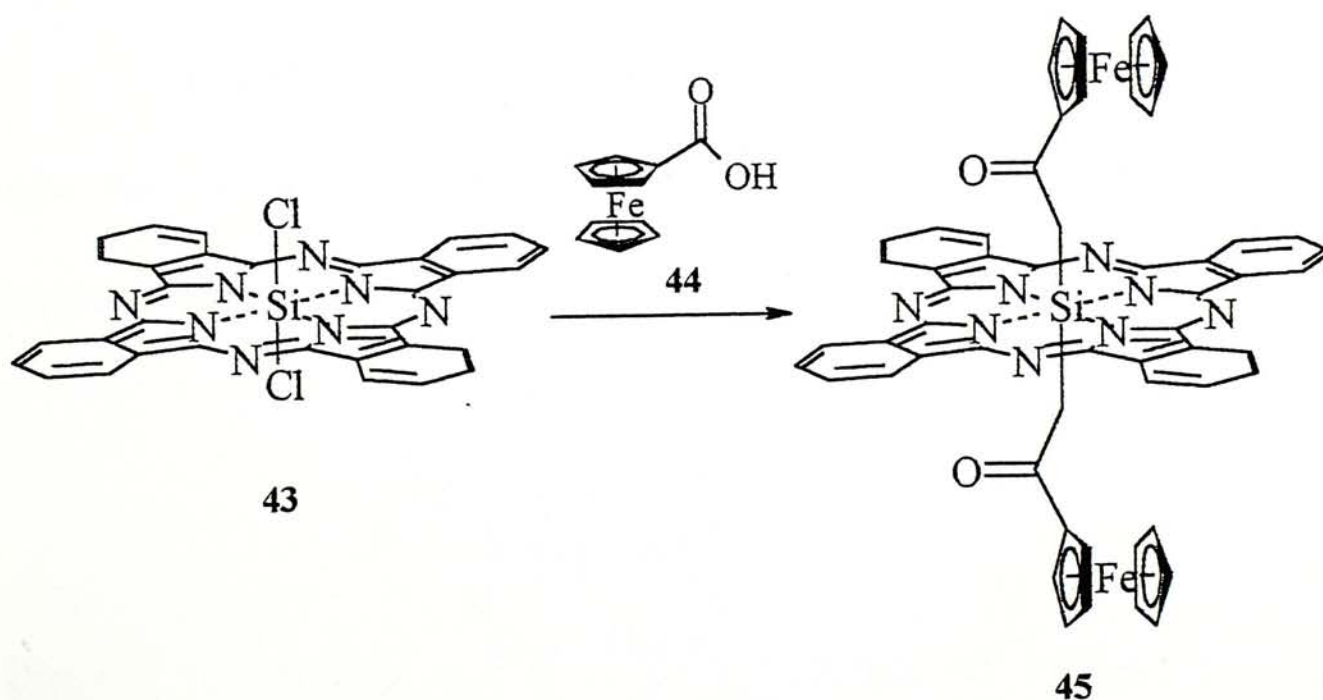


**Figure 15.** (a) Cyclic voltammogram ( $\nu = 200 \text{ mV s}^{-1}$ ) and (b) differential pulse voltammogram ( $\nu = 5 \text{ mV s}^{-1}$ ) of **42** (0.05 mM) in  $\text{CH}_2\text{Cl}_2$  containing 0.1 M  $[\text{NBu}_4][\text{PF}_6]$ .

Phthalocyanines containing ferrocenyl moieties as axial ligands have also been reported.<sup>36</sup> The silicon diferrocenyl phthalocyanine **45** has been prepared by treating dichloro(phthalocyaninato)silicon(IV) (**43**) with ferrocenecarboxylic acid (**44**) (Scheme 3). The cyclic voltammogram of **45** shows one oxidation couple at 1.23 V and two reduction couples at -0.55 and -1.02 V, all of which are due to the phthalocyanine ring. The ferrocenyl oxidation couple appears at 0.69 V with no observable splitting, indicating the absence of electronic interaction between the ferrocenyl moieties.

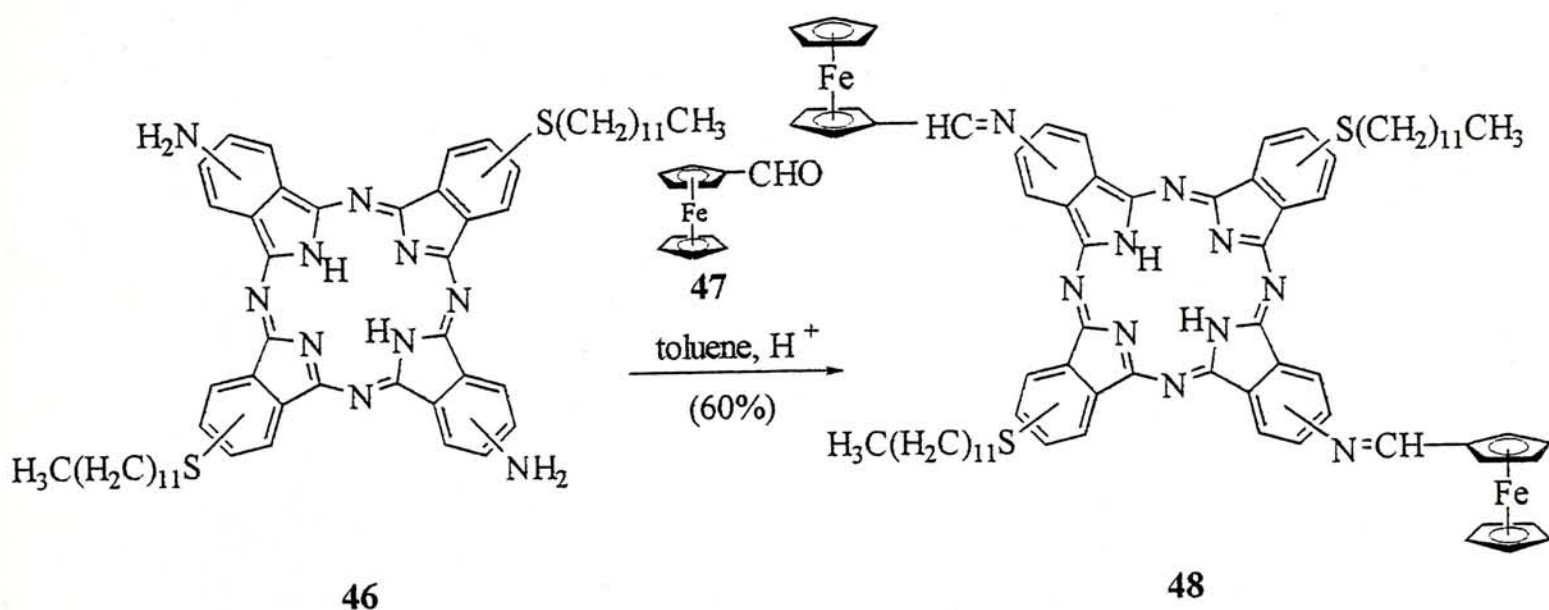
**Scheme 3**



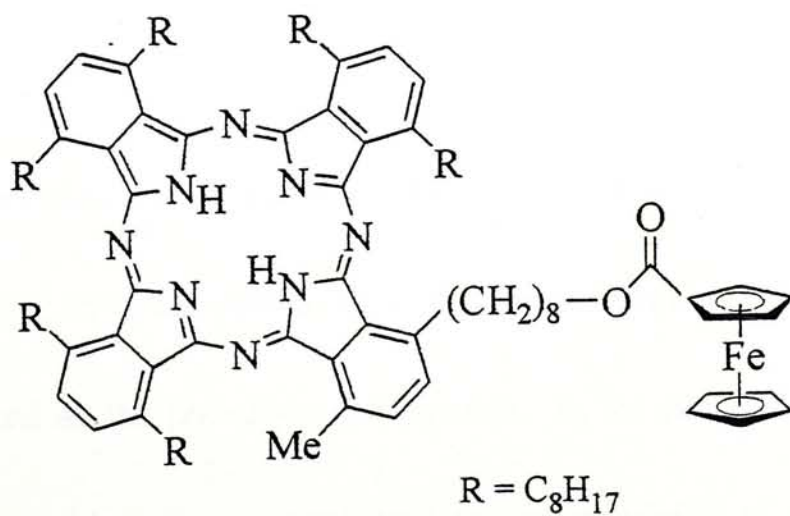


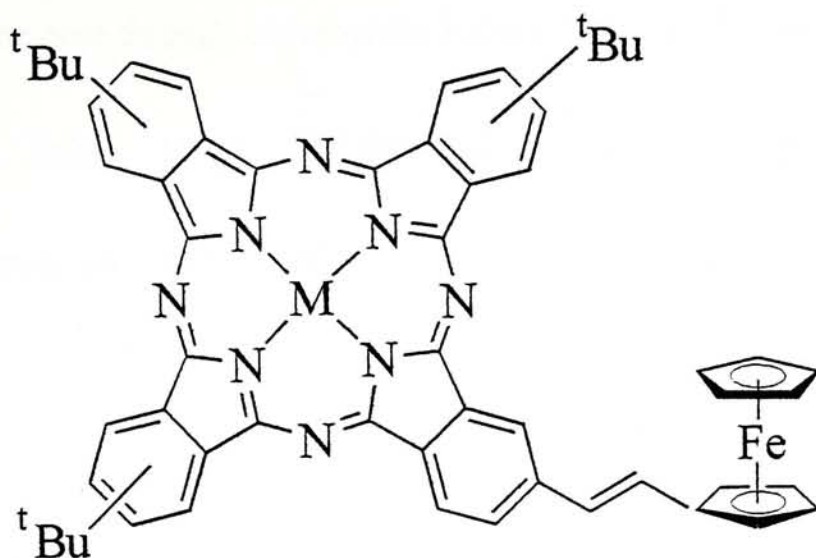
The bis(ferrocenyl)phthalocyanine **48** has also been prepared by heating **46** with ferrocenecarboxaldehyde (**47**) using a catalytic amount of acid (Scheme 4).<sup>37</sup> The electrical conductivity of **48** has been briefly examined but no electrochemical data have been given.

**Scheme 4**

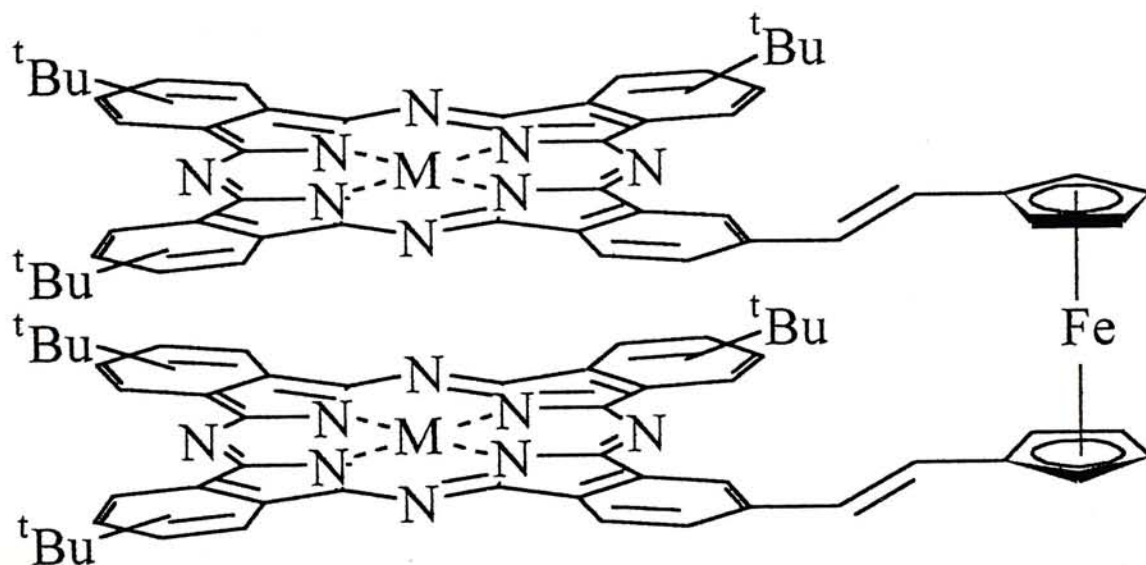


Apart from the above phthalocyanines containing more than one ferrocenyl units, there are several monoferrocene-phthalocyanine conjugates appearing in literatures which are given below.<sup>38,39</sup>





M = Zn, Co



M = Zn, Co

This thesis describes the preparation, spectroscopic, and electrochemical studies of two series of ferrocene-containing tetrapyrrole derivatives. Special emphasis has been placed on the phthalocyanine system. In the first series, four, eight, and sixteen ferrocenyl units are connected to the periphery of a Zn(II)

phthalocyanine core through oxyethylene linkers.<sup>40</sup> In another series, the ferrocenyl groups are linked to a 5,15-diphenylporphyrin, phthalocyanine, or 2,3-naphthalocyanine core through ethynyl moieties. The findings are described in the following section.

## 2. RESULTS AND DISCUSSION

### 2.1 Ferrocenylphthalocyanines with Oxyethylene Linkers

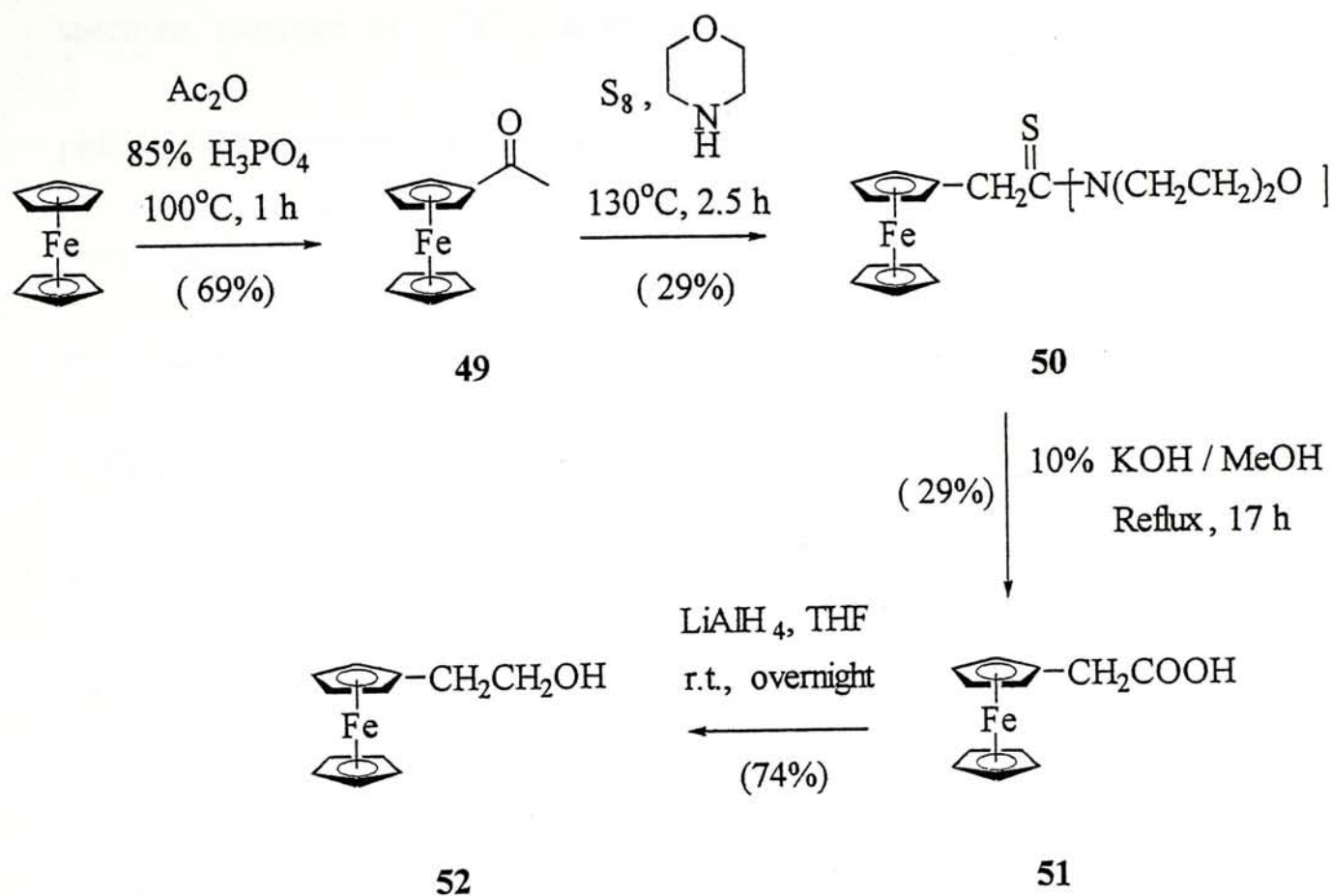
#### 2.1.1 Synthesis and Characterization

##### 2.1.1.1 Preparation of Tetrakis(2-ferrocenylethoxy)phthalocyaninatozinc(II) (55)

The preparation of this tetraferrocenyl macrocycle involves 2-ferrocenylethanol (**52**) as the starting material, which was prepared by the literature method with minor modification (Scheme 5).<sup>41</sup> Ferrocene was treated with acetic anhydride in 85% phosphoric acid to generate the acetylferrocene (**49**). Subsequent treatment of **49** with sulfur and morpholine gave the thioamide **50**, which was converted to **51** by the action of 10% KOH in MeOH. Reduction of **51** by  $\text{LiAlH}_4$  led to the formation of 2-ferrocenylethanol (**52**).



Scheme 5

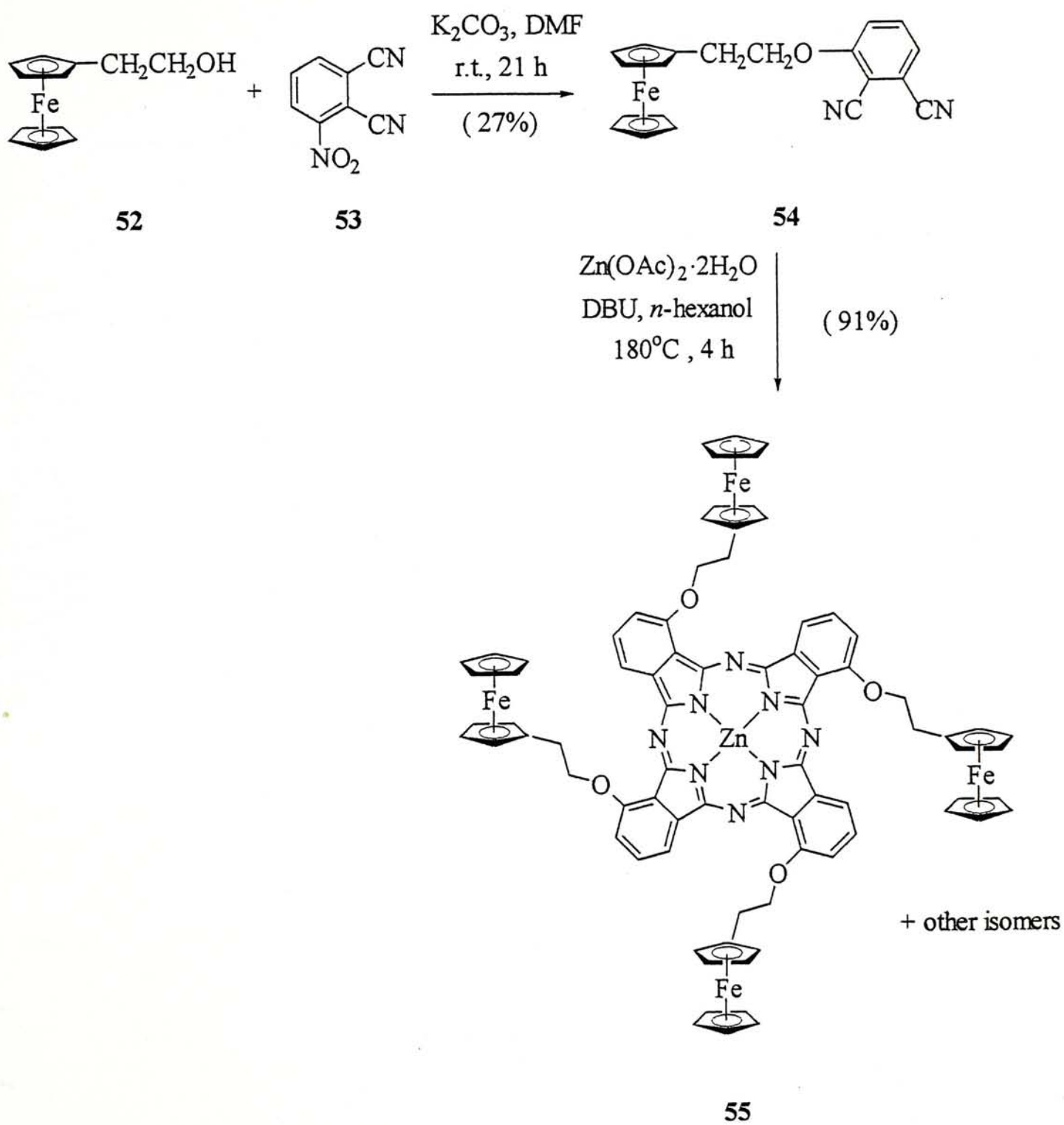


Treatment of **52** with 3-nitrophthalonitrile (**53**) and potassium carbonate in DMF afforded the dinitrile **54**. Cyclization of this precursor in the presence of 1,8-diazabicyclo[5.4.0]undec-7-ene (DBU) and  $\text{Zn}(\text{OAc})_2 \cdot 2\text{H}_2\text{O}$  in *n*-hexanol gave the tetrakis(2-ferrocenylethoxy)phthalocyaninatozinc(II) (**55**) as a mixture of constitutional isomers (Scheme 6). In an attempt to prepare a single 1,8,15,22-tetrasubstituted isomer, **54** was treated with lithium in *n*-octanol at lower temperature ( $70^\circ\text{C}$ ).<sup>42</sup> After acidification with acetic acid, a deep green solid was obtained of which the UV-Vis spectrum showed characteristic pattern for metal-free

phthalocyanines [ $\lambda_{\text{max}}$  ( $\text{CHCl}_3$ ): 320, 356, 629, 695, 730 nm]. Its  $^1\text{H}$  NMR spectrum recorded in  $\text{CDCl}_3$ , however, exhibited complex multiples for the phthalocyanine ring protons indicating that a mixture of isomers was produced. It is worth noting that, under similar reaction conditions, a single isomers could be obtained for phthalocyanines containing substituents such as  $-\text{OCH}_2\text{C}_6\text{H}_4\text{Bu}$ ,  $-\text{OCH}_2^t\text{Bu}$ ,  $-\text{OMe}$ , and  $-\text{OCH}_2\text{Et}$  at the 1,8,15,22-positions.<sup>42,43</sup> It appears that the steric as well as the electronic nature of the substituent is crucial in the formation of single isomer in the cyclization of 3-substituted phthalonitriles.<sup>42b,44</sup>

The  $^1\text{H}$  NMR spectrum of **55** in  $\text{CDCl}_3$  is shown in Figure 16, which confirms the existence of a mixture of constitutional isomers. The several downfield broad bands at  $\delta$  6.9-8.9 are assignable to the aromatic ring protons. The broad signals at  $\delta$  4.6-4.9 and  $\delta$  2.8-3.5 are due to the  $-\text{OCH}_2$  and  $-\text{CH}_2\text{Fc}$  protons, respectively. The relatively sharp multiplets at  $\delta$  4.1-4.4 are attributed to the ferrocenyl protons. The formation of this compound was also confirmed by MALDI-TOF mass spectrometry. The spectrum showed an isotopic cluster peaking at  $m/z$  1490.2, which could be assigned to the molecular ion of **55**.

Scheme 6



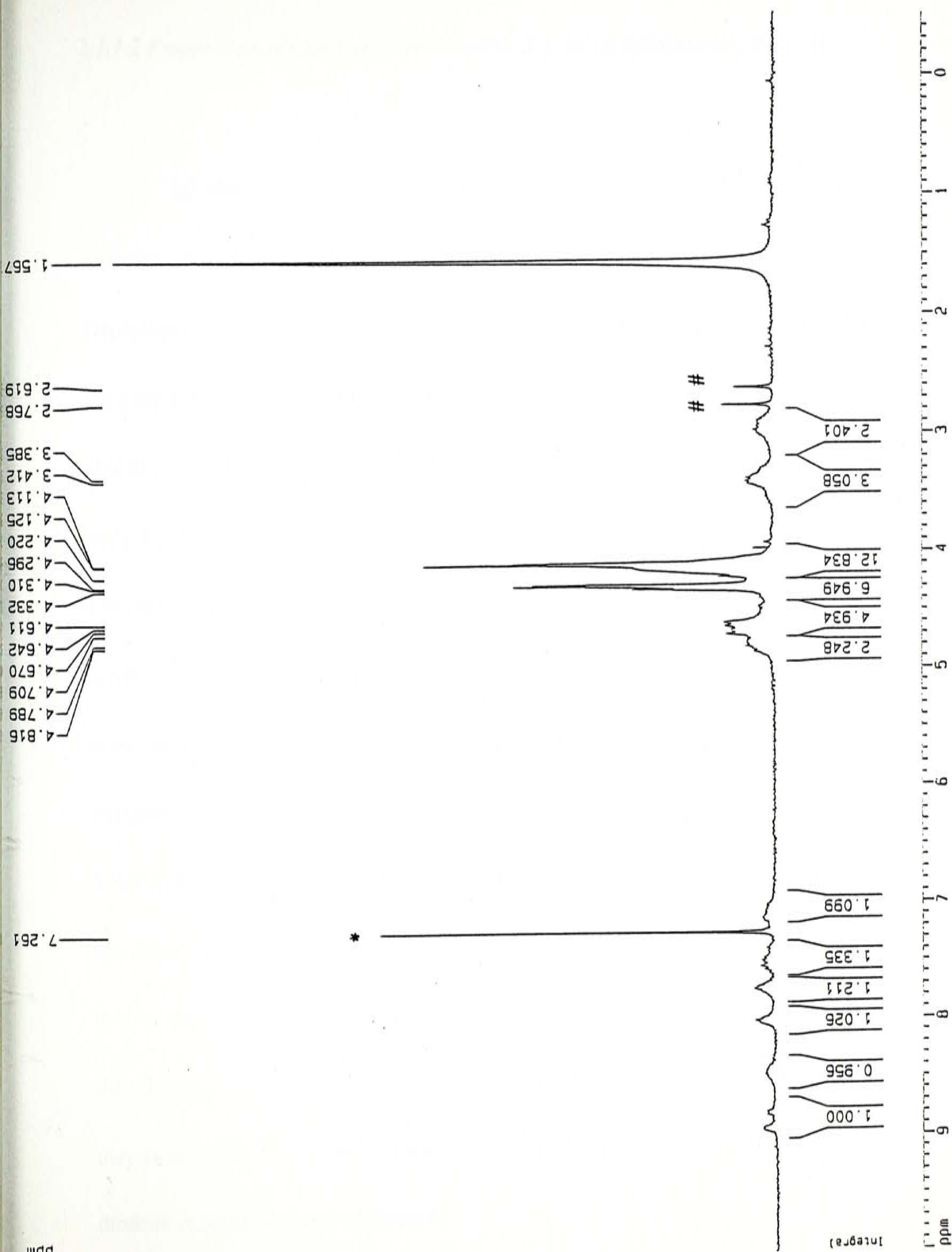


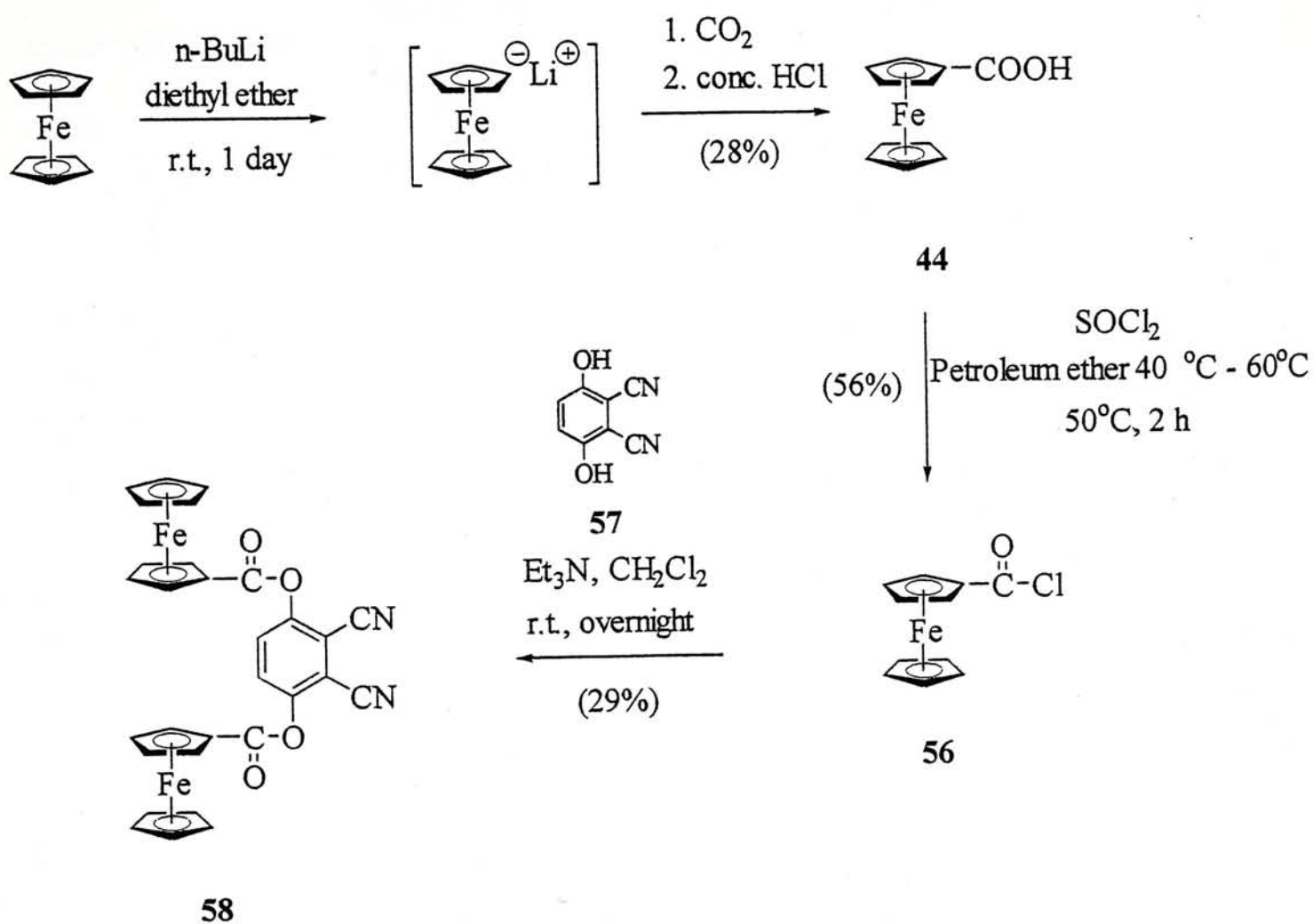
Figure 16.  $^1\text{H}$  NMR spectrum of **55** in  $\text{CDCl}_3$ ; \* indicates solvent peak; # indicates impurities.



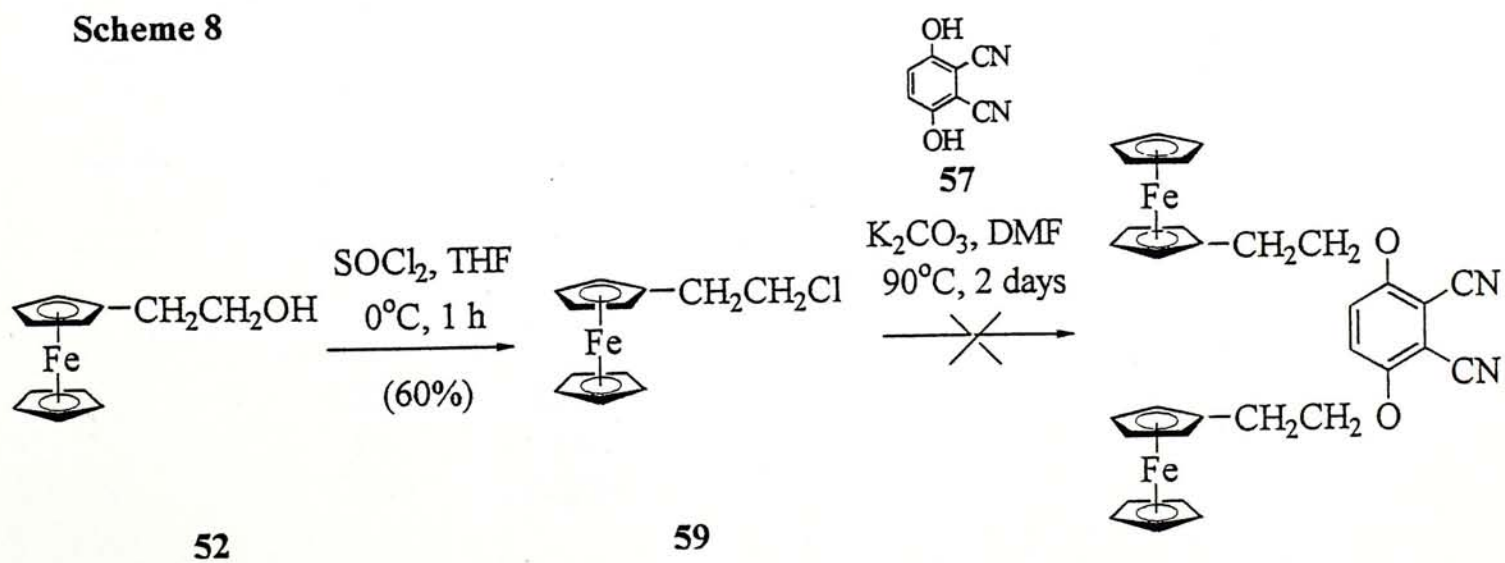
### 2.1.1.2 Preparation of Octakis(2-ferrocenylethoxy)phthalocyaninatozinc(II) (62)

In attempts to prepare octaferrocenylphthalocyanines linked with ester moieties, the dinitrile **58** was prepared by the method shown in Scheme 7. Deprotonation of ferrocene with *n*-butyllithium followed by carbonylation with dry ice gave the ferrocenecarboxylic acid (**44**) which was then chlorinated with thionyl chloride to generate ferrocenecarbonyl chloride (**56**).<sup>45</sup> Treatment of compound **56** with 2,3-dicyanohydroquinone (**57**) under alkaline conditions gave the dinitrile **58**. Unfortunately, attempts to cyclize this compound with  $\text{Zn}(\text{OAc})_2 \cdot 2\text{H}_2\text{O}$  and DBU in *n*-pentanol were not successful. This might be due to the alkaline hydrolysis of the ester groups. Cyclization was also performed in quinoline, but again no phthalocyanine could be obtained. To avoid hydrolysis of the ester groups, 1-chloro-2-ferrocenylethane (**59**), which was prepared by chlorination of **52**,<sup>46</sup> was treated with 2,3-dicyanohydroquinone (**57**) under alkaline conditions (Scheme 8). However, the desired dinitrile **60** could not be obtained which might be due to the low reactivity of the chloride. Thus, 2-ferrocenylethyl tosylate (**61**), which was obtained by the tosylation of **52**,<sup>46</sup> was used instead in the substitution reaction giving the desired dinitrile in moderate yield (Scheme 9).

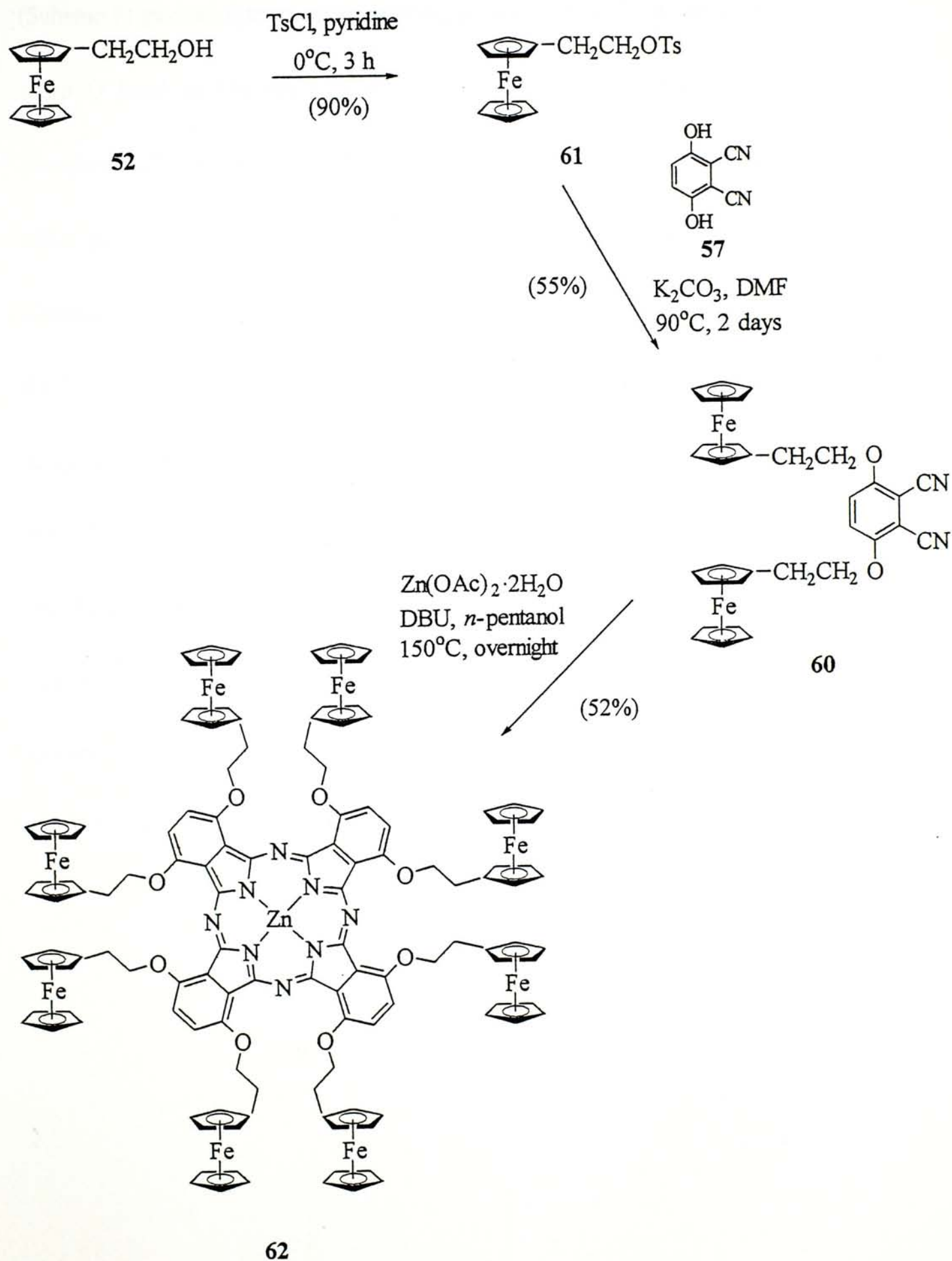
Scheme 7



Scheme 8



Scheme 9



Treatment of **60** with  $\text{Zn}(\text{OAc})_2 \cdot 2\text{H}_2\text{O}$  and DBU in *n*-pentanol at 150°C (Scheme 9) gave an intense green mixture, of which the UV-Vis spectrum showed a sharp Q band at 736 nm indicating the formation of a metallophthalocyanine. Compound **62** was unstable and turned yellow during chromatographic purification in silica gel. However, the compound could be purified by chromatography on basic alumina columns using chloroform and THF (v/v 5 : 1) as eluent. Figure 17 displays the  $^1\text{H}$  NMR spectrum of **62** in  $\text{C}_6\text{D}_6$ , which shows a broad downfield signal at  $\delta$  7.59 assignable to the eight equivalent aromatic protons, broad signals at  $\delta$  5.15 and 3.38 assignable to the  $-\text{OCH}_2$  and  $\text{FcCH}_2$ -protons, sharp singlets at  $\delta$  4.40 and 4.03 which are due to the substituted ferrocenyl Cp ring and a sharp singlet at  $\delta$  4.15 assignable to the unsubstituted ferrocenyl Cp ring. The MALDI-TOF mass spectrum of **62** showed the molecular ion peaks as an isotopic cluster peaking at  $m/z$  2404.6 with predicted isotopic pattern (Figure 18).



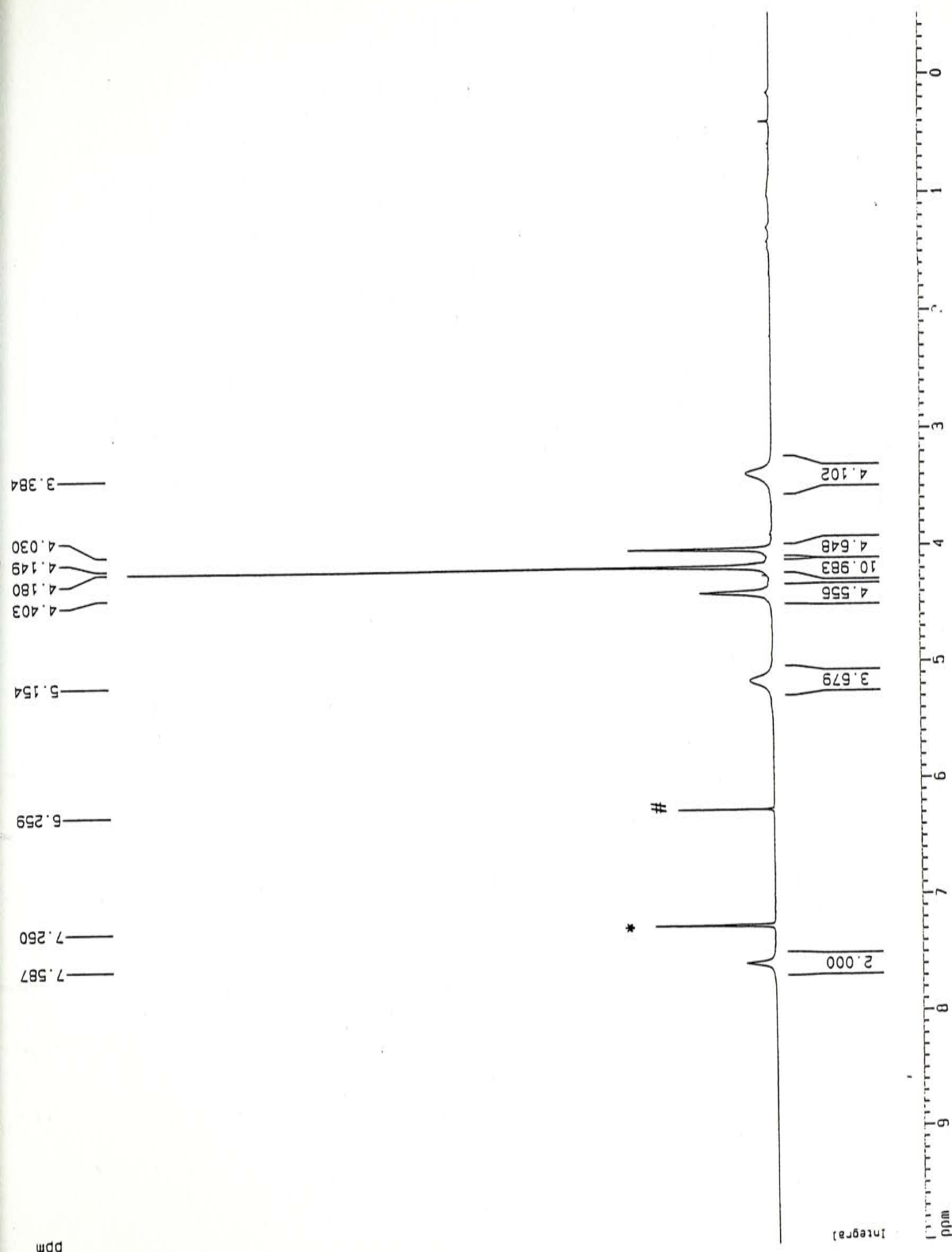
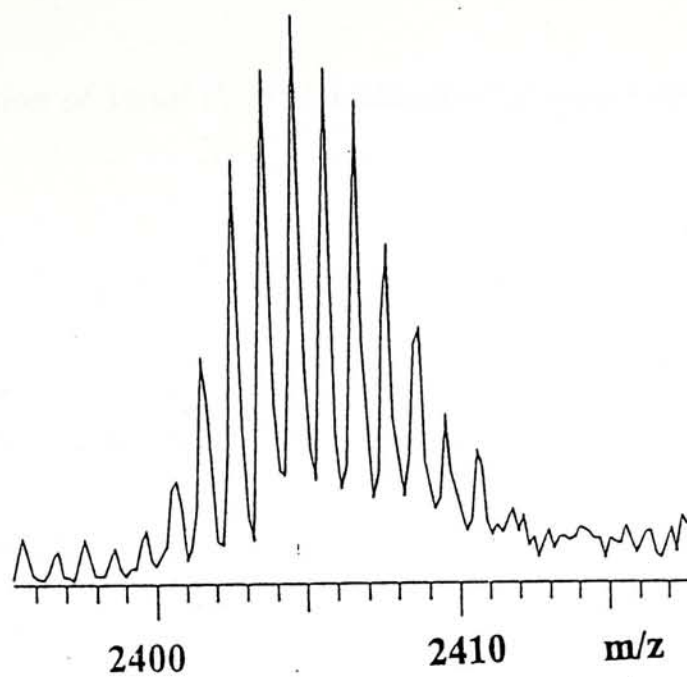
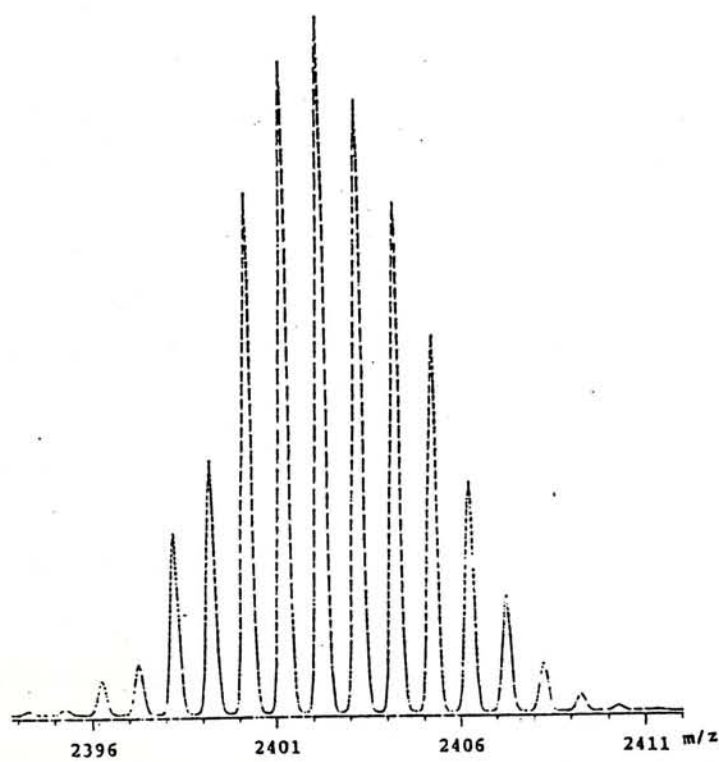


Figure 17.  $^1\text{H}$  NMR spectrum of 62 in  $\text{C}_6\text{D}_6$ ; \* indicates solvent peak; # indicates impurity peak.



(a)



(b)

**Figure 18.** (a) Experimental and (b) simulated pattern for the molecular ion of 62.

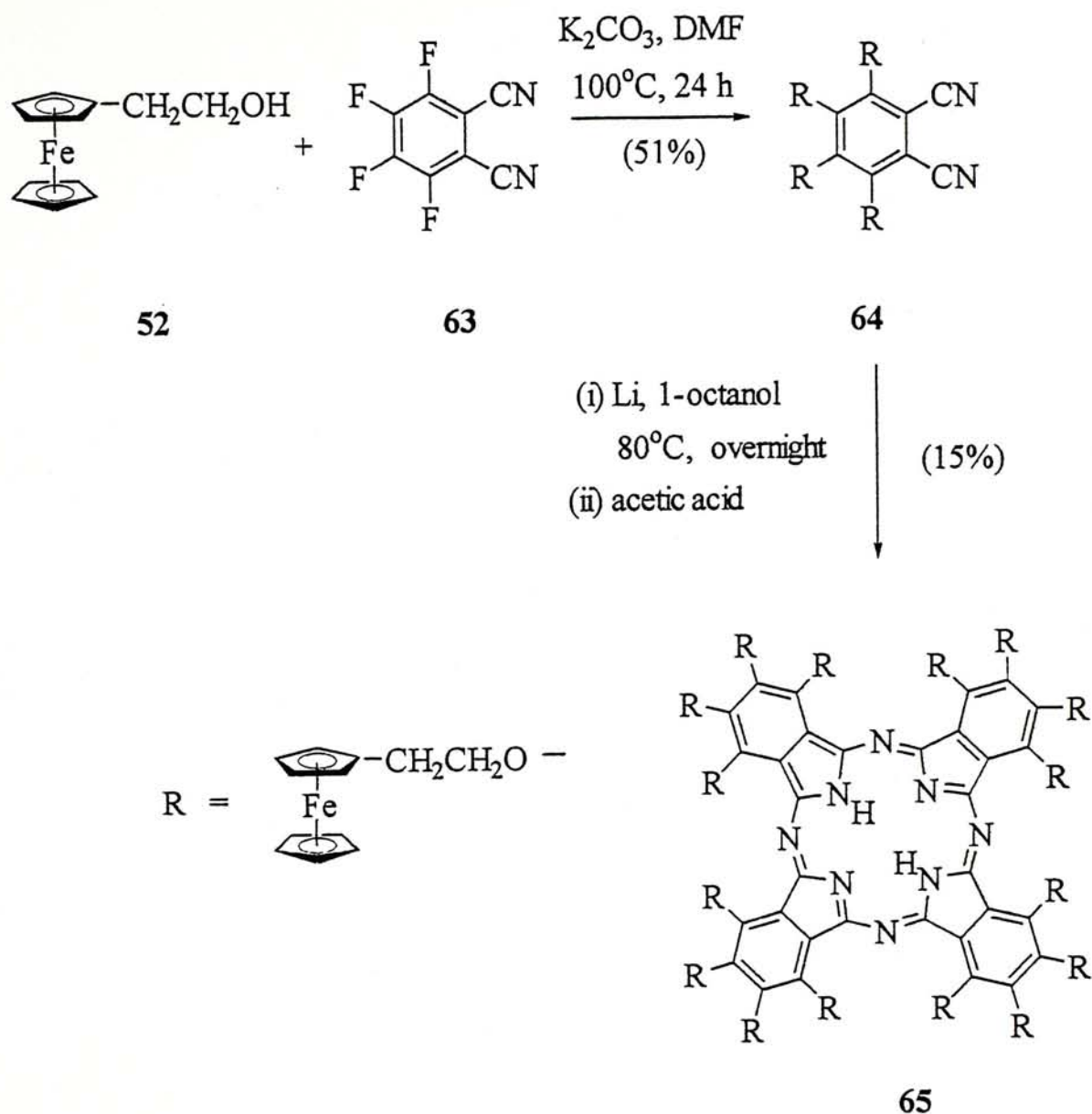
### 2.1.1.3 Preparation of Metal Free Hexadecakis(2-ferrocenylethoxy)phthalocyanine

(65)

The tetraferrocenyl dinitrile **64** was prepared using tetrafluorophthalonitrile (**63**) and 2-ferrocenylethanol (**52**) as the starting materials (Scheme 10).<sup>47</sup> Substitution occurred in the presence of  $K_2CO_3$  giving **64** in moderate yield. Attempts to prepare the corresponding zinc phthalocyanine using the above procedure were not successful. Cyclization of **64** in *N,N*-dimethylaminoethanol was also performed, but the reaction also did not lead to the formation of the expected phthalocyanine. The metal-free hexadecakis(2-ferrocenylethoxy)phthalocyanine (**65**), however, could be prepared in 15% yield using lithium in *n*-octanol followed by acid treatment. The reaction temperature was critical in the preparation of **65** and should be controlled at ca. 120-130°C. Higher reaction temperatures would lead to the formation of black mixtures with no indication of the presence of **65**.

As expected, the  $^1H$  NMR spectrum of **65** in  $CDCl_3$  (Figure 19) does not show downfield aromatic signals. Several broad bands at ca.  $\delta$  3-5 appear which can be ascribed to the methylene and ferrocenyl protons. The MALDI-TOF mass spectrum of **65** showed an isotopic cluster peaking at  $m/z$  4168.6, which could be assigned to the molecular ion of **65**.

# Scheme 10



In attempts to prepare ferrocenyl phthalocyanines with shorter linkers, the ferrocenylmethanol (**66**) was prepared by formylation of ferrocene followed by reduction (Scheme 11).<sup>48</sup> Treatment of **66** with 3-nitrophthalonitrile (**53**) or tetrafluorophthalonitrile (**63**) however did not result in the formation of the desired phthalocyanine precursors.



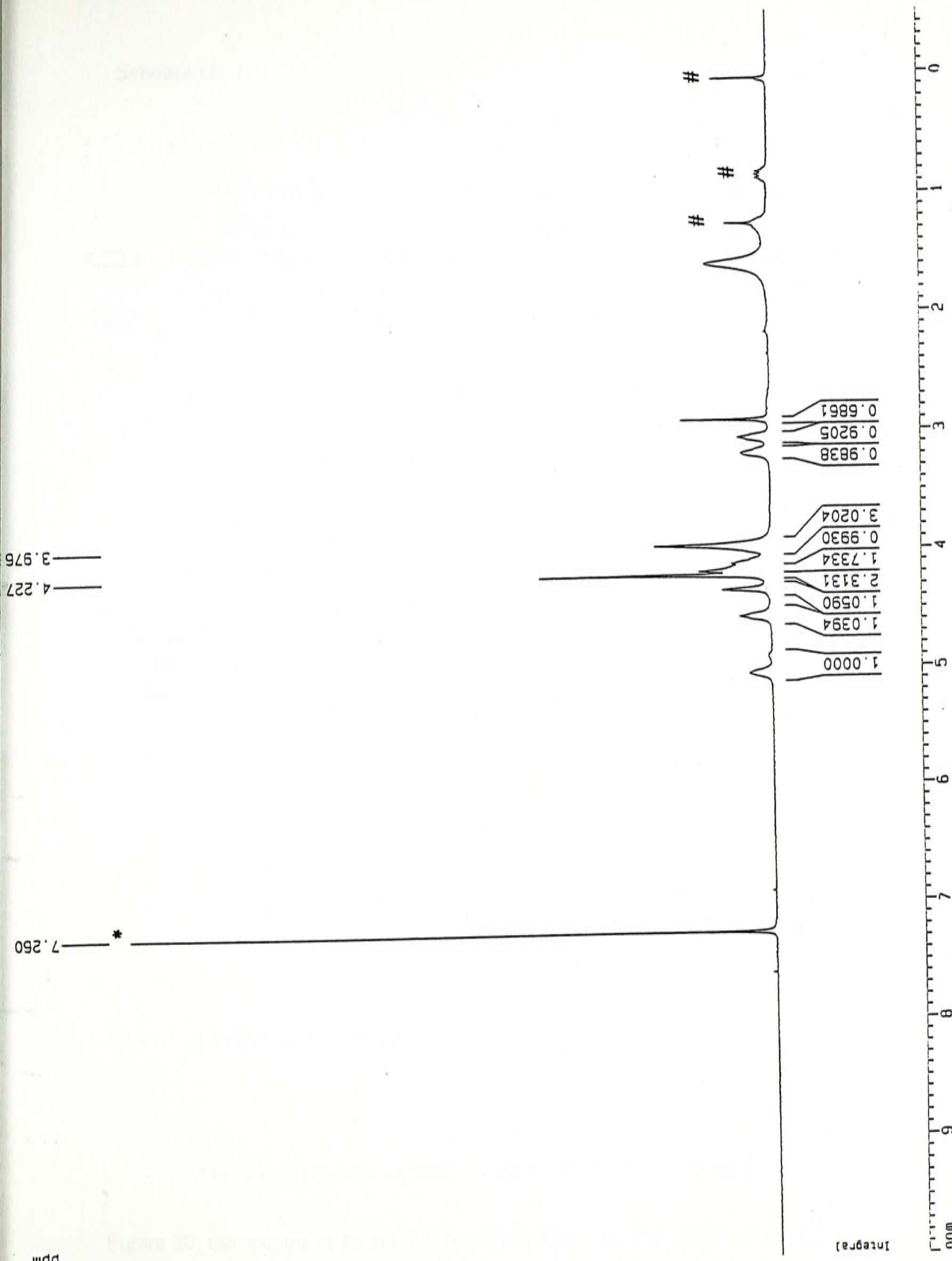
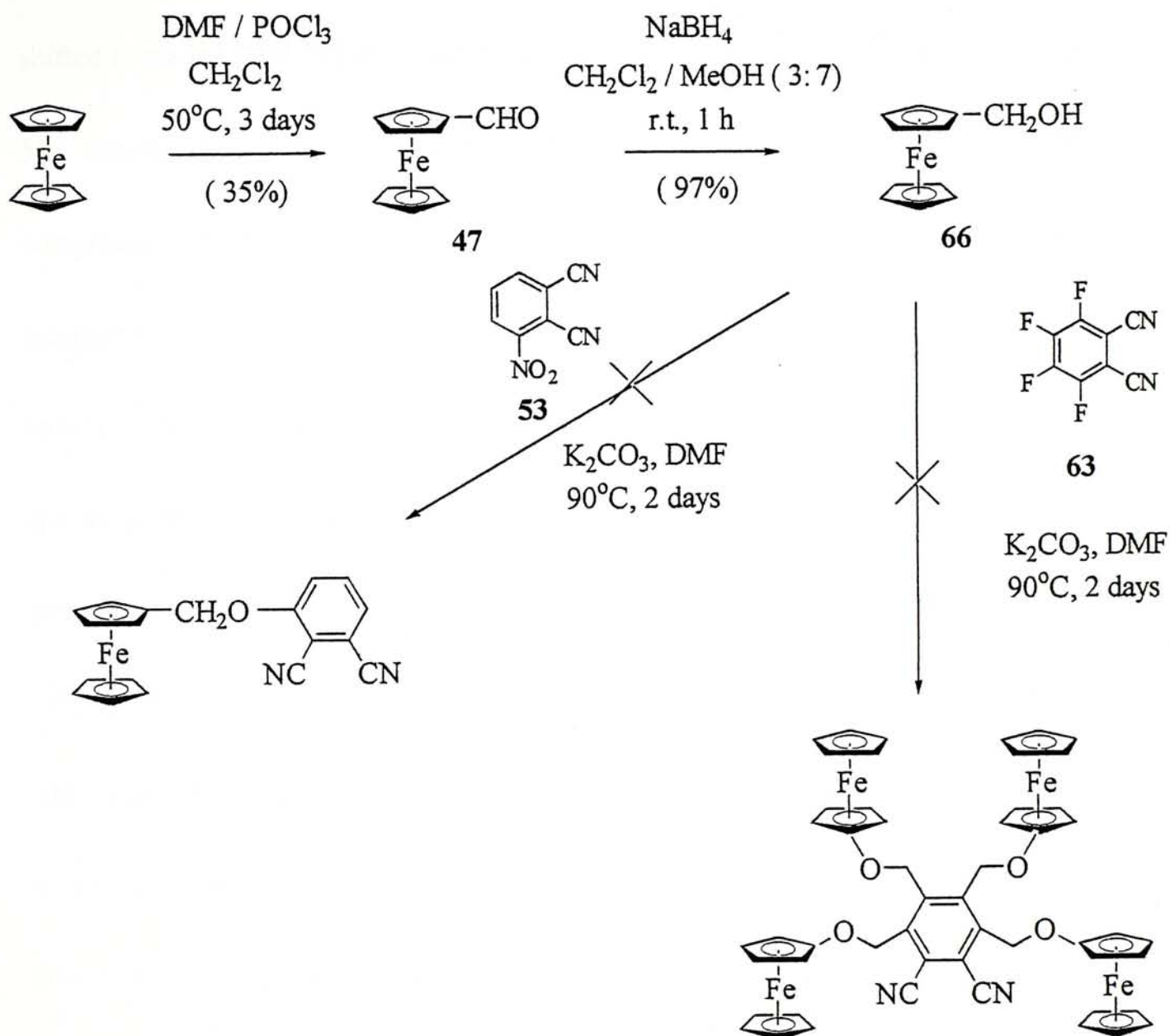


Figure 19.  $^1\text{H}$  NMR spectrum of 65 in  $\text{CDCl}_3$ ; \* indicates solvent peak; # indicates impurities.

## Scheme 11



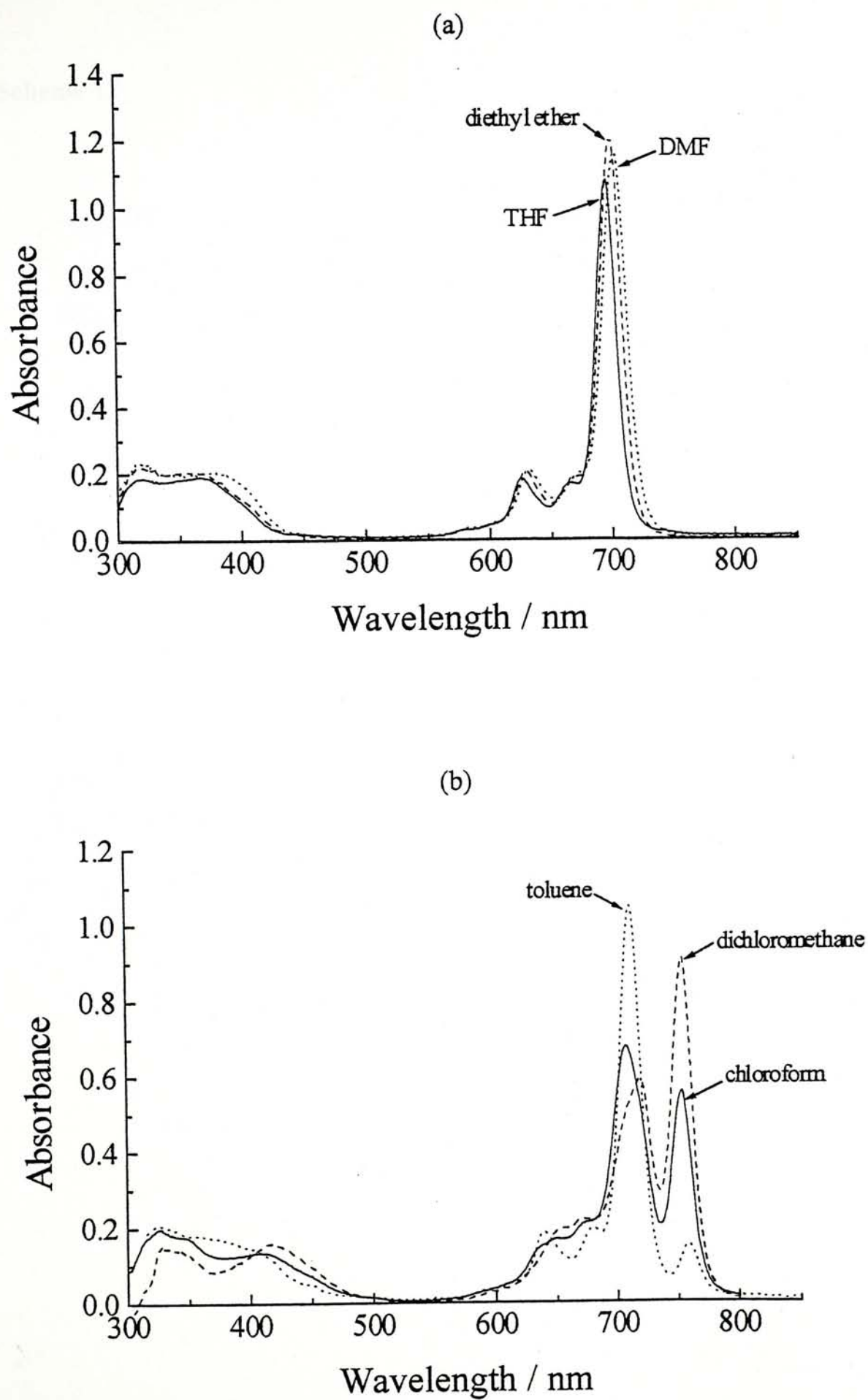
### 2.1.2 Electronic Absorption Spectra

The UV-Vis spectra of **55** are peculiar and worth mentioning. As shown in Figure 20, the spectra of **55** are solvent dependent. In THF, DMF, and diethyl ether solutions, the spectra show a typical Q band at 695-701 nm along with broad signals

at 316-379 nm due to the phthalocyanine (B band) and ferrocene. In less polar solvents such as toluene,  $\text{CHCl}_3$ , and  $\text{CH}_2\text{Cl}_2$ , the Q band is broadened and slightly shifted to the red (707-718 nm), and an additional band emerges at 752-758 nm (Table 5). Similar phenomena were observed previously for the  $\text{Mg(II)}$  and  $\text{Zn(II)}$  (70) complexes of 1,8,15,22-tetrakis(3-pentyloxy)phthalocyanine and the longest-wavelength band was tentatively attributed to a slipped face-to-face dimer.<sup>43b</sup> In order to reveal the origin of this band, the concentration dependency of the absorption spectra of 55 and 70 was studied. The latter was prepared according to the literature method as shown in Scheme 12.<sup>43b</sup> For compound 55 in toluene (Figure 21) or  $\text{CH}_2\text{Cl}_2$  (Figure 22), the intensity of the "monomer" band at ca. 700 nm decreased while that of the "dimer" band at ca. 760 nm increased with decreasing concentration of phthalocyanines (from  $1 \times 10^{-5}$  to  $2 \times 10^{-7}$  mol  $\text{dm}^{-3}$ ). Similar results were also observed for 70 (Figure 23).

	Diethyl ether	THF	DMF	Toluene	$\text{CH}_2\text{Cl}_2$	$\text{CHCl}_3$
Q band	698	695	701	710, 758	718, 753	707, 752
Ferrocenyl $\pi$ - $\pi^*$ transition	353	366	379	-----	417	413
B band	316	319	321	326	327	326

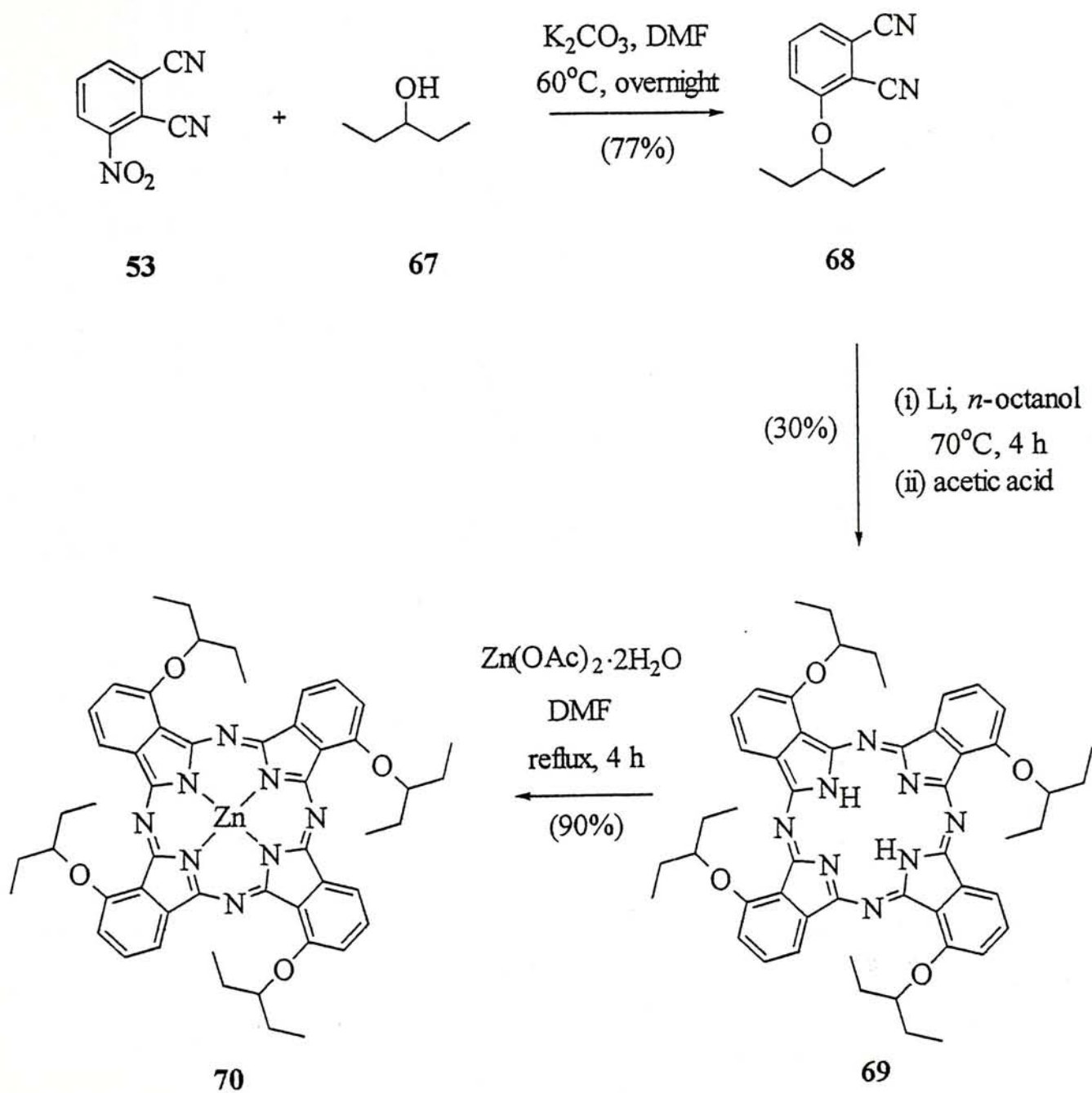
**Table 5.** UV-Vis spectral data of 55 in different solvents (in nm).



**Figure 20.** UV-Vis spectra of **55** (a) in diethyl ether, THF and DMF (b) in toluene,  $\text{CH}_2\text{Cl}_2$  and  $\text{CHCl}_3$ .



**Scheme 12**



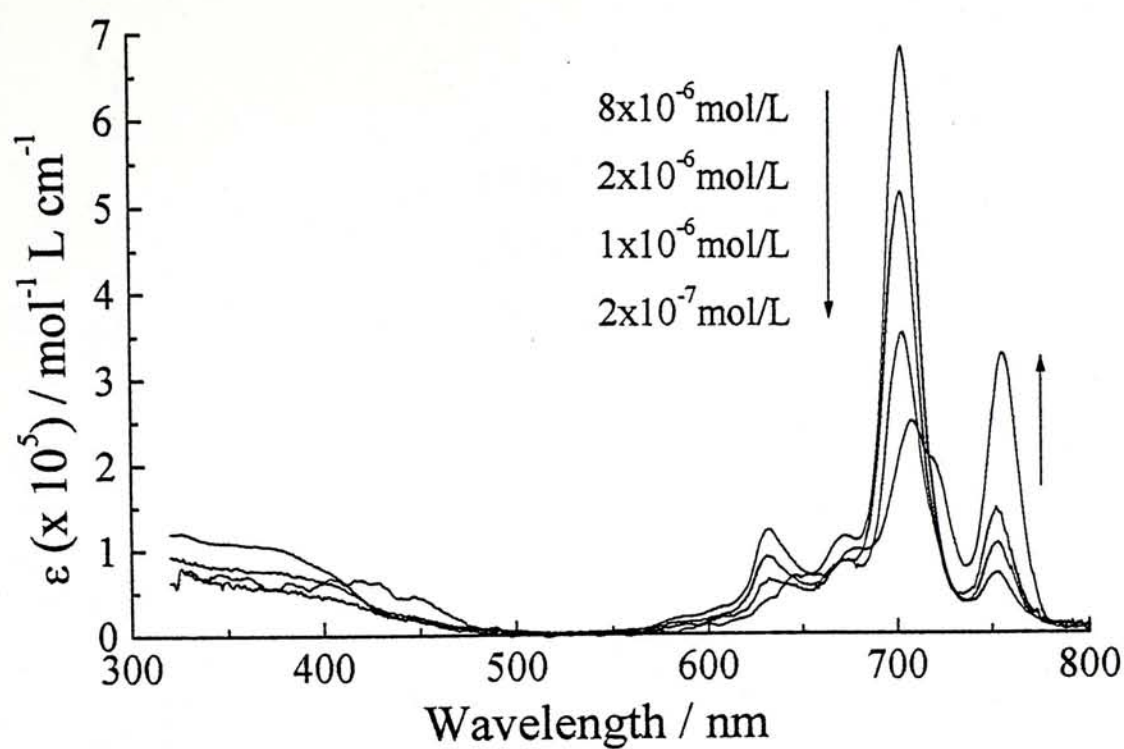


**Figure 21.** UV-Vis spectra of **55** in toluene with different concentration.

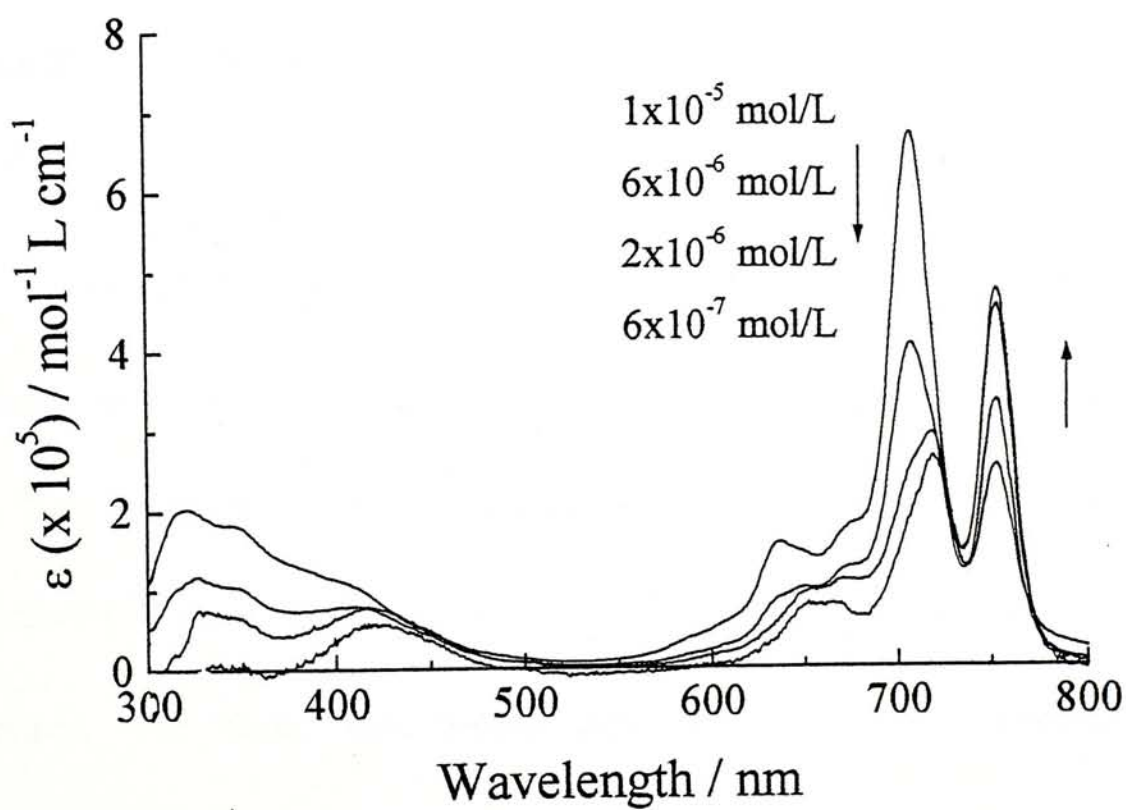


**Figure 22.** UV-Vis spectra of **55** in  $\text{CH}_2\text{Cl}_2$  with different concentration.

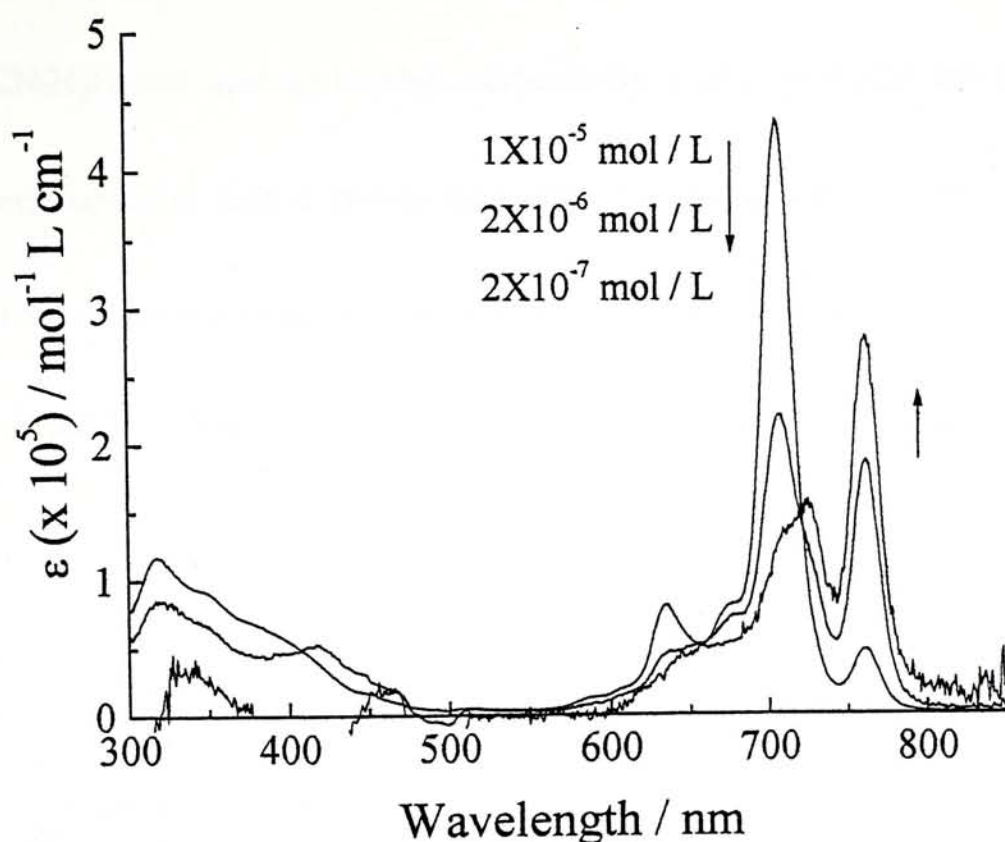


**Figure 23.** UV-Vis spectra of **70** in  $\text{CH}_2\text{Cl}_2$  with different concentration.

Compound **70** showed a fluorescence emission at 714 nm in  $\text{CH}_2\text{Cl}_2$  upon excitation at 630 nm (Figure 24); no emission was observed at a wavelength longer than 760 nm indicating that the species absorbing at 760 nm was not fluorescent. The spectral changes of a  $\text{CH}_2\text{Cl}_2$  solution of **70** after ultrasonic treatment were also examined. The “dimer” band became more intense while the “monomer” band together with the fluorescence at 714 nm was significantly weakened. All the observation suggested that the longer-wavelength absorption may not be due to a cofacial dimer which is expected to be dominant in higher concentrations as in the

cases of zinc(II)<sup>49</sup> and aluminum(III)<sup>50</sup> complexes of tetrasulfonatophthalocyanine in MeCN/H<sub>2</sub>O and aqueous alcohol, respectively, which were also assumed to adapt a dimeric structure with a face-to-face slipped or tilted conformation. The dimer of the former zinc(II) complex was also found to be emissive which again contradicts our results.<sup>49</sup> Thus the exact nature of this band remains to be explored.

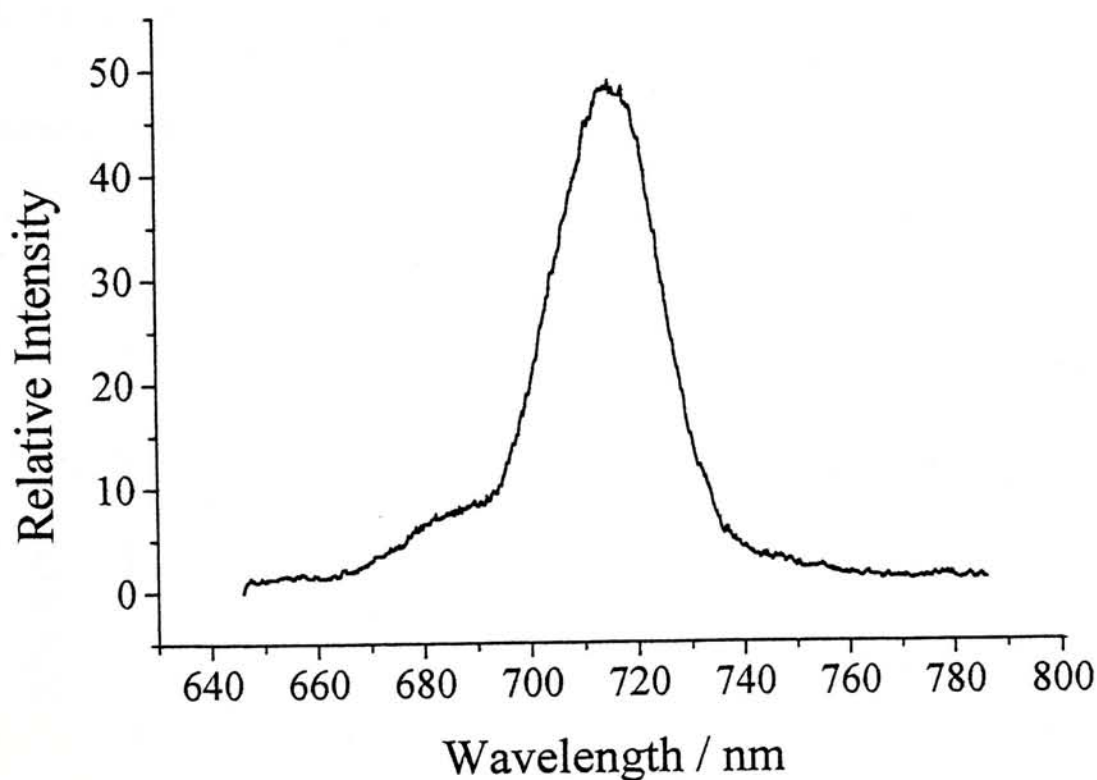


**Figure 24.** Fluorescence spectrum of **70** in CH<sub>2</sub>Cl<sub>2</sub> upon excitation at 630 nm.



The UV-Vis spectra of phthalocyanines **62** (Figure 25) and **65** (Figure 26) in THF were also recorded and the data are tabulated in Table 6. By comparing these two spectra with that of **55**, the Q band shifts to the red as the number of electron donating ferrocenylethoxyl groups increases. All the spectra show relatively sharp Q band indicating that the degree of aggregation is not significant for these compounds in THF. The spectrum of **65** shows a shoulder near the Q band. This is consistent with the typically split Q bands for metal-free phthalocyanines which are not well resolved in this case.

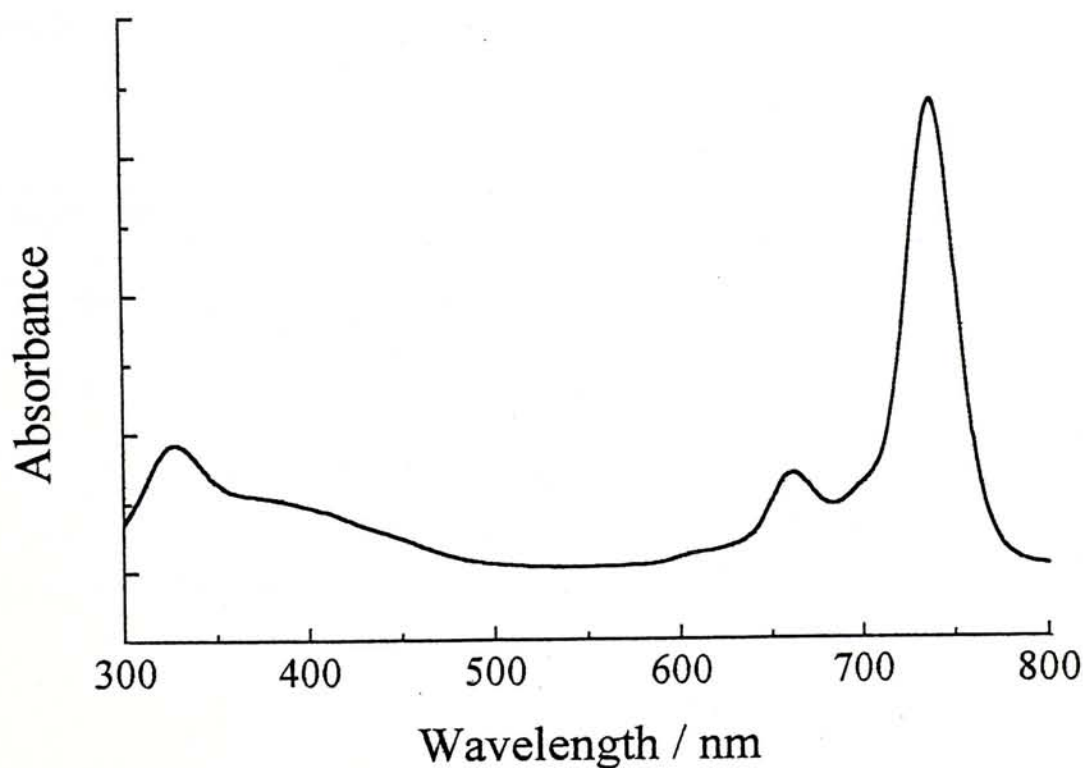


**Figure 25.** UV-Vis spectrum of **62** in THF.

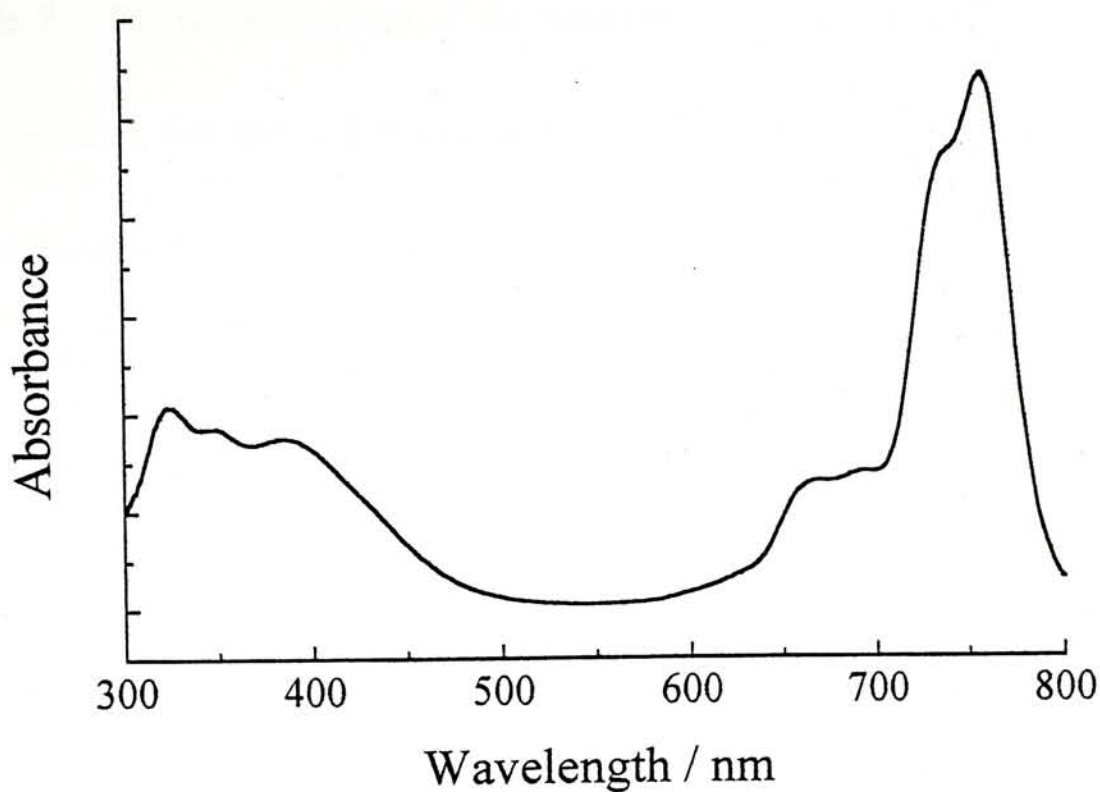


**Figure 26.** UV-Vis spectrum of **65** in THF.

Compound	Q band	Ferrocenyl band	B band
<b>55</b>	695	366	319
<b>62</b>	737	382	326
<b>65</b>	756	381	325

**Table 6.** UV-Vis spectral data of **55**, **62**, and **65** in THF (in nm).

### 2.1.3 *Electrochemical Studies*

The electrochemical properties of all the ferrocenyl phthalonitriles and phthalocyanines were investigated by cyclic voltammetry and the data are collected in

Table 7. The voltammograms of the dinitriles **54**, **60** and **64** in DMF showed two couples at ca. 0.0 and -2.0 V assignable to the ferrocene (oxidation to ferrocenium cation) and dicyanobenzene (reduction to the corresponding radical anion) moieties, respectively. By comparing the reduction potential of benzonitrile (-2.32 V vs. SCE or -2.63 V vs. Ag-Ag<sup>+</sup> in MeCN),<sup>51,52</sup> phthalonitrile (**34**), and these compounds (Table 7), it is clear that the electron withdrawing cyano group greatly facilitates the addition of electron to the  $\pi$  system while the electron donating 2-ferrocenylethoxy group makes the reduction more difficult. Based on the separation between the anodic and cathodic potentials ( $\Delta E$ ) and the plots of peak current vs. square root of the scan rate which showed deviation from a straight line at higher scan rates, all these couples were regarded as quasi-reversible, except the phthalonitrile reduction of **64** which was basically irreversible. Addition of ferrocene to the solution of **64** only increased the cathodic and anodic current without significantly shifting or splitting the potential. This indicated that the ferrocenyl units in **64** are electrochemically very similar to free ferrocene. The voltammogram of ferrocene was also recorded under identical conditions. The peak currents for the ferrocene-ferrocenium couple were much lower than those of **64** in the same concentration showing that **64** may undergo a multi-electron redox process.

Ferrocene			Phthalonitrile/Phthalocyanine									
Compound	$E_{1/2}(\text{ox})$	$\Delta E^b$	$ i_{\text{pa}}/i_{\text{pc}} $	$E_{1/2}(\text{ox1})$	$\Delta E^b$	$ i_{\text{pa}}/i_{\text{pc}} $	$E_{1/2}(\text{red1})$	$\Delta E^b$	$ i_{\text{pa}}/i_{\text{pc}} $	$E_{1/2}(\text{red2})$	$\Delta E^b$	$ i_{\text{pa}}/i_{\text{pc}} $
34	---	---	---	---	---	---	-1988	91	0.95	---	---	---
54	43	79	1.02	---	---	---	-2008	93	0.89	---	---	---
60	20	70	1.02	---	---	---	-2013	70	0.91	---	---	---
64	63	76	0.97	---	---	---	-2078	154	0.53	---	---	---
55 <sup>c</sup>	44	72	1.01	288	56	0.54	-1306	72	1.12	-1784	104	0.63
62 <sup>d</sup>	43	93	1.01	215	57	0.66	-1348	53	0.80	-1788	89	0.78
65 <sup>e</sup>	79	226	0.37	342 <sup>f</sup>	---	---	-1209	106	0.59	-1493	138	0.93

<sup>a</sup> Recorded with  $[\text{Bu}_4\text{N}][\text{ClO}_4]$  as electrolyte in DMF (0.1 mol dm<sup>-3</sup>) at ambient temperature with a scan rate of 100 mV s<sup>-1</sup>, unless otherwise stated.

Potentials are expressed in mV vs. Ag-Ag<sup>+</sup> in MeCN. <sup>b</sup>  $\Delta E = |E_{\text{pc}} - E_{\text{pa}}|$ . <sup>c</sup>  $\Delta E_{1/2}(\text{red3})$  for phthalocyanine appeared at -1982 mV

with  $\Delta E = 111$  mV. <sup>d</sup> Scan rate = 20 mV s<sup>-1</sup>.  $E_{1/2}(\text{ox2})$  for phthalocyanine appeared at 490 mV with  $\Delta E = 43$  mV. <sup>e</sup> In  $\text{CH}_2\text{Cl}_2$ .  $E_{\text{pc}}(\text{ox2})$

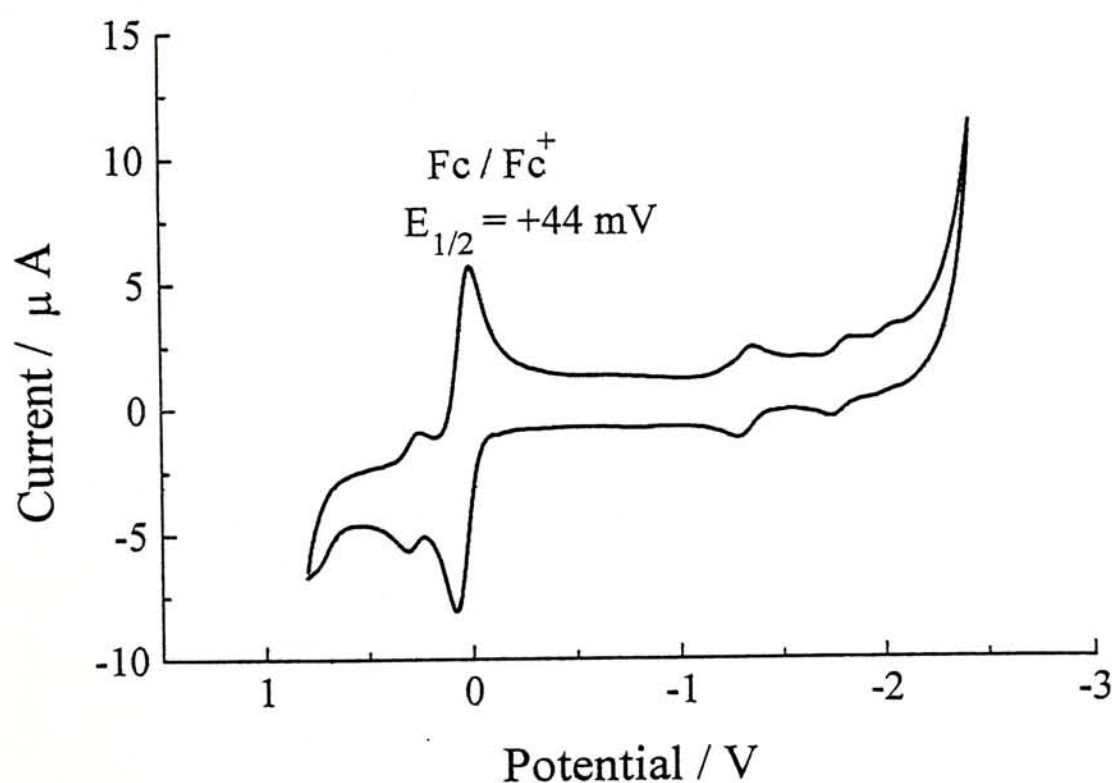
and  $E_{\text{pc}}(\text{red3})$  for phthalocyanine appeared at 610 and -1852 mV, respectively. <sup>f</sup>  $E_{\text{pc}}$ .

Table 7. Electrochemical data of the dinitriles 34, 54, 60, and 64, and the phthalocyanines 55, 62, and 65.<sup>a</sup>



All the voltammograms of phthalocyanines **55** (Figure 27), **62** (Figure 28) and **65** (Figure 29) showed a quasi-reversible oxidation attributed to the ferrocenyl units together with one to two quasi-reversible oxidation and up to three quasi-reversible reductions due to the phthalocyanine  $\pi$  system (Table 7).<sup>53</sup> As **65** was not soluble in DMF, the voltammogram was recorded in  $\text{CH}_2\text{Cl}_2$ . The potential difference between the first oxidation and reduction couples for phthalocyanines is related to the energy gap between their HOMO and LUMO. The values for these ferrocenylphthalocyanines are very similar and fall in the normal region (1.5-1.7 V) reported for other phthalocyanines.<sup>53</sup> As shown in Figures 27-29, a remarkable trend is the increase of relative peak currents of the ferrocene couple with respect to either one of the phthalocyanine couples as the number of ferrocenyl units increased from four, eight to sixteen in a molecule. A sharp cathodic stripping peak was observed for the ferrocene couple of **65** with a peak current ratio  $|i_{pa}/i_{pc}|$  much smaller than unity (0.37). This waveform suggested that adsorption of the oxidized product onto the electrode may occur which was also seen for some ferrocene-containing dendrimers.<sup>24,25,35</sup> Addition of a small amount of MeCN (v/v 1:5 to  $\text{CH}_2\text{Cl}_2$ ) reduced the peak-to-peak separation ( $\Delta E$ ) of the ferrocene couple to 126 mV. This however could not solve the problem of adsorption ( $|i_{pa}/i_{pc}| = 0.25$ ) and the other redox couples for phthalocyanine turned to be even weaker. The voltammogram of **65** in

THF gave a higher peak current ratio ( $|i_{pa}/i_{pc}| = 0.57$ ) for the ferrocene couple showing that this solvent can better dissolve the oxidized product and relieve the adsorption. The couple however became less reversible as shown by the large peak-to-peak separation (420 mV). In all cases, no splitting of the ferrocene couple was observed. It appeared that all the ferrocenyl moieties attached to these phthalocyanines behave independently and are oxidized at the same potential.



**Figure 27.** Cyclic voltammogram of **55** in DMF containing 0.1 M  $[\text{NBu}_4][\text{ClO}_4]$  at a scan rate of  $100 \text{ mV s}^{-1}$ .

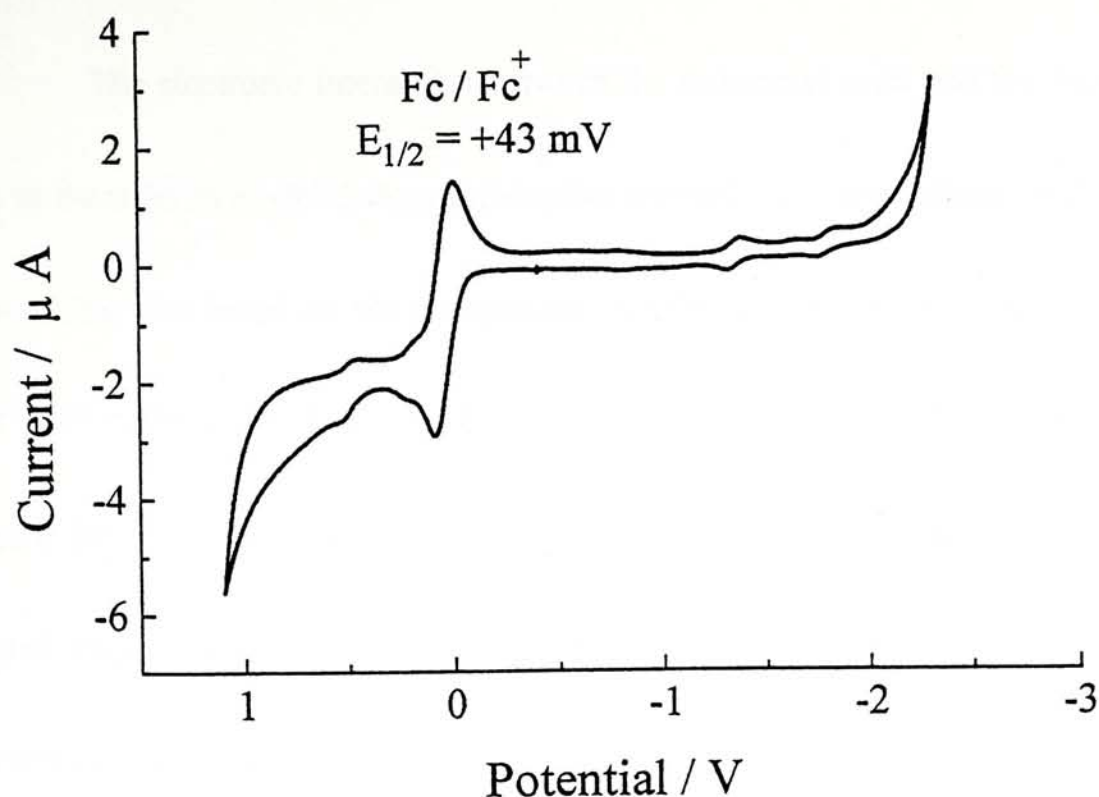


**Figure 28.** Cyclic voltammogram of **62** in DMF containing 0.1 M  $[\text{NBu}_4][\text{ClO}_4]$  at a scan rate of  $20 \text{ mV s}^{-1}$ .

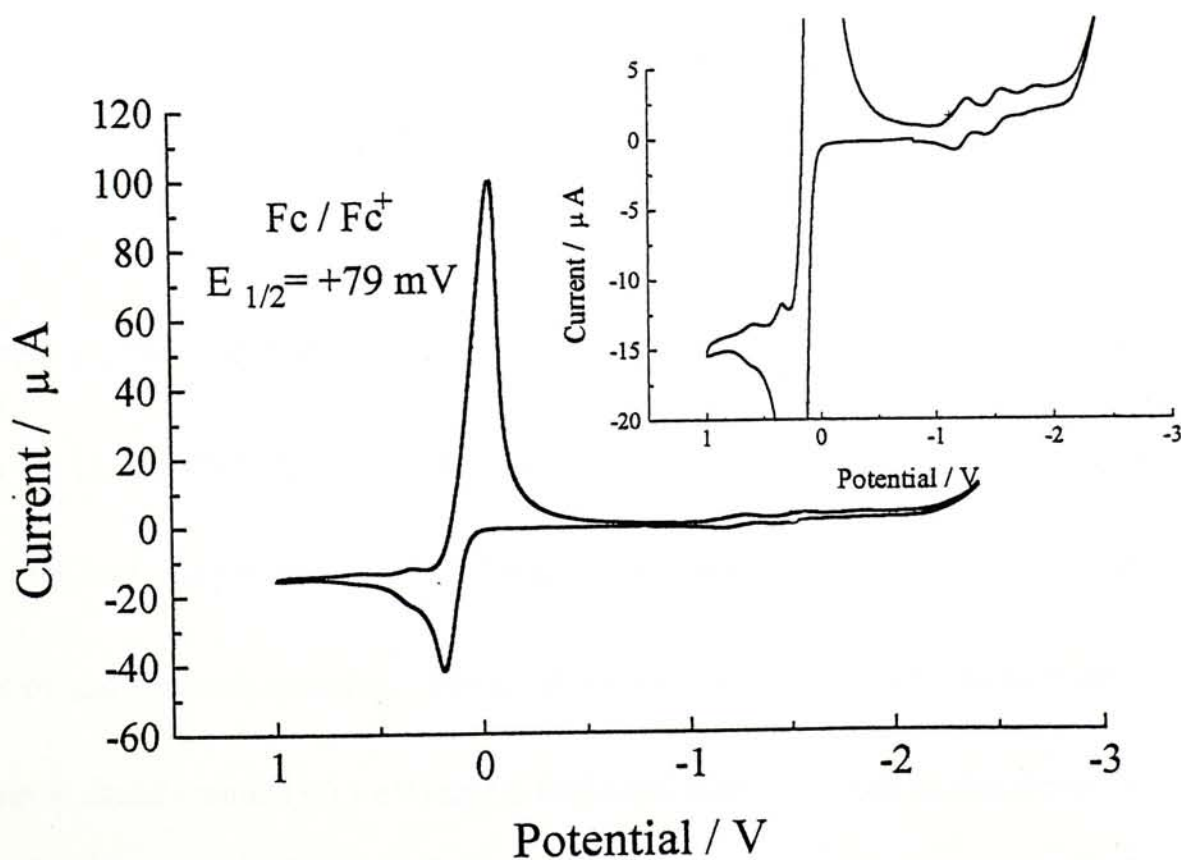


**Figure 29.** Cyclic voltammogram of **65** in  $\text{CH}_2\text{Cl}_2$  containing 0.1 M  $[\text{NBu}_4][\text{ClO}_4]$  at a scan rate of  $100 \text{ mV s}^{-1}$ .



The electronic interaction between the ferrocenyl units and the macrocyclic core in these ferrocenylphthalocyanines also seemed to be insignificant in the ground state. This was based on the observation that the absorption spectrum of **70** mixed with four equivalents of ferrocene was almost identical with that of **55** in  $\text{CHCl}_3$  (Figure 30). The ferrocenyl moieties, however, were very efficient to quench the excited state of **55** for which no fluorescence was observed. We attributed this quenching to a photoinduced electron transfer (PET) in which ferrocene behaves as an electron donor. The overall free energy change for this PET was determined by the Rehn-Weller equation.<sup>54</sup>

$$\Delta G^0 = e[E_{1/2}(\text{D}^+/\text{D}) - E_{1/2}(\text{A}/\text{A}^-)] - \Delta E(0,0) - w_p$$

where  $e$  is the charge on the electron,  $E_{1/2}$  is half-wave reduction for potential either for the donor ( $\text{D}^+/\text{D}$ ) or acceptor ( $\text{A}/\text{A}^-$ ) couples in volts,  $\Delta E(0,0)$  is the relevant singlet state energy, and  $w_p$  is a Coulombic interaction term between the oxidized donor and reduced acceptor. For polar solvents with a high dielectric constant, this term is usually small ( $<0.1$  eV) and is neglected here.<sup>9j</sup> Based on the electrochemical data for **55** (Table 7) and the value of  $\Delta E(0,0)$  for phthalocyaninatozinc(II) (1.83 eV),<sup>55</sup> the value of  $\Delta G^0$  was determined to be  $-0.48$  eV showing that this PET is a



thermodynamically favorable process. The alternative quenching pathway by energy transfer from the phthalocyanine's  $S_1$  state to ferrocene is excluded because of its endothermic nature (the  $S_1$  state of ferrocene at 2.46 eV).<sup>56</sup> The estimated value of  $\Delta G^\circ$  for this system is of the same order with and lies between those of octamethylporphyrins linked with a ferrocenyl group at a meso-position (ca. -0.1 eV)<sup>9h</sup> and the ferrocenylporphyrin containing three cationic pyridinium moieties at the meso-positions (-0.66 eV).<sup>9j</sup>

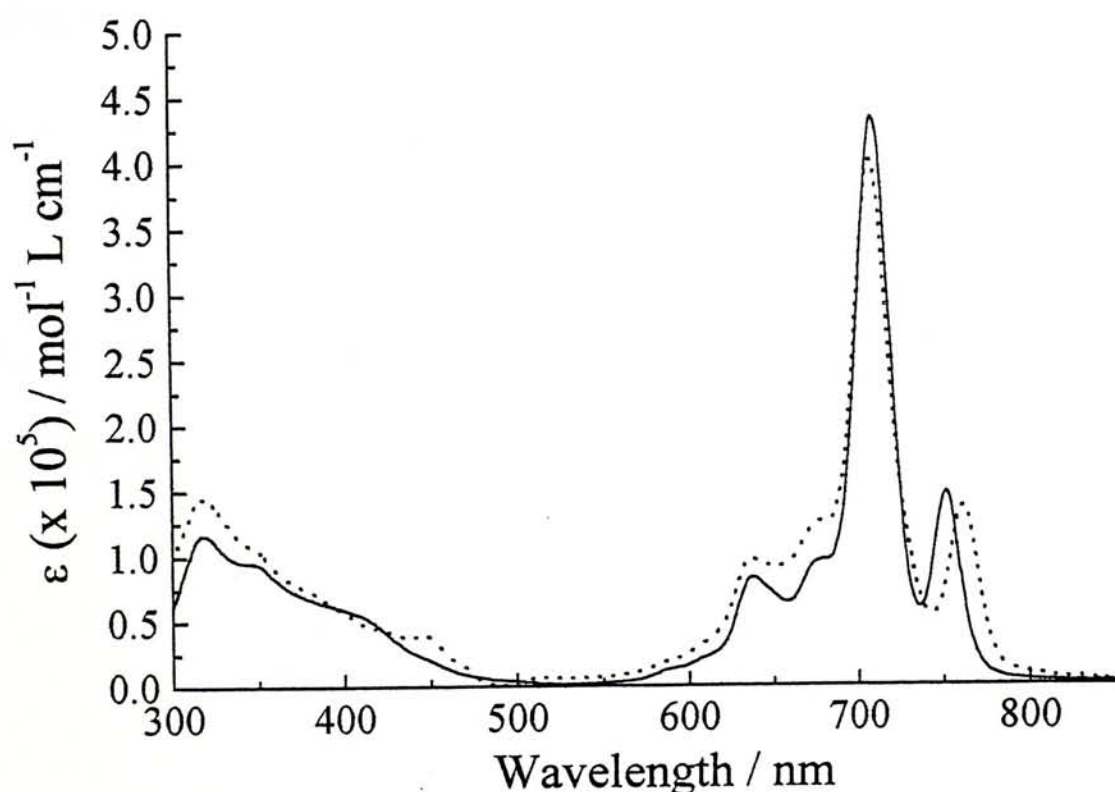


**Figure 30.** Absorption spectra of a mixture of ferrocene and **70** (4:1) (···) and **55** (—) in  $\text{CHCl}_3$ .

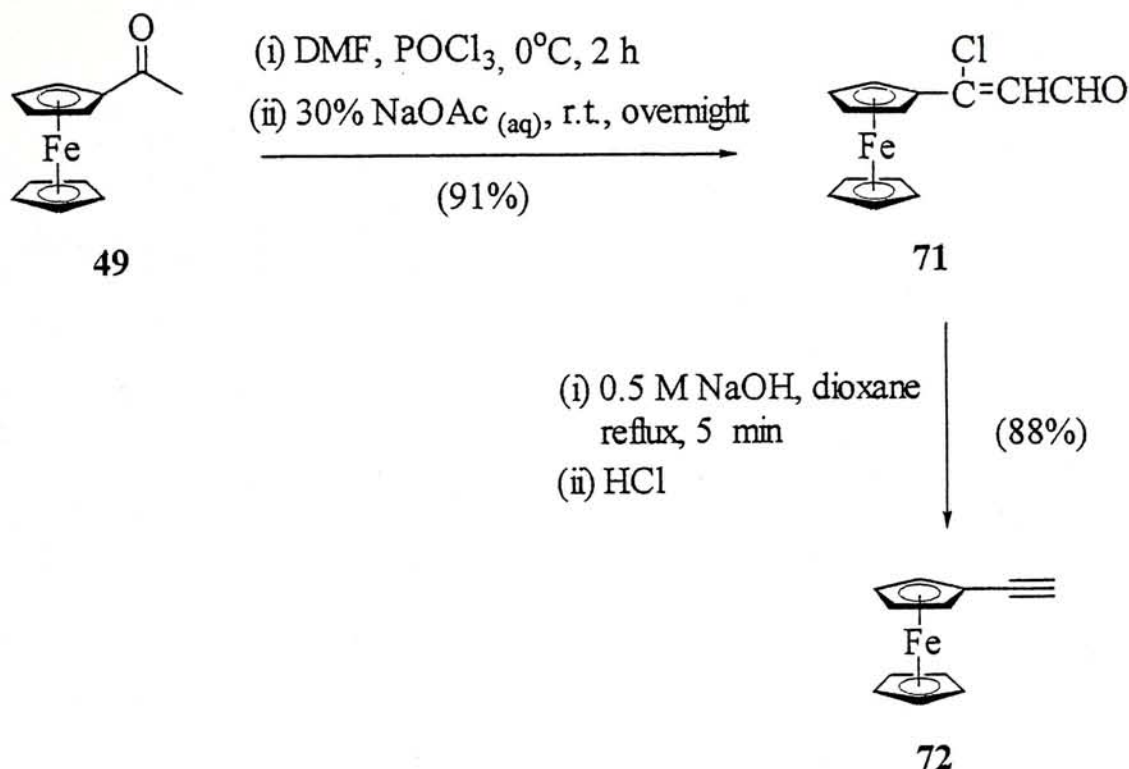
## 2.2 Ferrocenyl Tetrapyrroles with Ethynyl Linkers

### 2.2.1 *Synthesis and Characterization*

As the shortage of electronic interactions between the ferrocenyl groups in **55**, **62**, and **65** may be attributed to the saturated nature of the linkers, we therefore prepared another series of tetrapyrrole derivatives in which the ferrocenyl units are connected to the macrocycles with unsaturated ethynyl bridges. The synthesis involved ferrocenylethyne and dicyano-dihalobenzene and naphthalene as the starting materials which were prepared by the published methods.

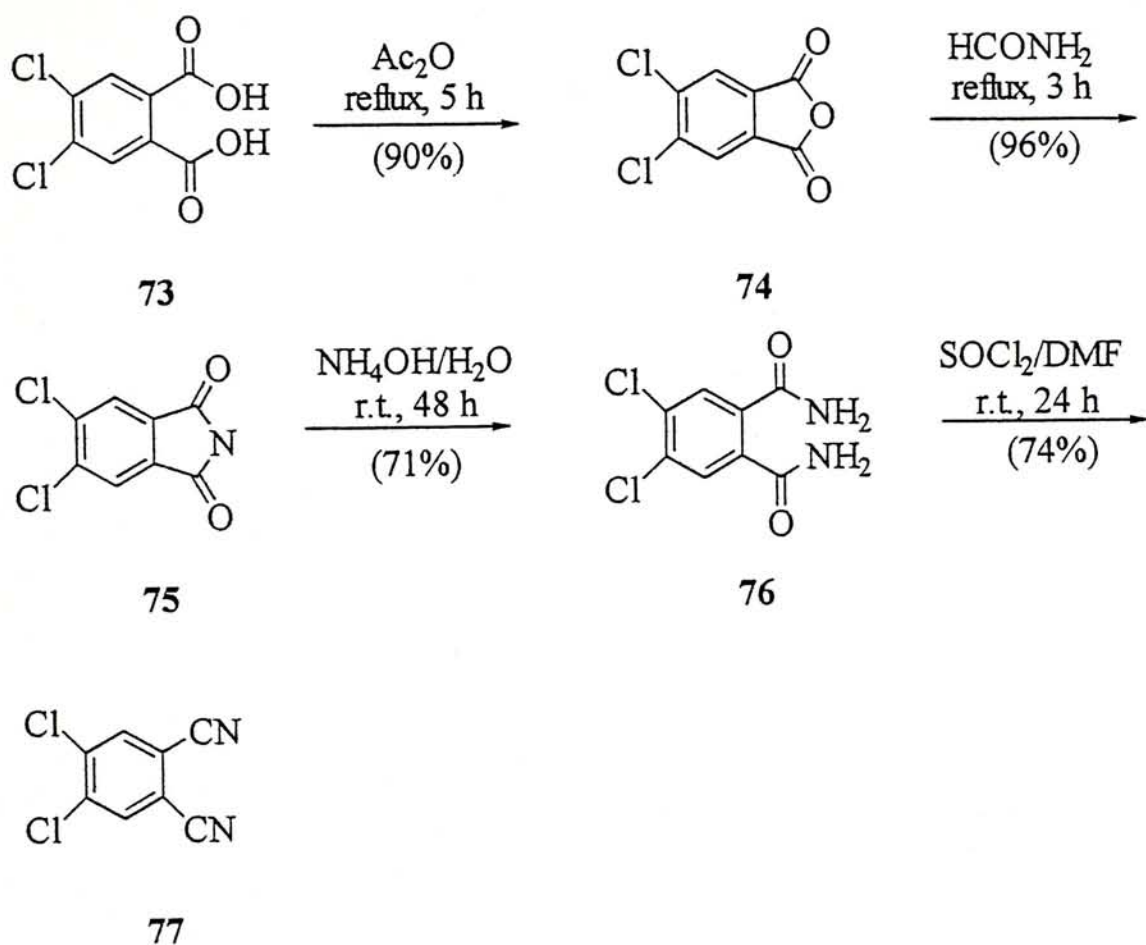
Formylation of acetylferrocene (**49**) followed by basic workup gave (1-chloro-2-formylvinyl)ferrocene (**71**), which upon basic hydrolysis, was converted to ferrocenylethyne (**72**) (Scheme 13).<sup>57</sup>

### Scheme 13



Treatment of 4,5-dichloro-1,2-benzenedicarboxylic acid (**73**) with acetic anhydride gave 5,6-dichloro-1,3-isobenzofurandione (**74**), which was then refluxed in formamide to generate 5,6-dichloro-1*H*-isoindole-1,3(2*H*)-dione (**75**). Compound **75** was then converted to 4,5-dichloro-1,2-benzenedicarboxamide (**76**) by the action of ammonia solution. Upon treatment with thionyl chloride in DMF, compound **76** was further transformed to 1,2-dichloro-4,5-dicyanobenzene (**77**) in good yield (Scheme 14).<sup>58</sup>

# Scheme 14

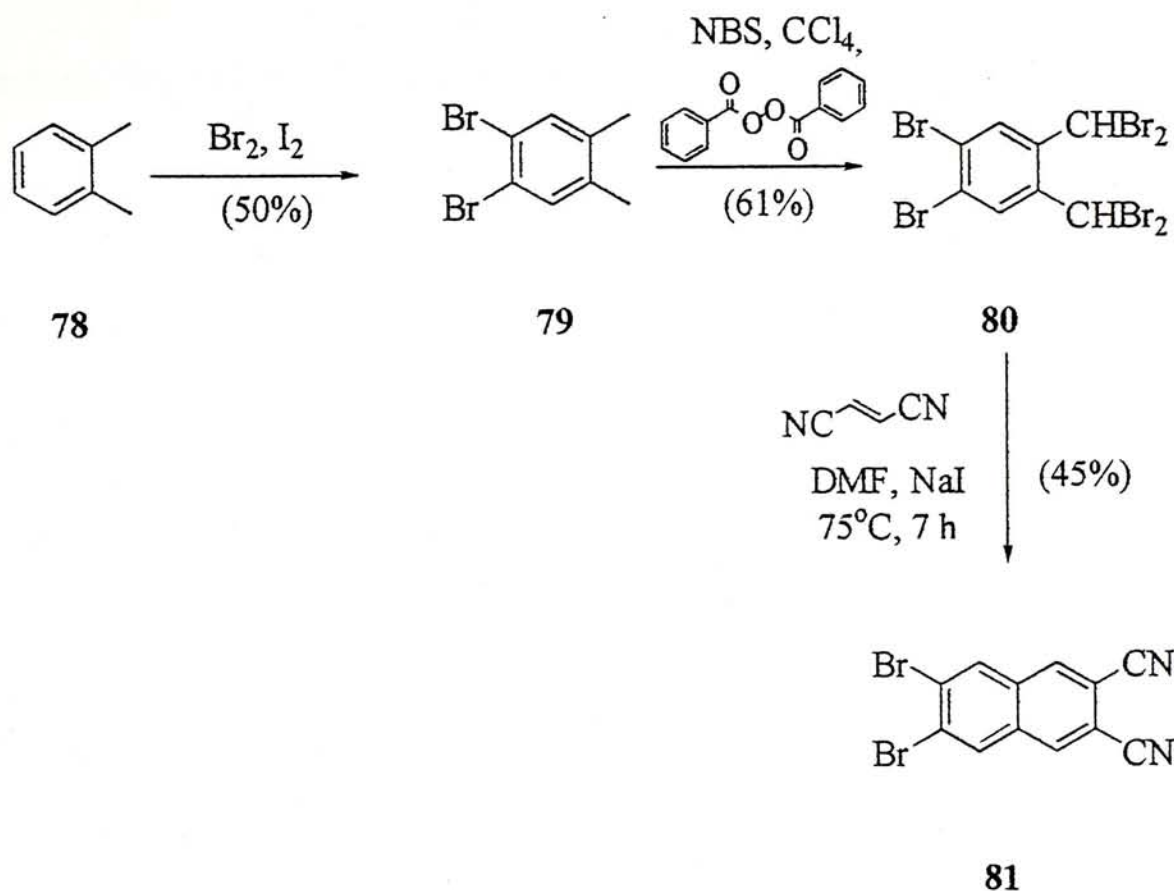


The dibromonaphthalene analog **81** was prepared according to Scheme 15.<sup>59</sup>

Bromination of *o*-xylene (**78**) in the presence of iodine generated 1,2-dibromo-4,5-dimethylbenzene (**79**). In the presence of dibenzoyl peroxide, compound **79** was further brominated using *N*-bromosuccinimide to give 1,2-dibromo-4,5-bis(dibromomethyl)benzene (**80**). Reaction of **80** with fumaronitrile and sodium iodide afforded 2,3-dibromo-6,7-dicyanonaphthalene (**81**) in a moderate yield (Scheme 15).



### Scheme 15



#### 2.2.1.1 Preparation of Octakis(ferrocenylethynyl)phthalocyaninatozinc(II) (83)

By using the well-established palladium-mediated cross-coupling reactions,<sup>60</sup> ferrocenylethyne (72) was coupled with 1,2-dichloro-4,5-dicyanobenzene (77) to afford the dinitrile 82, which underwent typical cyclization in the presence of DBU and  $\text{Zn}(\text{OAc})_2 \cdot 2\text{H}_2\text{O}$  in *n*-pentanol to give the desired phthalocyanine 83 (Scheme 16). This compound, having a large conjugated  $\pi$ -system, was found to be highly aggregated and could only be purified by Soxhlet extraction; the macrocycle was stuck in silica gel or alumina columns during chromatography. The compound was preliminary characterized with MALDI-TOF mass spectroscopy which showed

an isotopic cluster peaking at  $m/z$  2242.6 assignable to the  $M^+$  species. The UV-Vis spectrum recorded in THF showed only a weak Q band at 732 nm. Due to the molecular association, the B band was embedded in the background signal which was very intense. In order to relieve the extent of aggregation, a mixed cyclization was performed using the dinitriles **82** and **84** (15 : 1),<sup>61</sup> which contains three long dodecyloxy carbon chains. Under identical conditions, the reaction produced the expected self-cyclized product **83** in 2% yield together with a trace amount of the “3 + 1” unsymmetrical product **85** (Scheme 17). To our surprise, both of these compounds could be purified by column chromatography. It is likely that the  $\pi$ - $\pi$  interactions between the molecules of **83** are disrupted by **85** which facilitates the chromatographic purification. The MALDI-TOF mass spectrum of **83**, obtained by this mixed-cyclization method, also showed an isotopic cluster corresponding to the molecular ion, but the intensity was higher than that for the product isolated in the self-cyclization procedure. This suggested that the laser-assisted desorption process is easier for samples with less significant molecular aggregation. The UV-Vis spectrum of **83** (Figure 31), purified by chromatography, is well-resolved and displays a typical spectrum of non-aggregated phthalocyanines. Due to the presence of eight ferrocenylethynyl moieties, both of the B (377 nm) and Q (736 nm) bands are bathochromic shifted comparing with those of the unsubstituted analog ( $\lambda_{\text{max}} = 345$

and 672 nm in DMSO).<sup>62</sup> The  $^1\text{H}$  NMR spectrum of **83** in  $\text{CDCl}_3$  or pyridine- $\text{d}_5$  showed only the signals due to the ferrocenyl moieties; the aromatic signal could not be observed. As the concentration of solution for  $^1\text{H}$  NMR measurements is usually much higher (about two order of magnitude) than that for UV-Vis spectroscopic studies, the absence of the aromatic signal may be due to an aggregation phenomenon as suggested previously.<sup>63</sup> The IR spectrum of **83** showed a sharp peak at  $2200\text{ cm}^{-1}$ , which indicates the presence of triple bonds in the molecule. Attempts to obtain satisfactory analytical data of **83**, unfortunately, were not successful which may be due to the presence of traces of impurities or the difficulty in complete combustion of this type of compounds.<sup>64</sup> The formation of the unsymmetrical analog **85** was supported by MALDI-TOF mass spectroscopy ( $\text{M}^+$  cluster at  $m/z$  2485.5).

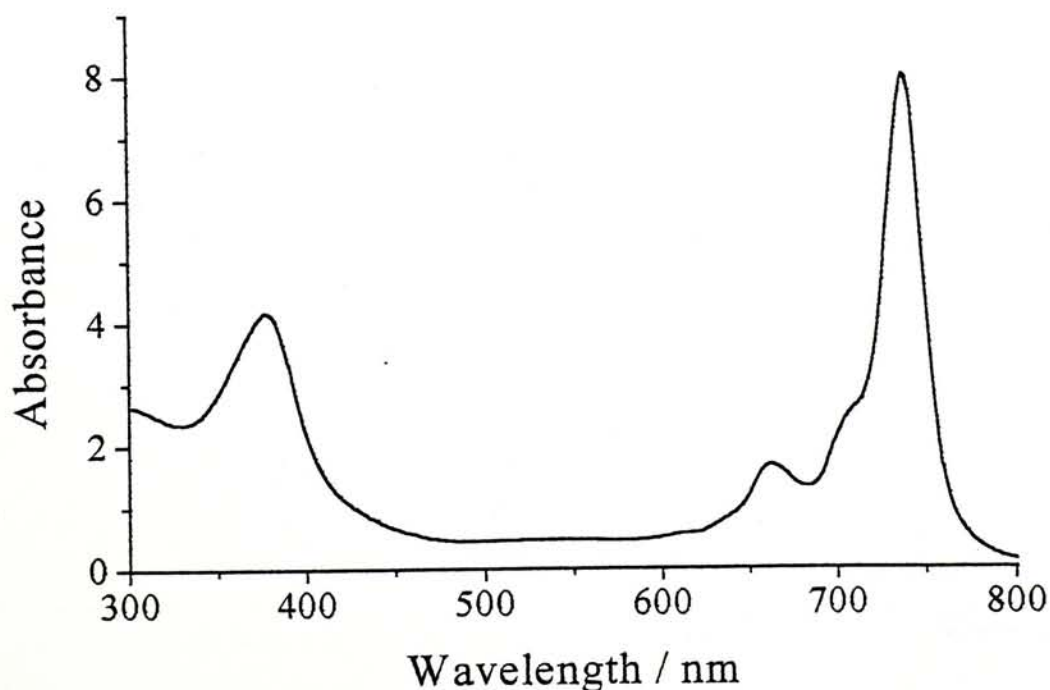
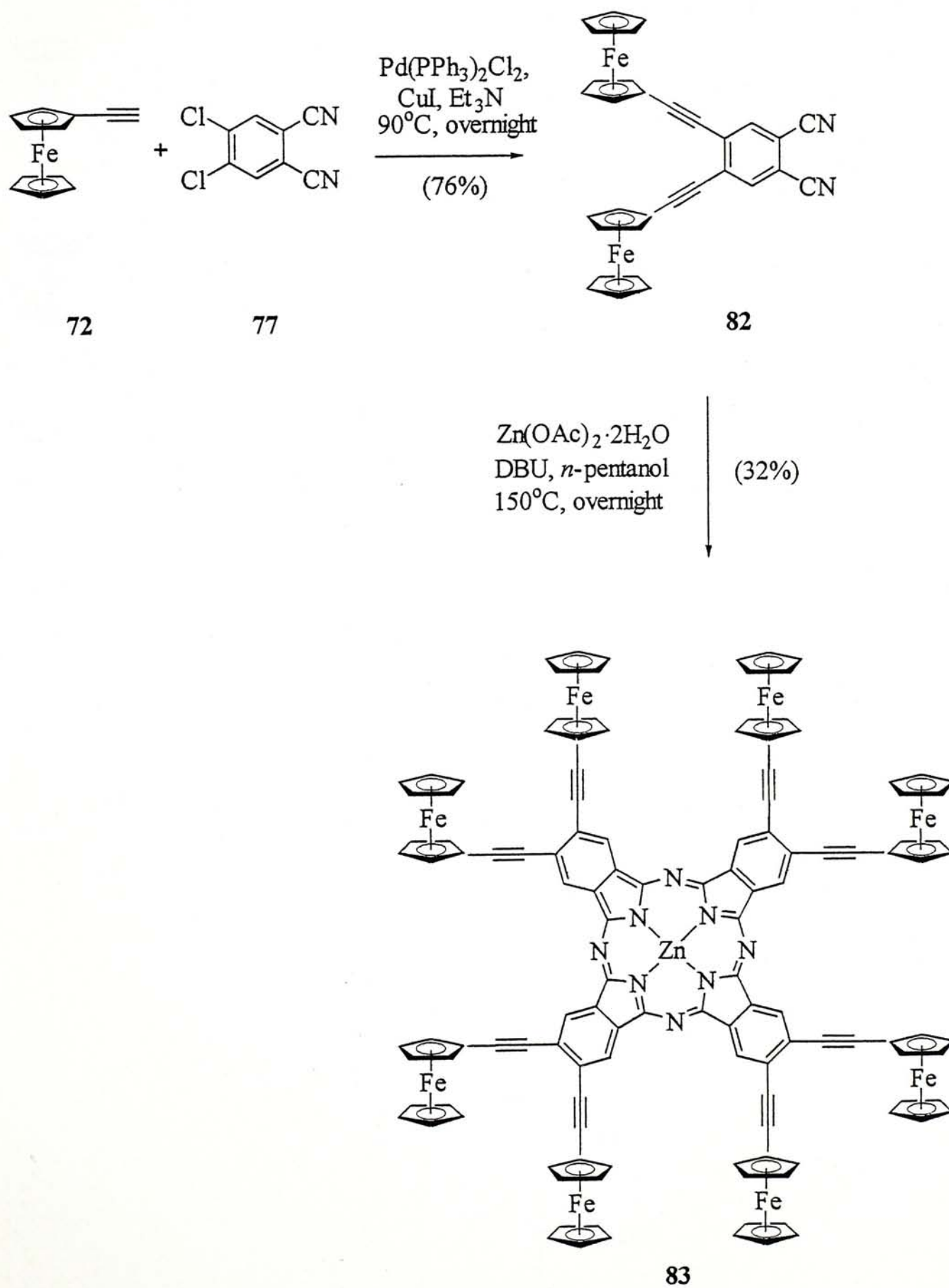


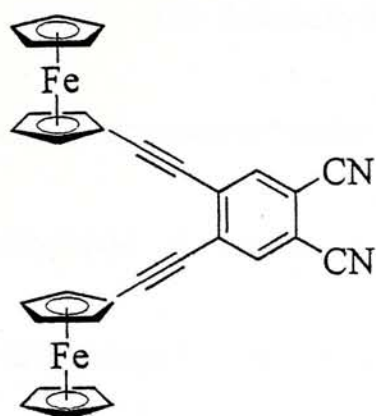
**Figure 31.** UV-Vis spectrum of **83** in THF.

Scheme 16

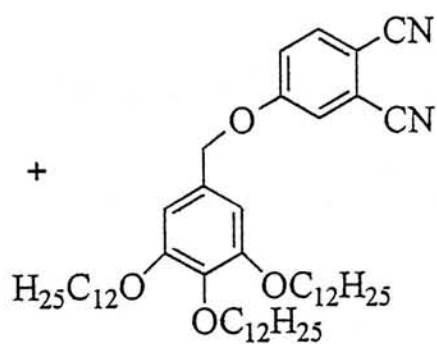




Scheme 17



82



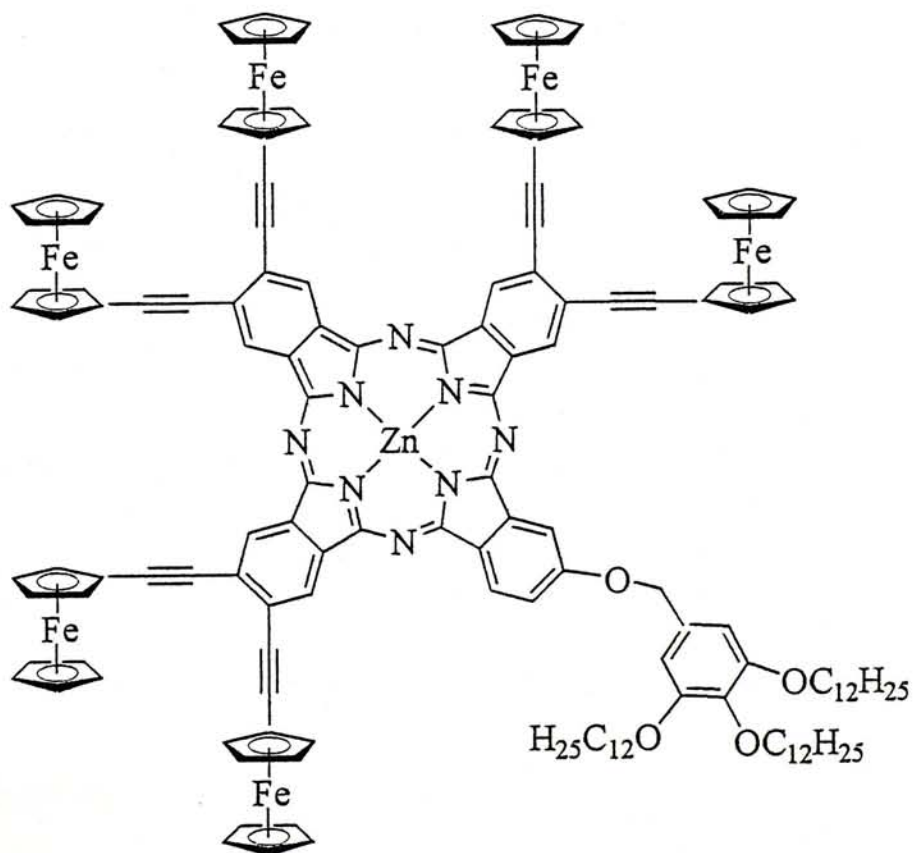
84

$\text{Zn(OAc)}_2 \cdot 2\text{H}_2\text{O}$   
DBU, *n*-pentanol  
150°C, overnight

83

(2%)

+



85

trace amount

#### 2.2.1.2 Preparation of Octakis(ferrocenylethynyl)naphthalocyaninatozinc(II) (**87**)

The ferrocenynaphthalocyanine **87** was also prepared in a similar manner using dicyanonaphthalene **86** as the precursor, which was generated by palladium-mediated cross-coupling reaction of ferrocenylethyne (**72**) and 2,3-dibromo-6,7-dicyanonaphthalene (**81**) (Scheme 18). Self-cyclization of dinitrile **86** in the presence of DBU and  $\text{Zn}(\text{OAc})_2 \cdot 2\text{H}_2\text{O}$  in *n*-pentanol gave the first ferrocenyl naphthalocyanine **87** in 31% yield. Again, due to the problem of aggregation, this compound could only be purified by Soxhlet extraction. The formation of this novel macrocycle was confirmed by MALDI-TOF mass spectroscopy which showed the molecular ion cluster at  $m/z$  2442.0. The UV-Vis spectrum of **87** in THF showed a typical naphthalocyanine spectrum, but again aggregation seemed to be significant. We therefore employed the mixed cyclization procedure as shown in Scheme 19. Treatment of 15 equiv. of **86** with 1 equiv. **84**, under normal cyclization conditions, gave the self-cyclized product **87** and the “3 + 1” product **88**, which could be separated by column chromatography.

The MALDI-TOF mass spectrum of **87**, obtained by this mixed cyclization method, also showed the molecular ion isotopic cluster with a relatively high intensity. The corresponding cluster for **88** appeared at  $m/z$  2635.9. Both compounds gave

well-resolved UV-Vis spectra (Figures 32 and 33) showing that aggregation is not significant for these compounds under these conditions. As expected, the Q band (87: 792 nm; 88: 763 nm) was red-shifted comparing with that of 83 and the unsubstituted analog.<sup>63</sup> The IR spectra of 87 and 88 exhibited a strong band at 2200  $\text{cm}^{-1}$  indicating the existence of the  $\text{C}\equiv\text{C}$  triple bonds in the molecule. Very intense C-H stretching bands at 2853 and 2923  $\text{cm}^{-1}$  were also observed for 88. Attempts to obtain satisfactory NMR data for these macrocycles, unfortunately, were not successful which could be related to the highly aggregation tendency for these large  $\pi$ -systems. Analytical data for this compound again were not entirely satisfactory as in the case of phthalocyanine 83.

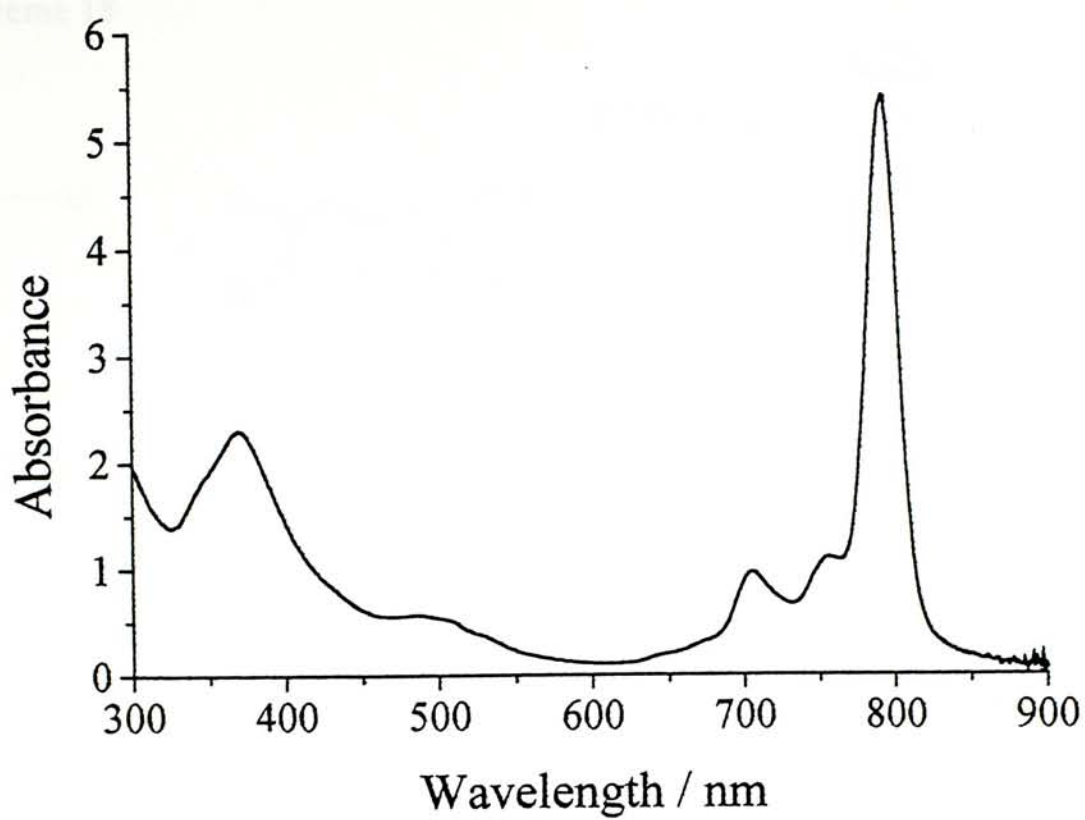


**Figure 32.** UV-Vis spectrum of **87** in THF.

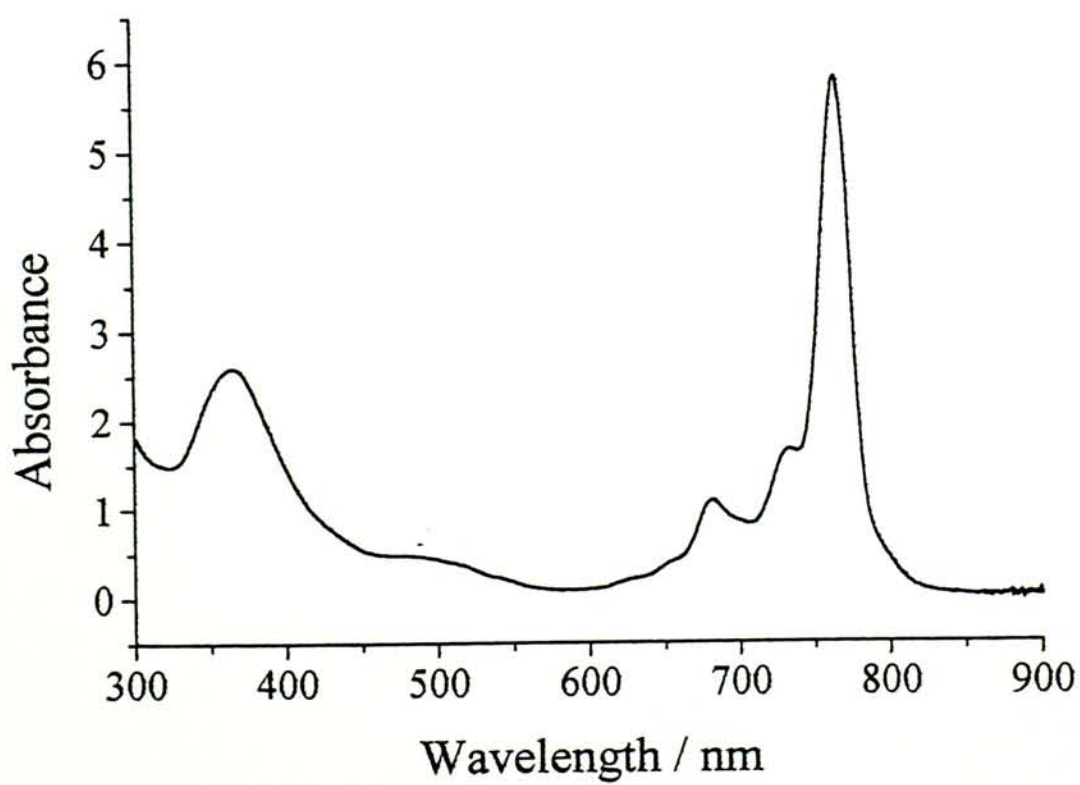
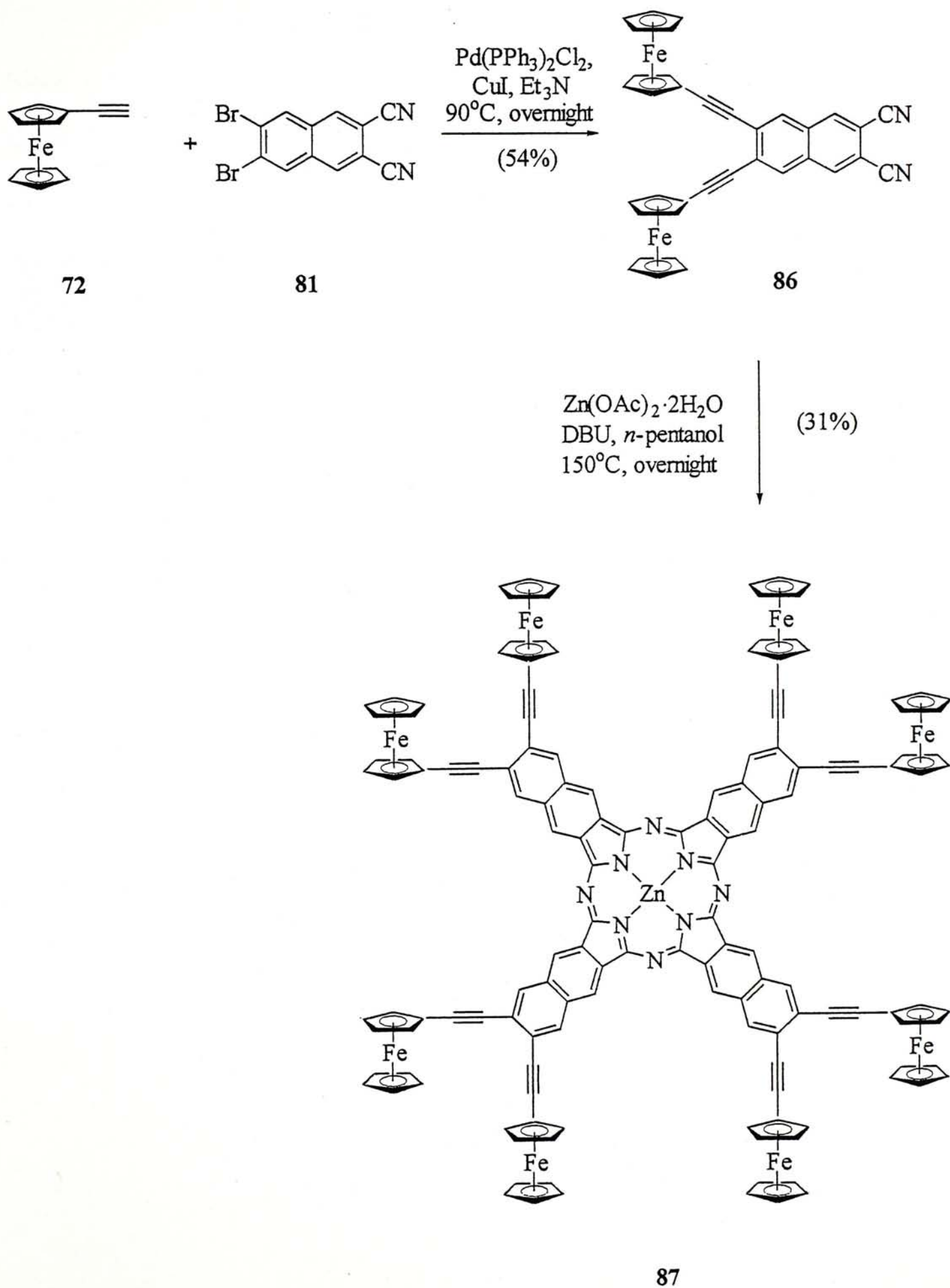


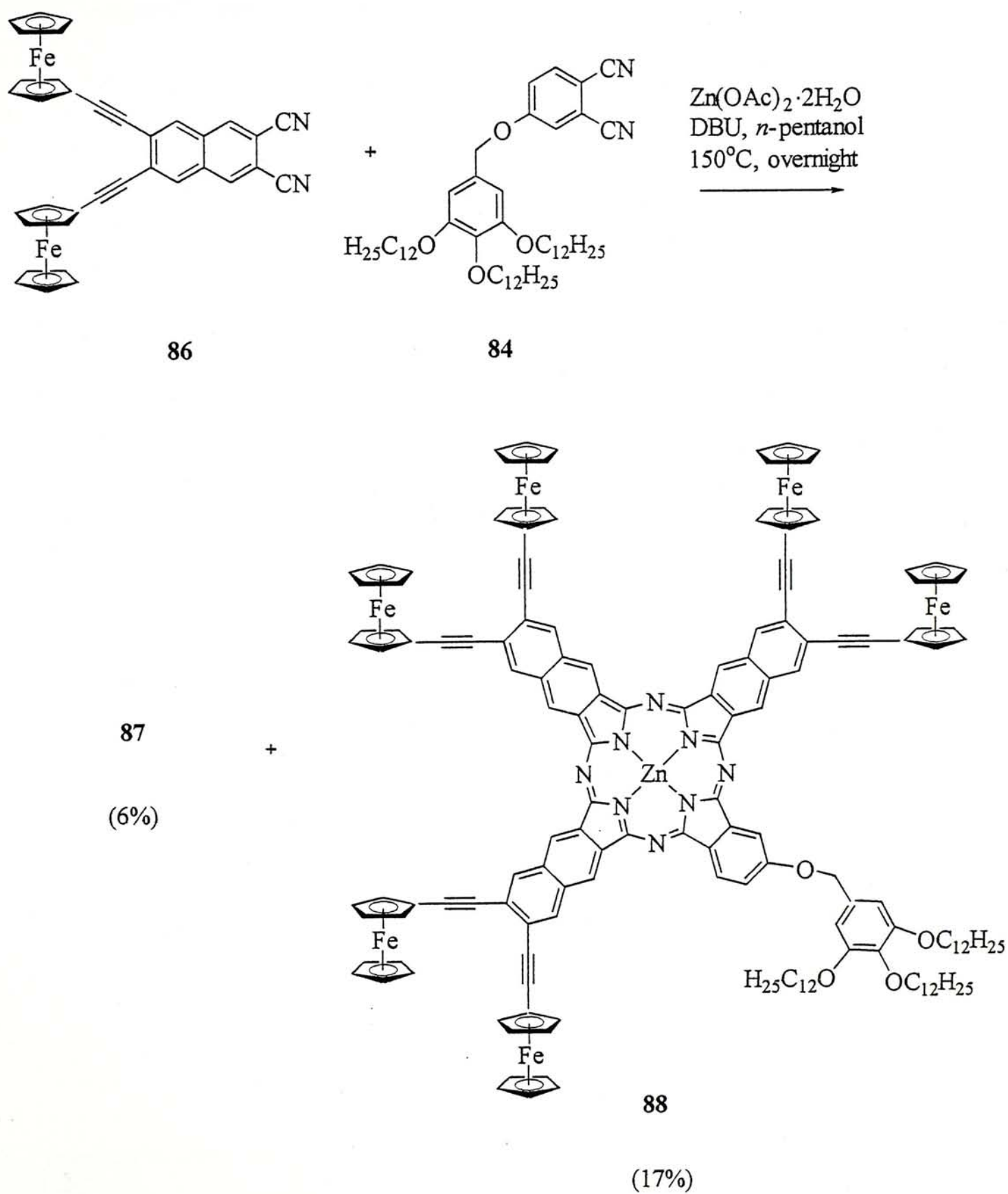
**Figure 33.** UV-Vis spectrum of **88** in THF.



Scheme 18

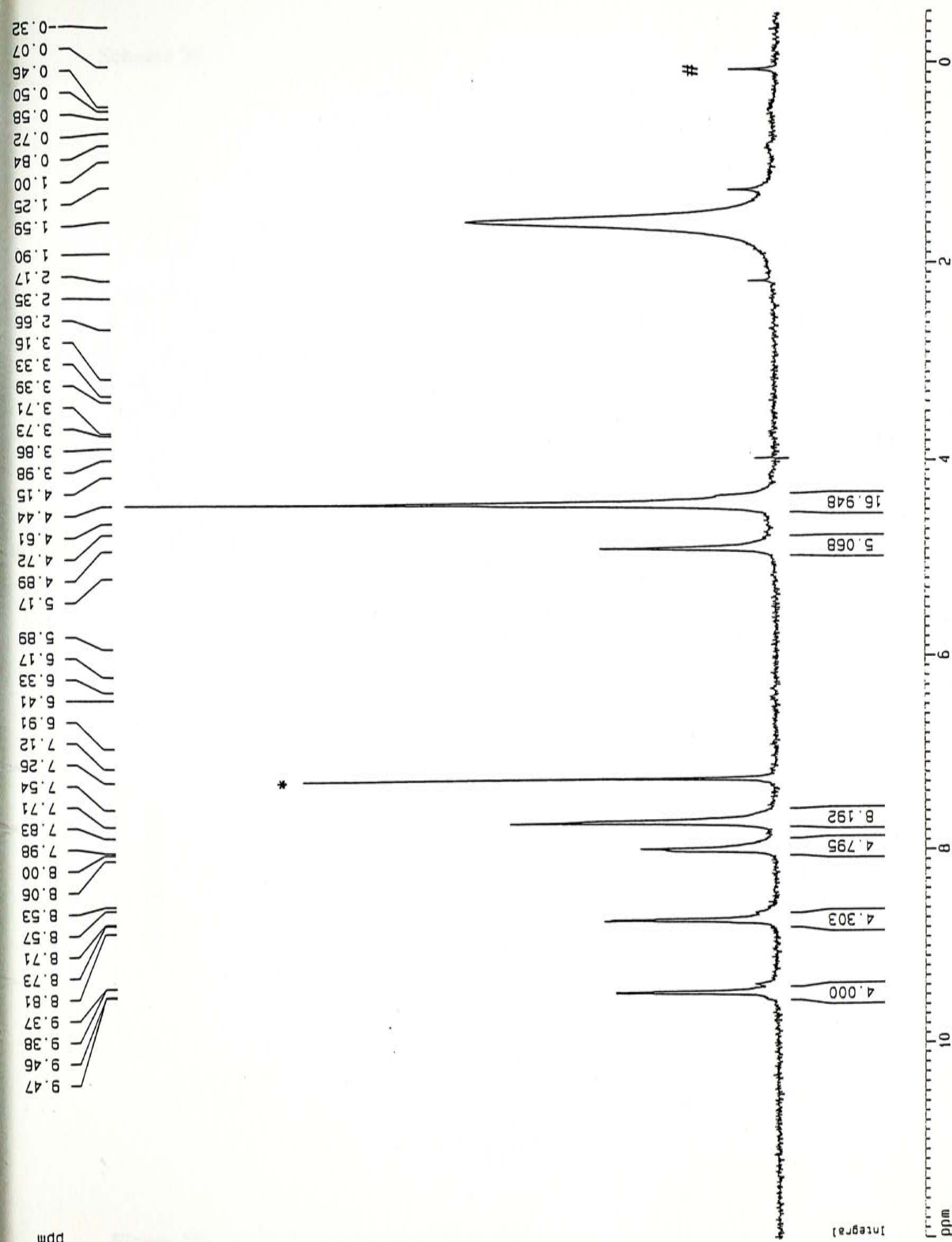


Scheme 19



### 2.2.1.3 Preparation of 5,15-bis(ferrocenylethynyl)-10,20-diphenylporphyrinato-nickel(II) (**90**)

The bis(ferrocenyl)porphyrin **90** was prepared by palladium-catalyzed coupling reaction of **72** and dibromo-porphyrin **89**, which could be prepared readily by the literature method.<sup>64</sup> (Scheme 20). Figure 34 displays the <sup>1</sup>H NMR spectrum of **90** in CDCl<sub>3</sub>, which shows two downfield doublets at  $\delta$  9.46 and 8.72 assignable to the pyrrolic protons, two broad signals at  $\delta$  8.00 and 7.71 assignable to the phenyl protons, and two broad signals at  $\delta$  4.89 and 4.44 which are due to the ferrocenyl protons. The UV-Vis spectrum of **90** (Figure 35) is typical for metalloporphyrins and exhibits a Q band at 624 nm and a Soret band at 433 nm. As expected, the Soret band of **90** is significantly shifted to the red by comparing with that of **89** (420 nm), due to the two conjugated ferrocenylethynyl moieties. No fluorescence emission of **83**, **87**, and **90** in CHCl<sub>3</sub> could be observed. As ferrocene is a well known electron donor, the quenching could be attributed to a photo-induced electron transfer process in which an electron is transfer for one of the ferrocenyl groups to the excited macrocyclic core.





Scheme 20

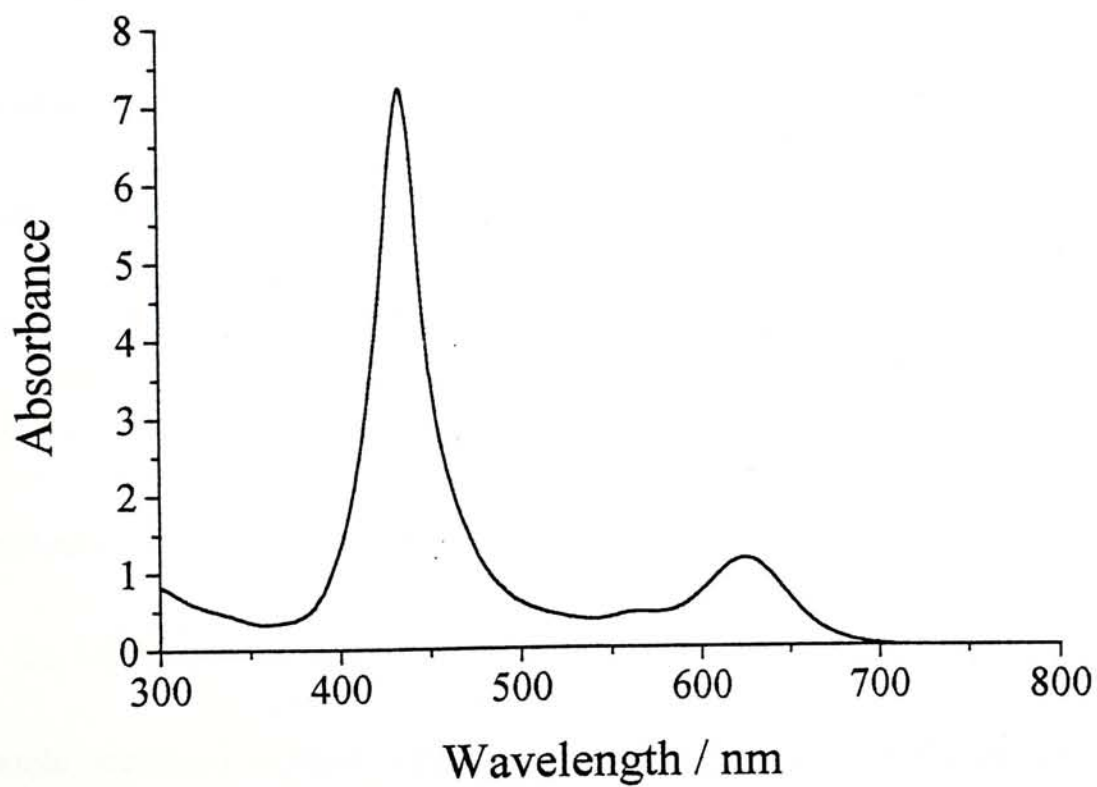
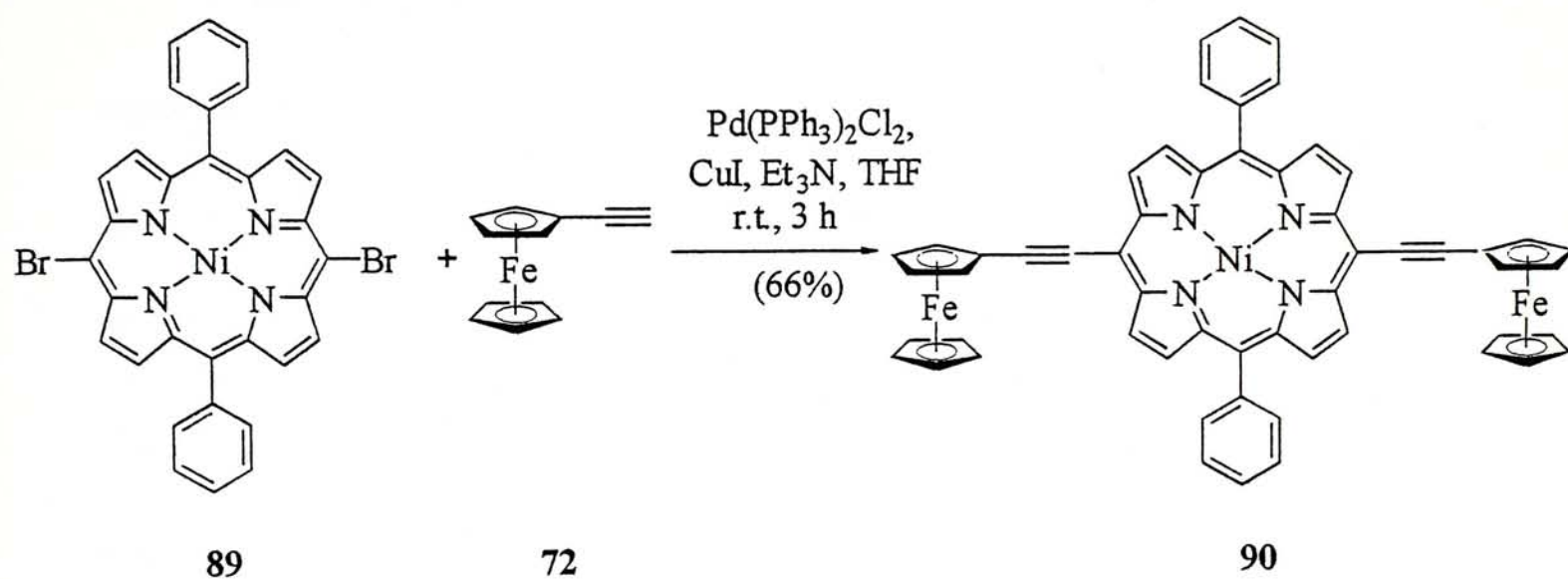


Figure 35. UV-Vis spectrum of **90** in THF.

### 2.2.2 *Electrochemical Studies*

The electrochemical properties of the ferrocenyl phthalonitrile **82**, naphthalonitrile **86**, and the tetrapyrrole derivatives **83**, **87**, and **90** were investigated by cyclic voltammetry and the data are summarized in Table 8. The voltammograms of the dinitriles **82** and **86** in  $\text{CH}_2\text{Cl}_2$  exhibited two couples at ca. 0.3 and  $-1.7$  V (Table 8), which can be attributed to the oxidation of the ferrocenyl groups and the reduction of the cyano-benzene on naphthalene moieties, respectively. The  $\text{Fc}/\text{Fc}^+$  potentials are more positive while the ring reduction potentials are less negative by comparing with those of the dinitriles **54**, **60**, and **64** (Table 7). These results showed that, due to the conjugation effects, the oxidation of the ferrocenyl moieties is more difficult and the reduction of the dicyanobenzene and naphthalene becomes easier in **82** and **86**. Based on the separation between the anodic and cathodic potentials ( $\Delta E$ ), all these couples were regarded as quasi-reversible, except the ferrocenyl oxidation of **86** which was basically irreversible. After adding ferrocene to the solutions of these dinitriles, the cathodic and anodic currents for the  $\text{Fc}/\text{Fc}^+$  couple increased without significantly shifting or splitting the potentials. This indicated that the ferrocenyl units in these dinitriles are electrochemically very similar to free ferrocene. As the peak currents for the  $\text{Fc}/\text{Fc}^+$  couple were approximately

two-fold higher than those for the ring reduction, the former may be attributed to a two-electron redox process.

Figures 36-38 give the cyclic voltammograms of **83**, **87**, and **90** using a platinum disc working electrode. Both voltammograms of **83** and **87** show a quasi-reversible oxidation at 230-250 mV due to the ferrocenyl substituents, and for the latter, two more quasi-reversible ring reduction processes are also revealed (Figures 36 and 37). As shown in Figure 38, the voltammogram of the porphyrin analog **90** displays extra oxidation couples. The oxidation wave at 0.31 V is due to the  $\text{Fc}/\text{Fc}^+$  oxidation while the two other waves at ca. 0.8 V are due to the  $\text{Ni(II)}/\text{Ni(III)}$  and porphyrin ring oxidation. It is worth noting that the anodic peaks for the oxidation couples diminished and vanished eventually after repeated scans. This is probably due to the deposition of insoluble oxidized species on the electrode surface, which can be remedied by polishing the electrode surface after every scan. Based on the peak currents for the  $\text{Fc}/\text{Fc}^+$  couple and the  $\text{ring}/\text{ring}^-$  couple, it is likely that the oxidation of the ferrocenyl groups is a multi-electron process.

All the voltammograms exhibit no splitting of the ferrocenyl couple even at a very slow scan rate (up to  $10 \text{ mV s}^{-1}$ ). Interestingly, when a platinum microsphere working electrode was used, the ferrocenyl couple for all these tetrapyrrole derivatives exhibited a splitting at slow scan rates. As shown in Figure 39, there are

two poorly-resolved couples for the oxidation of ferrocene with a separation of 63 mV (Table 9). This suggests that the ferrocenyl units in **83** are weakly coupled. The voltammograms of **87** and **90** are peculiar (Figures 40 and 41). There is a diffusion controlled anodic peak but the cathodic peak is clearly split into two. Moreover, adsorption of the oxidized product on the electrode is significant, in particular, for the naphthalocyanine **87**. The splitting of the cathodic peak may also be ascribed to a metal-metal interaction. However, it is also possible that there are two different types of layers on the electrode surface which undergo electrochemical reduction at different potentials. Thus, the exact origin for the splitting remains elusive and further investigation is needed to clarify this point.



Ferrocene				Dinitrile/Tetrapyrrole								
Compound	$E_{1/2}(\text{ox})$	$\Delta E^b$	$ i_{\text{pa}}/i_{\text{pc}} $	$E_{1/2}(\text{ox})$	$\Delta E^b$	$ i_{\text{pa}}/i_{\text{pc}} $	$E_{1/2}(\text{red1})$	$\Delta E^b$	$ i_{\text{pa}}/i_{\text{pc}} $	$E_{1/2}(\text{red2})$	$\Delta E^b$	$ i_{\text{pa}}/i_{\text{pc}} $
82	393	98	1.25	-----	---	----	-1630	100	1.38	-----	---	----
86 <sup>c</sup>	303	214	2.89	-----	---	----	-1786	88	1.68	-----	---	----
83 <sup>d,e</sup>	250	1.24	1.35	-----	---	----	-----	---	----	-----	---	----
87 <sup>d</sup>	230	100	1.74	-----	---	----	-1280	100	1.16	-1707	55	2.15
90 <sup>f</sup>	314	108	0.52	917	190	1.84	-1424	104	0.66	-----	---	----

<sup>a</sup> Recorded with  $[\text{Bu}_4\text{N}][\text{ClO}_4]$  as electrolyte in  $\text{CH}_2\text{Cl}_2$  (0.1 mol dm<sup>-3</sup>) at ambient temperature with a scan rate of 100 mV s<sup>-1</sup>, unless otherwise stated. Potentials are expressed in mV vs. Ag-Ag<sup>+</sup> in MeCN. <sup>b</sup>  $\Delta E = |E_{\text{pc}} - E_{\text{pa}}|$ . <sup>c</sup>  $[\text{Bu}_4\text{N}][\text{PF}_6]$  as electrolyte. <sup>d</sup> In THF with a scan rate of 20 mV s<sup>-1</sup>. <sup>e</sup> The couples due to the phthalocyanine are too weak to be observed. <sup>f</sup> The Ni(II)/Ni(III) couple appears at 841 mV with a  $\Delta E$  value of 239 mV.

Table 8. Electrochemical data of the dinitriles 82 and 86, and the tetrapyrroles 83, 87, and 90, using a platinum disc working electrode. <sup>a</sup>

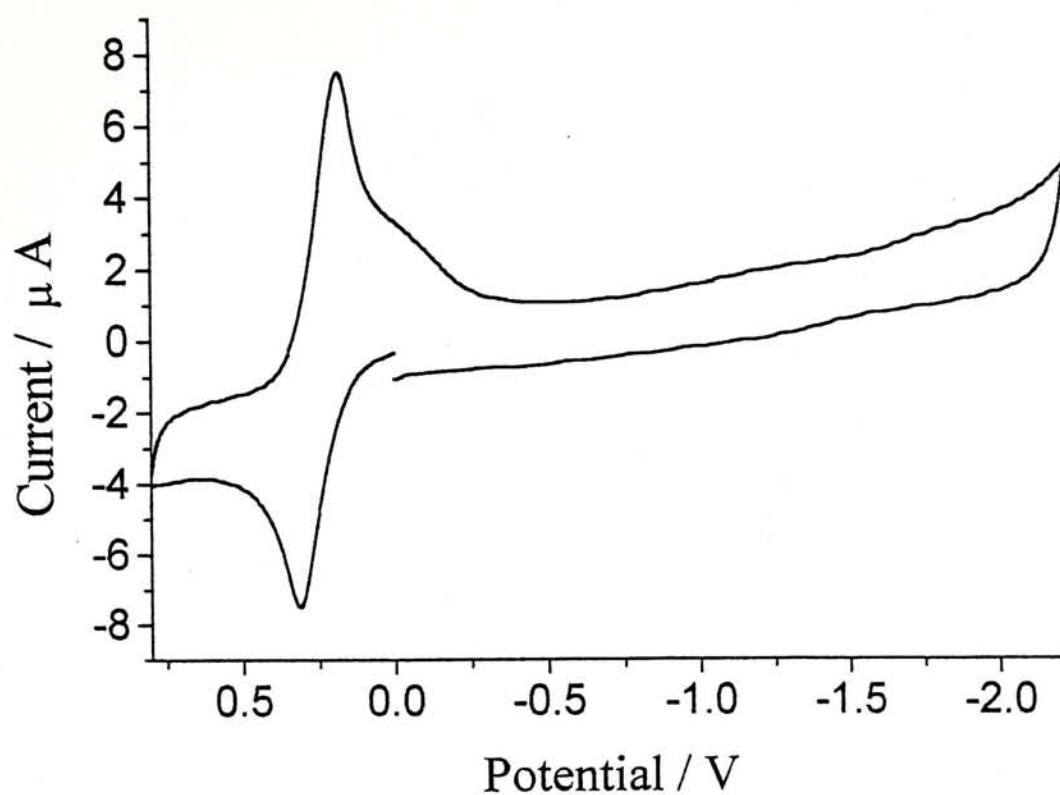


**Figure 36.** Cyclic voltammogram of **83** in THF containing 0.1 M [NBu<sub>4</sub>][ClO<sub>4</sub>] at a scan rate of 20 mV s<sup>-1</sup> (using a platinum disc working electrode).

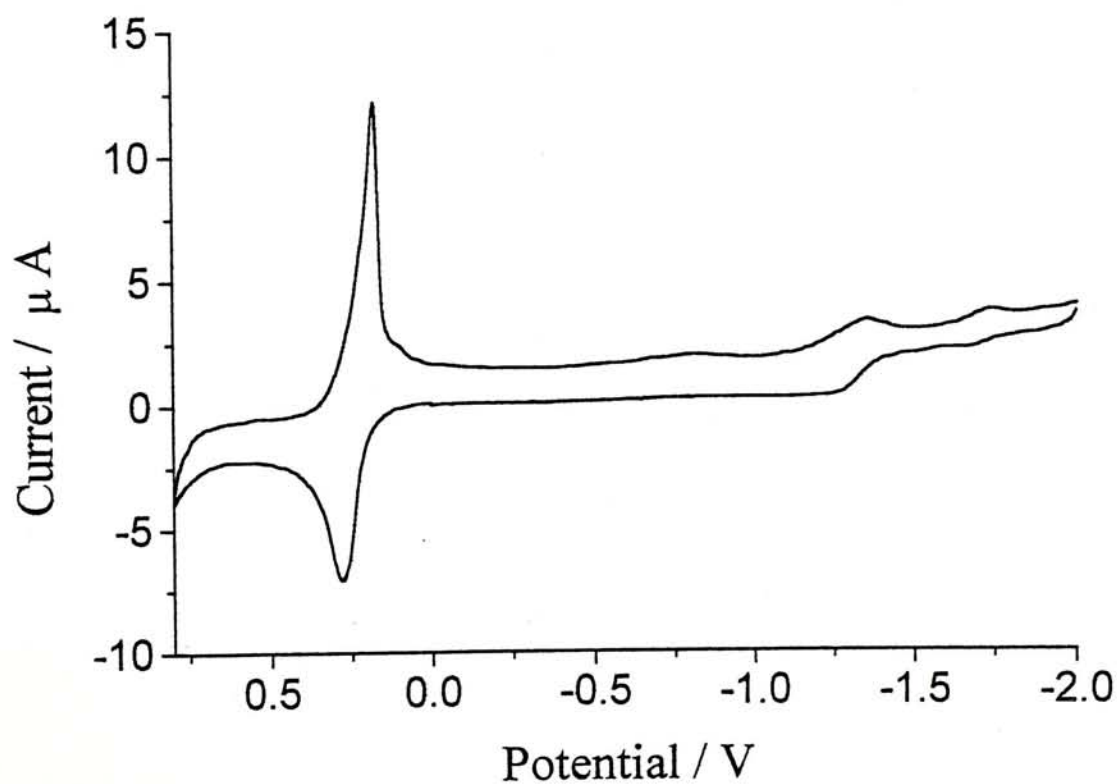


**Figure 37.** Cyclic voltammogram of **87** in THF containing 0.1 M [NBu<sub>4</sub>][ClO<sub>4</sub>] at a scan rate of 20 mV s<sup>-1</sup> (using a platinum disc working electrode).

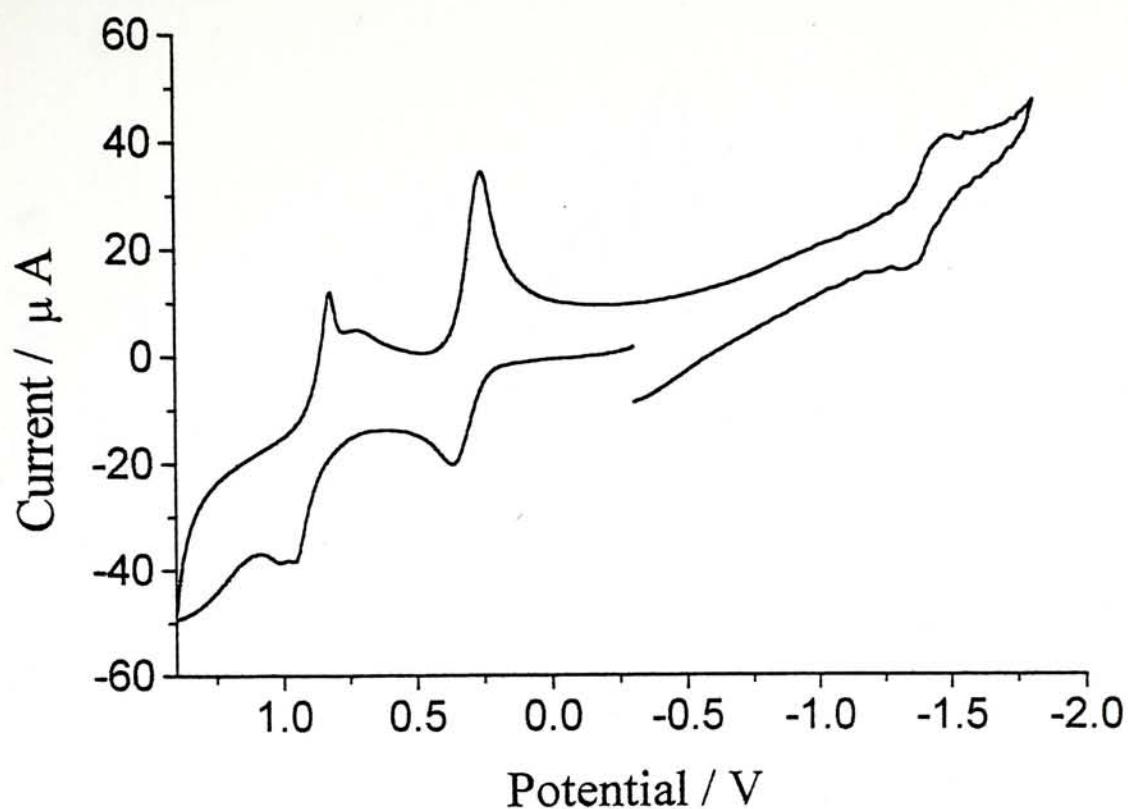


**Figure 38.** Cyclic voltammogram of **90** in  $\text{CH}_2\text{Cl}_2$  containing 0.1 M  $[\text{NBu}_4][\text{ClO}_4]$  at a scan rate of  $100 \text{ mV s}^{-1}$  (using a platinum disc working electrode).

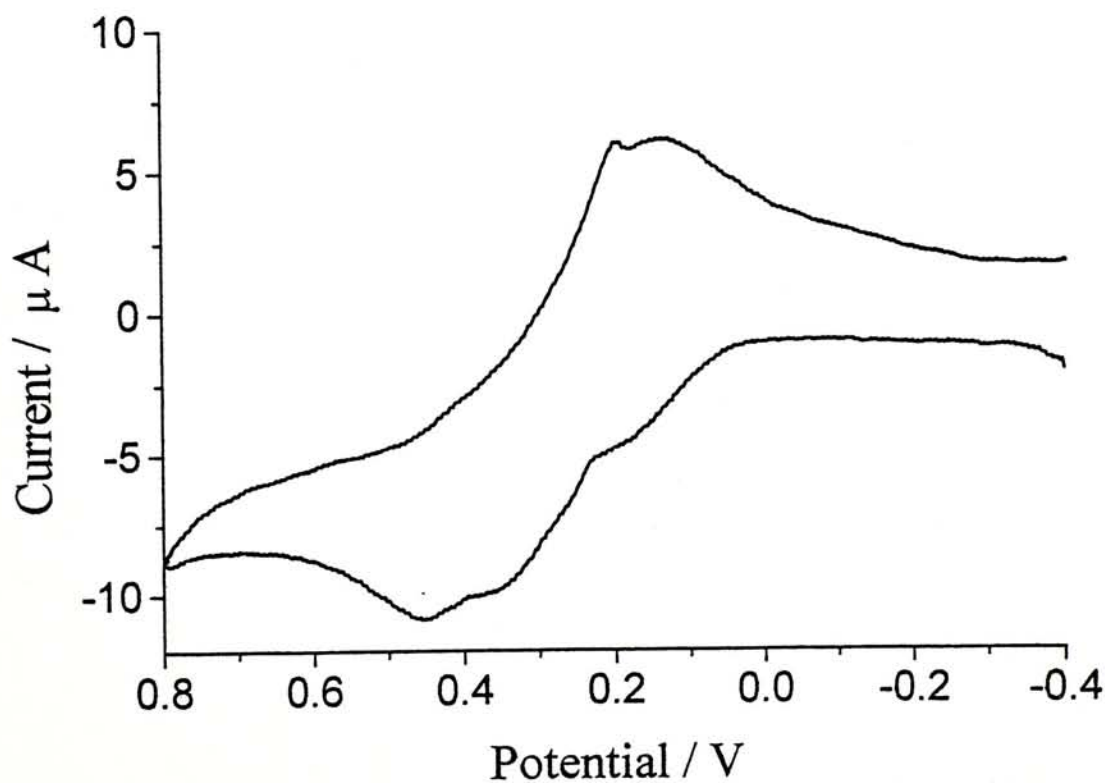


**Figure 39.** Cyclic voltammogram of **83** in THF containing 0.1 M  $[\text{NBu}_4][\text{ClO}_4]$  at a scan rate of  $20 \text{ mV s}^{-1}$  (using a platinum microsphere working electrode).

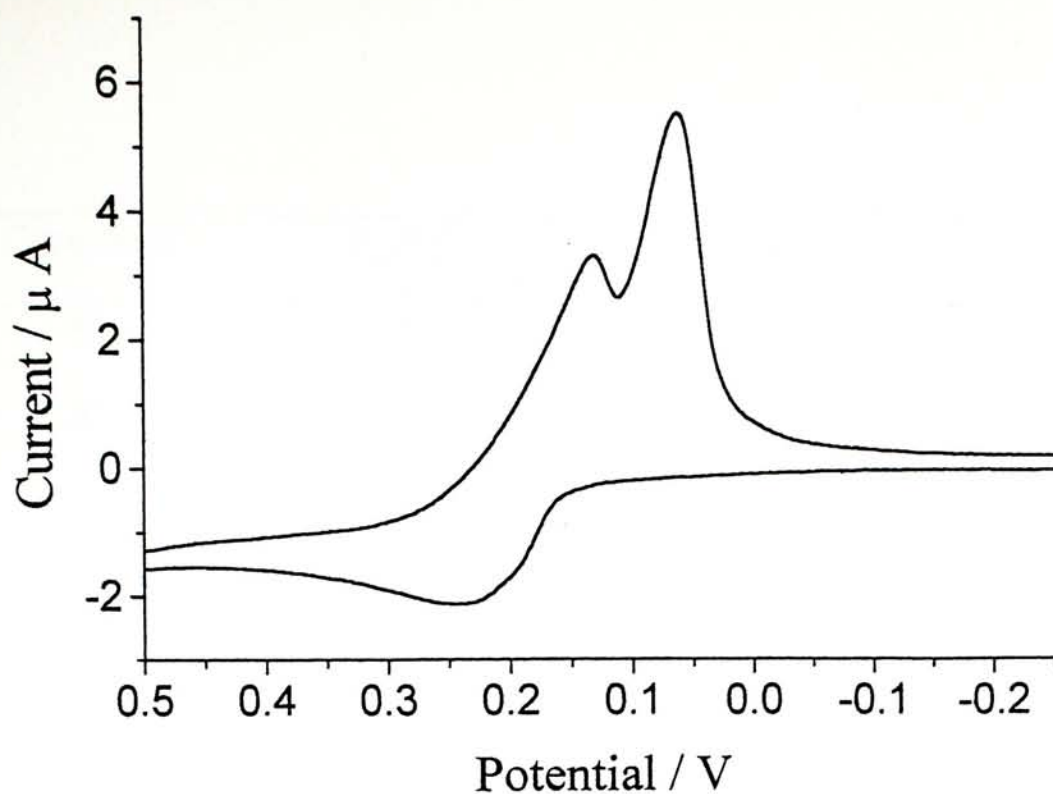


**Figure 40.** Cyclic voltammogram of **87** in THF containing 0.1 M  $[\text{NBu}_4][\text{ClO}_4]$  at a scan rate of  $20 \text{ mV s}^{-1}$  (using a platinum microsphere working electrode).

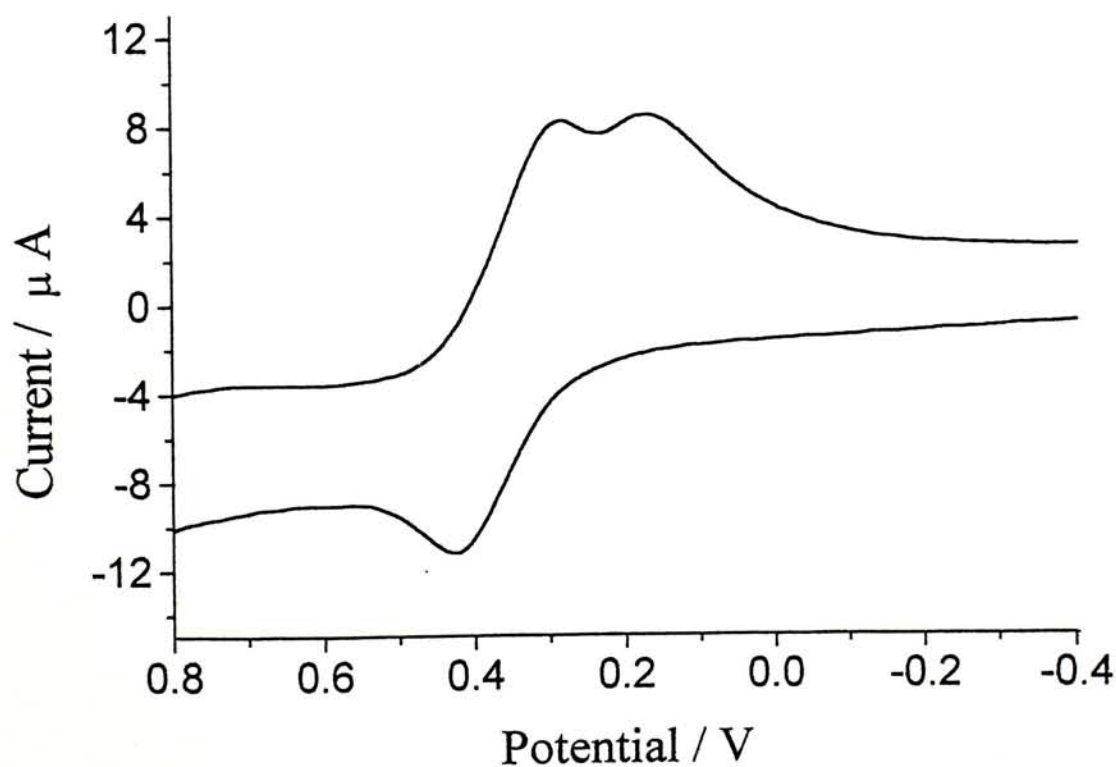


**Figure 41.** Cyclic voltammogram of **90** in  $\text{CH}_2\text{Cl}_2$  containing 0.1 M  $[\text{NBu}_4][\text{ClO}_4]$  at a scan rate of  $10 \text{ mV s}^{-1}$  (using a platinum microsphere working electrode).



Compound	$E_{pc}(1)^b$	$E_{pc}(2)^b$	$\Delta E$
<b>83</b>	137	200	63
<b>87</b>	64	133	69
<b>90<sup>c</sup></b>	174	286	112

<sup>a</sup> Recorded with  $[NBu_4][ClO_4]$  as electrolyte in THF ( $0.1 \text{ mol dm}^{-3}$ ) at ambient temperature with a scan rate of  $20 \text{ mV s}^{-1}$ , unless otherwise stated. <sup>b</sup>  $E_{pc}$  = cathodic potential. <sup>c</sup> In  $CH_2Cl_2$  with a scan rate of  $10 \text{ mV s}^{-1}$ .

**Table 9.** Electrochemical data of the  $Fc/Fc^+$  couples for **83**, **87**, and **90** using a platinum microsphere working electrode.<sup>a</sup>

## 2.3 Conclusion

We have prepared two series of ferrocenyl tetrapyrrole derivatives. The first series contains four, eight, and sixteen 2-ferrocenylethoxy moieties on the periphery of a zinc(II) phthalocyanine core. Due to the saturated nature of the linkers, the ferrocenyl units appear to be electrochemically independent and oxidize at the same potential. In the other series, the ferrocenyl groups are connected to a porphyrin, phthalocyanine, and 2,3-naphthalocyanine core through unsaturated ethynyl bridges. Electrochemical studies showed that the redox-active ferrocenyl units are weakly coupled in these systems.

### 3. EXPERIMENTAL SECTION

#### 3.1 General Methods

Reactions were performed under an atmosphere of nitrogen. THF and diethyl ether were distilled from sodium benzophenone ketyl. *n*-Pentanol and *n*-hexanol were distilled from sodium prior to use. Triethylamine was distilled from potassium hydroxide. Hexanes used in column chromatography and petroleum ether were distilled from anhydrous  $\text{CaCl}_2$ . Column chromatographic purifications were carried out on silica gel column (Macherey-Nagel, 70-230 mesh) with the indicated eluents unless otherwise stated. The electrolyte  $[\text{Bu}_4\text{N}][\text{ClO}_4]$  and  $[\text{Bu}_4\text{N}][\text{PF}_6]$  were recrystallized from dry acetone and THF, respectively, three times prior to use. All other reagents and solvents were of reagent grade and used as received.

#### 3.2 Physical Measurements

Melting points were uncorrected.  $^1\text{H}$  and  $^{13}\text{C}$  NMR spectra were recorded on a Bruker DPX300 spectrometer ( $^1\text{H}$ , 300;  $^{13}\text{C}$ , 75.4 MHz) in  $\text{CDCl}_3$  solutions unless otherwise stated. Spectra were referenced internally using the residual solvent ( $^1\text{H}$ :  $\text{CDCl}_3$ ,  $\delta$  7.26) or solvent ( $^{13}\text{C}$ :  $\text{CDCl}_3$ ,  $\delta$  77.0) resonances relative to

SiMe<sub>4</sub>. IR spectra were measured on a Nicolet Magna 550 FT-IR spectrometer as KBr pellets. UV-Vis and fluorescence spectra were taken on a Hitachi U-3300 spectrophotometer and Hitachi F-4500 spectrofluorometer, respectively. LSI mass spectra were recorded on a Bruker APEX 47e FT-ICR mass spectrometer with a 3-nitrobenzyl alcohol matrix. MALDI-TOF spectra were obtained on a Bruker bench TOF mass spectrometer equipped with a standard UV-laser desorption source, using  $\alpha$ -cyano-4-hydroxycinnamic acid as matrix. Elemental analyses were performed by the Shanghai Institute of Organic Chemistry, Chinese Academy of Sciences.

Electrochemical measurements were carried out on a BAS CV-50W voltammetric analyzer. The cell comprised inlets for a platinum-sphere (or platinum disk) working electrode, a platinum-plate counter electrode, and a Ag-AgNO<sub>3</sub> (0.1 mol dm<sup>-3</sup> in MeCN) reference electrode which was connected to the solution by a Luggin capillary whose tip was placed close to the working electrode. Typically, a 0.1 mol dm<sup>-3</sup> solution of [Bu<sub>4</sub>N][PF<sub>6</sub>] in CH<sub>2</sub>Cl<sub>2</sub> (unless otherwise stated) containing 1.0 mmol dm<sup>-3</sup> of sample was purged with nitrogen for 20 min., then the voltammograms were recorded at ambient temperature. Potentials were referenced to the Ag-Ag<sup>+</sup> couple in MeCN.



### 3.3 Synthesis of Ferrocenylphthalocyanines with Oxyethylene Linkers

**Acetylferrocene (49).**<sup>41</sup> A mixture of ferrocene (34 g, 0.18 mol), acetic anhydride (90.0 mL, 0.95 mmol), and 85% phosphoric acid (7.3 mL, 0.13 mmol) was stirred at 100°C for 1 h. The resulting mixture was briefly cooled then poured into ice (500 mL), and was allowed to stand overnight.  $\text{Na}_2\text{CO}_3$  (73 g) was added carefully to neutralize the mixture. The orange-brown paste was filtered and washed with water (4 x 100 mL). The product was purified by column chromatography with hexanes as eluent first to remove all the unreacted ferrocene and then with ethyl acetate to afford an orange-brown solid (9.4 g, 69%).  $^1\text{H}$  NMR:  $\delta$  4.77 (t,  $J = 1.8$  Hz, 2 H, Fc), 4.50 (t,  $J = 1.8$  Hz, 2 H, Fc), 4.20 (s, 5 H, Fc), 2.39 (s, 3 H,  $\text{CH}_3$ ).

**Thiomorphylamidomethylferrocene (50).**<sup>41</sup> A mixture of 49 (9.5 g, 41.7 mmol), sulfur (1.9 g, 59.0 mmol), and morpholine (2.5 mL, 59.0 mmol) was stirred at 130°C for 2.5 h. The resulting dark brown mixture was extracted with hot methanol (150 mL) which was then poured into water (4 L) to precipitate the product. The product was collected by suction filtration and purified by column chromatography with ethyl acetate as eluent to afford an orange solid (4.0 g, 29%).  $^1\text{H}$  NMR:  $\delta$  4.28 (t,  $J = 4.5$  Hz, 2 H, Fc), 4.23 (br. s, 2 H, Fc), 4.17 (s, 5 H, Fc), 4.11 (br. s, 2 H,  $\text{CH}_2$ ), 4.07 (br. s, 2 H,  $\text{CH}_2$ ), 3.71 (m, 4 H,  $\text{CH}_2$ ), 3.53 (m, 2 H,  $\text{CH}_2$ ).

**2-Ferrocenylethanoic acid (51).**<sup>41</sup> A mixture of **50** (929 mg, 2.8 mmol) and KOH (1 g, 18 mmol) in methanol (13 mL) was stirred at reflux for 17 h. The resulting mixture was poured into ice water (200 mL) which was washed with diethyl ether (200 mL) to remove unreacted **50**. The aqueous layer was collected and neutralized with conc. HCl to give a fine yellow precipitate which was filtered and then purified by column chromatography with ethyl acetate as eluent to give a yellow solid (200 mg, 29%). <sup>1</sup>H NMR:  $\delta$  4.25 (br. s, 2 H, Fc), 4.16 (br. s, 7 H, Fc), 3.38 (s, 2 H, CH<sub>2</sub>).

**2-Ferrocenylethanol (52).**<sup>41</sup> To a suspension of LiAlH<sub>4</sub> (0.78 g, 20.0 mmol) in THF (50 mL) was added dropwise a solution of **51** (2.0 g, 8.2 mmol) in THF (100 mL). The mixture was stirred at r.t. for 1 h, then water (10 mL) was added to destroy the excess LiAlH<sub>4</sub>. The resulting mixture was extracted with diethyl ether (3 x 40 mL) and the combined extracts were dried and evaporated. The residue was purified by column chromatography with ethyl acetate as eluent to afford a brown solid (1.4 g, 74%). <sup>1</sup>H NMR:  $\delta$  4.14 (s, 9 H, Fc), 3.72 (q,  $J = 4.8$  Hz, 2 H, CH<sub>2</sub>), 2.59 (t,  $J = 6.6$  Hz, 2 H, CH<sub>2</sub>), 1.65 (br. s, 1 H, OH). <sup>13</sup>C {<sup>1</sup>H} NMR:  $\delta$  84.9, 68.6, 68.5, 67.7, 63.4, 32.8.

**3-(2-Ferrocenylethoxy)phthalonitrile (54)** – A mixture of **52** (1.15 g, 5.0 mmol), 3-nitrophthalonitrile (**53**) (0.43 g, 2.5 mmol) and potassium carbonate



(0.69 g, 5.0 mmol) in DMF (3 mL) was stirred at r.t. for 21 h. The volatiles were then removed under reduced pressure giving a brown precipitate which was subjected to chromatography using THF/hexane (1 : 4) as eluent. Compound **54** was isolated as orange-yellow microcrystals (0.24 g, 27%; mp 163-166°C).  $^1\text{H}$  NMR ( $\text{CD}_3\text{SOCD}_3$ ):  $\delta$  7.84 (dd,  $J = 7.5, 8.4$  Hz, 1 H, ArH), 7.66 (d,  $J = 8.4$  Hz, 1 H, ArH), 7.64 (d,  $J = 7.5$  Hz, 1 H, ArH), 4.32 (t,  $J = 6.6$  Hz, 2 H,  $\text{OCH}_2$ ), 4.23 (t,  $J = 1.8$  Hz, 2 H, Fc), 4.15 (s, 5 H, Fc), 4.08 (t,  $J = 1.8$  Hz, 2 H, Fc), 2.80 (t,  $J = 6.6$  Hz, 2 H,  $\text{FcCH}_2$ ).  $^{13}\text{C}$   $\{^1\text{H}\}$  NMR:  $\delta$  161.3, 134.4, 125.0, 117.0, 116.6, 115.3, 113.1, 104.9, 83.8, 70.6, 69.3, 69.0, 68.2, 29.6. IR (KBr):  $\nu = 2227\text{m cm}^{-1}$  ( $\text{C}\equiv\text{N}$ ). HRMS (LSI):  $m/z$  calcd for  $\text{C}_{20}\text{H}_{16}^{56}\text{FeN}_2\text{O}$  ( $\text{M}^+$ ) 356.0612, found 356.0607. Anal. Calcd for  $\text{C}_{20}\text{H}_{16}\text{FeN}_2\text{O}$ : C, 67.44; H, 4.53; N, 7.86. Found: C, 67.45; H, 4.54; N, 7.81.

**Tetrakis(2-ferrocenylethoxy)phthalocyaninatozinc (II) (55)** – A mixture of **54** (100 mg, 0.28 mmol) and  $\text{Zn}(\text{OAc})_2 \cdot 2\text{H}_2\text{O}$  (22 mg, 0.10 mmol) in *n*-hexanol (3 mL) was heated to 90°C, then DBU (0.01 mL, 0.07 mmol) was added. The mixture was stirred at 150°C for 16 h, then the volatiles were removed under reduced pressure. The resulting deep green residue was subjected to chromatography using  $\text{CHCl}_3$  as eluent to give **55** as a green solid (80 mg, 77%).  $^1\text{H}$  NMR:  $\delta$  8.38-8.98 (m, 4 H, ArH), 7.66-8.08 (m, 4 H, ArH), 7.00-7.64 (m, 4 H, ArH), 4.54-4.92 (m, 8 H,  $\text{OCH}_2$ ), 4.02-4.38 (m, 36 H, Fc), 2.86-3.50 (m, 8 H,  $\text{FcCH}_2$ ). UV-Vis (THF) [ $\lambda_{\text{max}}$  nm (log

$\epsilon$ ]: 316 (5.41), 347 (5.35), 629 (5.29), 664 (sh), 698 (5.94). MS (MALDI-TOF): an isotopic cluster peaking at  $m/z$  1490.2 ( $M^+$ ). Anal. Calcd for  $C_{80}H_{64}Fe_4N_8O_4Zn$ : C, 64.48; H, 4.33; N, 7.52. Found: C, 65.28; H, 4.63; N, 7.32.

**Ferrocenecarboxylic acid (44).**<sup>45</sup> To a solution of ferrocene (10 g, 54 mmol) in diethyl ether (120 mL) was added *n*-BuLi in 1.6 M *n*-hexanes (35 mL, 56 mmol). The reaction mixture was stirred at r.t. for 2 days, then poured into a beaker of dry ice (600 mL). Water (150 mL) was added after all the dry ice evaporated to give two layers. The aqueous layer was separated and acidified with conc. HCl until all the product precipitated. The orange powder (3.5 g, 28%) was filtered and dried under vacuum.  $^1H$  NMR:  $\delta$  4.87 (br. s, 2 H, Fc), 4.48 (br. s, 2 H, Fc), 4.27 (s, 5 H, Fc). IR (KBr):  $\nu = 1643s$  (C=O)  $cm^{-1}$ .

**Ferrocenecarbonyl chloride (56).**<sup>45</sup> To a solution of **44** (460mg, 2.0 mmol) in petroleum ether (bp 40–60°C) (20 mL) was added dropwise an excess of thionyl chloride (1.3 mL, 16 mmol) at r.t. The resulting mixture was heated to 50°C for 2 h, then the solvent was removed under reduced pressure and the residue was extracted with petroleum ether (bp 40–60°C) (3 x 50 mL). The combined extracts were evaporated using a rotatory evaporator to afford a red solid which was used without further purification (278 mg, 56%).  $^1H$  NMR:  $\delta$  4.92 (br. s, 2 H, Fc), 4.64 (br. s, 2 H, Fc), 4.34 (s, 5 H, Fc). IR (KBr):  $\nu = 1751s$   $cm^{-1}$  (C=O).



**3,6-Bis(ferrocenecarboxylate)phthalonitrile (58).** To a solution of 2,3-dicyanohydroquinone (**57**) (144 mg, 0.9 mmol) in  $\text{CH}_2\text{Cl}_2$  (100 mL) was added triethylamine (0.5 mL, 3.6 mmol). The resulting mixture was stirred at r.t. for 5 min, then a solution of **56** (894 mg, 3.6 mmol) in  $\text{CH}_2\text{Cl}_2$  (20 mL) was added via a dropping funnel. The resulting mixture was refluxed overnight, then the volatiles were evaporated in vacuo to give an orange powder which was purified by column chromatography with ethyl acetate and hexane (1 : 3) as eluent (150 mg, 29%).  $^1\text{H}$  NMR:  $\delta$  7.74 (s, 2 H, ArH), 5.03 (br. s, 4 H, Fc), 4.62 (br. s, 4 H, Fc), 4.38 (s, 10 H, Fc).  $^{13}\text{C}$   $\{^1\text{H}\}$  NMR:  $\delta$  169.0, 150.4, 128.7, 112.0, 73.0, 71.0, 70.6, 67.4. IR (KBr):  $\nu$  = 2238w ( $\text{C}\equiv\text{N}$ ), 1708s ( $\text{C}=\text{O}$ )  $\text{cm}^{-1}$ . MS (LSI):  $m/z$  584 ( $\text{M}^+$ ).

**1-Chloro-2-ferrocenylethane (59).**<sup>46</sup> To a solution of **52** (500 mg, 2.18 mmol) in THF (30 mL) was added  $\text{SOCl}_2$  (0.3 mL, 4.1 mmol) at  $0^\circ\text{C}$ . The mixture was stirred at this temperature for 1 h, then at r.t. for a further 1 h. The resulting mixture was poured into ice (50 mL) before being extracted with  $\text{CH}_2\text{Cl}_2$  (3 x 30 mL). The combined extracts were washed with saturated aqueous  $\text{NaHCO}_3$  solution and  $\text{H}_2\text{O}$ , and then dried over anhydrous  $\text{Na}_2\text{SO}_4$ . After removing the volatiles under reduced pressure, the residue was purified by column chromatography with hexanes as eluent to give a yellow solid (324 mg, 60%).  $^1\text{H}$  NMR:  $\delta$  4.11 (br. s, 9 H, Fc), 3.60 (t,  $J$  = 7.5 Hz, 2 H,  $\text{OCH}_2$ ), 2.81 (t,  $J$  = 7.5 Hz, 2 H,  $\text{FcCH}_2$ ).  $^{13}\text{C}$   $\{^1\text{H}\}$  NMR:  $\delta$  85.2, 69.2,

69.0, 68.3, 45.2, 34.0. MS (EI):  $m/z$  248 ( $M^+$ ).

**2-Ferrocenylethyl tosylate (61).**<sup>46</sup> A mixture of **52** (1.0 g, 4.4 mol) and *p*-toluenesulfonyl chloride (1.0 g, 5.2 mol) in pyridine (5 mL) was stirred at 0°C for 3 h. The resulting brown solution was poured into ice (50 g) and extracted with  $\text{CHCl}_3$  (3 x 50 mL). The combined solution was successively washed with 5% HCl solution, a saturated aqueous  $\text{NaHCO}_3$  solution, and  $\text{H}_2\text{O}$ . The extract was dried with anhydrous  $\text{Na}_2\text{SO}_4$  and evaporated under reduced pressure. The residue was dissolved into hot *n*-hexanes and then filtered. Upon cooling to r.t., orange crystals appeared which were collected and dried in vacuo (1.5 g, 90%).  $^1\text{H}$  NMR  $\delta$  7.74 (d,  $J = 7.5$  Hz, 2 H, ArH), 7.32 (d,  $J = 7.5$  Hz, 2 H, ArH), 4.27 (br. s, 9 H, Fc), 4.06 (br. s, 2 H,  $\text{OCH}_2$ ), 2.54 (br. s, 2 H,  $\text{FcCH}_2$ ), 2.44 (s, 3 H,  $\text{CH}_3$ ).

**3,6-Bis(2-ferrocenylethoxy)phthalonitrile (60).** A mixture of 2,3-dicyanhydroquinone (**57**) (200 mg, 1.25 mmol) and  $\text{K}_2\text{CO}_3$  (700 mg, 5.07 mmol) in DMF (4 mL) was stirred at r.t. for 15 min. Then, **61** (1.0 g, 2.60 mmol) was then added and the mixture was stirred at 90°C for 2 days. The resulting dark brown solution was poured into  $\text{H}_2\text{O}$  (100 mL) then extracted with  $\text{CHCl}_3$  (3 x 50 mL). The combined extracts were dried with anhydrous  $\text{Na}_2\text{SO}_4$  and evaporated in vacuo. The residue was purified by column chromatography using  $\text{CHCl}_3$ /hexane (4 : 1) as eluent to obtain **60** as a yellow solid (400 mg, 55%; mp 198-200°C).  $^1\text{H}$  NMR:  $\delta$



7.04 (s, 2 H, ArH), 4.21 (s, 4 H, Fc), 4.14 (s, 10 H, Fc), 4.11 (s, 4 H, Fc), 4.08 (t,  $J = 6.3$  Hz, 4 H, OCH<sub>2</sub>), 2.87 (t,  $J = 6.3$  Hz, 4 H, FcCH<sub>2</sub>). <sup>13</sup>C {<sup>1</sup>H} NMR:  $\delta$  155.0, 118.2, 113.1, 105.3, 83.5, 70.8, 68.9, 68.6, 67.8, 29.7. IR (KBr):  $\nu = 2227$  cm<sup>-1</sup> (C $\equiv$ N). HRMS (LSI):  $m/z$  calcd for C<sub>32</sub>H<sub>28</sub><sup>56</sup>Fe<sub>2</sub>N<sub>2</sub>O<sub>2</sub> (M<sup>+</sup>) 584.0849, found 584.0856. Anal. Calcd for C<sub>32</sub>H<sub>28</sub>Fe<sub>2</sub>N<sub>2</sub>O<sub>2</sub>: C, 65.78; H, 4.83; N, 4.79. Found: C, 65.18; H, 4.67; N, 4.72.

**1,4,8,11,15,18,22,25-Octakis(2-ferrocenylethoxy)phthalocyaninatozinc (II)**

**(62).** A mixture of **60** (100 mg, 0.17 mmol) and Zn(OAc)<sub>2</sub>·2H<sub>2</sub>O (22 mg, 0.1 mmol) in *n*-pentanol (3 mL) was heated to 90°C, then DBU (0.01 mL, 0.07 mmol) was added. The mixture was stirred at 150°C overnight, then poured into a mixture of methanol and water (1 : 1, 50 mL). The precipitate formed was filtered and chromatographed on a base alumina column using CHCl<sub>3</sub>/THF (5 : 1) as eluent to give **62** as a green powder (54 mg, 53%). <sup>1</sup>H NMR (C<sub>6</sub>D<sub>6</sub>):  $\delta$  7.48 (br. s, 8 H, ArH), 5.04 (br. s, 16 H, OCH<sub>2</sub>), 4.29 (s, 16 H, Fc), 4.07 (s, 40 H, Fc), 3.92 (s, 16 H, Fc), 3.27 (br. s, 16 H, FcCH<sub>2</sub>). UV-Vis (THF) [ $\lambda_{\max}$  nm (log  $\epsilon$ ): 327 (5.15), 661 (5.04), 736 (5.72). MS (MALDI-TOF): an isotopic cluster peaking at  $m/z$  2404.6 (M<sup>+</sup>). Anal. Calcd for C<sub>128</sub>H<sub>112</sub>Fe<sub>8</sub>N<sub>8</sub>O<sub>8</sub>Zn: C, 63.99; H, 4.70; N, 4.66. Found: C, 62.66; H, 4.71; N, 4.45.

**3,4,5,6-Tetrakis(2-ferrocenylethoxy)phthalonitrile (64).** A mixture of **52**

(1.38 g, 6.0 mmol), tetrafluorophthalonitrile **63** (0.10 g, 0.5 mmol) and  $K_2CO_3$  (0.83 g, 6.0 mmol) in DMF (5 mL) was stirred at 100°C for 24 h, then poured into water (50 mL). The mixture was extracted with  $CHCl_3$  (3 x 30 mL) and the combined extracts were dried over anhydrous  $Na_2SO_4$  and removed in a rotatory evaporator. The crude product was purified by column chromatography with toluene as eluent to afford a yellow solid (265 mg, 51%, mp 139-141°C).  $^1H$  NMR:  $\delta$  4.0-4.3 (m, 44 H, Fc &  $OCH_2$ ), 2.76 (br. s, 4 H,  $FcCH_2$ ), 2.67 (br. s, 4 H,  $FcCH_2$ ).  $^{13}C$   $\{^1H\}$  NMR:  $\delta$  152.7, 150.7, 113.1, 104.5, 84.3, 83.8, 75.7, 74.9, 69.3, 69.2, 68.7, 68.2, 67.8, 30.5, 30.4. IR (KBr):  $\nu = 2231\text{ cm}^{-1}$  ( $C\equiv N$ ). MS (LSI): an isotopic cluster peaking at  $m/z$  1040.14 ( $M^+$ ). Anal. Calcd for  $C_{56}H_{52}Fe_4N_2O_4$ : C, 64.65; H, 5.04; N, 2.69. Found: C, 64.54; H, 5.06; N, 2.72.

**Hexadecakis(2-ferrocenylethoxy)phthalocyanine (65).** Lithium (10 mg, 1.44 mmol) was suspended in *n*-octanol (3 mL). The suspension was stirred at 150°C until the solution became clear. The homogenous solution was cooled to 90°C, then dinitrile **64** (100 mg, 0.10 mmol) was added. The temperature was increased to 120°C where the mixture was stirred for 4 h. Glacial acetic acid (3 mL) was then added and the mixture was kept at this temperature for 15 min before being poured into a mixture of methanol and water (1 : 1, 50 mL). The precipitate formed was filtered and subjected to column chromatography with  $CHCl_3$ /THF (10 : 1) as



eluent to give a green powder (15 mg, 15%).  $^1\text{H}$  NMR:  $\delta$  5.08 (br. s, 16 H,  $\text{OCH}_2$ ), 4.58 (br. s, 16 H,  $\text{OCH}_2$ ), 4.35 (br. s, 16 H, Fc), 4.08–4.23 (m, 96 H, Fc), 3.98 (br. s, 32 H, Fc), 3.18 (br. s, 16 H,  $\text{FcCH}_2$ ), 3.08 (br. s, 16 H,  $\text{FcCH}_2$ ). UV-Vis (THF) [ $\lambda_{\text{max}}$  nm (log  $\epsilon$ ): 323 (5.21), 349 (5.16), 386 (5.13), 669 (5.01), 692 (5.04), 732 (sh), 756 (5.62). MS (MALDI-TOF): an isotopic cluster peaking at  $m/z$  4168.6 ( $\text{M}^+$ ). Anal. Calcd for  $\text{C}_{224}\text{H}_{210}\text{Fe}_{16}\text{N}_8\text{O}_{16}$ : C, 64.62; H, 5.08; N, 2.69. Found: C, 64.31; H, 5.21; N, 2.66.

**Ferrocenecarboxyaldehyde (47).**<sup>48</sup> A mixture of DMF (10 mL) and  $\text{POCl}_3$  (11 mL) was stirred at r.t. for 1 h. Ferrocene (5.0 g, 27 mmol) was dissolved in  $\text{CH}_2\text{Cl}_2$  (20 mL) and added dropwise into this Vilsmeier reagent under vigorous stirring. The mixture was then heated at  $50^\circ\text{C}$  for 3 days under an atmosphere of nitrogen. After cooling to r.t., saturated NaOAc (100 mL) was added dropwise to quench the excess  $\text{POCl}_3$ . The mixture was then extracted with chloroform (3 x 50 mL) and the combined extracts were evaporated at reduced pressure. The crude product was purified by column chromatography with benzene as eluent to afford a dark red solid (2.0 g, 35%).  $^1\text{H}$  NMR:  $\delta$  9.96 (s, 1 H, CHO), 4.79 (br. s, 2 H, Fc), 4.61 (br. s, 2 H, Fc), 4.28 (s, 5 H, Fc).

**Ferrocenylmethanol (66).**<sup>48</sup> A suspension of 47 (100 mg, 0.47 mmol) and sodium borohydride (177 mg, 4.7 mmol) in  $\text{CH}_2\text{Cl}_2$  (3 mL) and methanol (7 mL) was

stirred at r.t. for 2 h. Water (20 mL) was then added and the mixture was extracted with chloroform (3 x 30 mL). The combined extracts were dried and the solvent was removed in a rotatory evaporator to give a residue which was purified by column chromatography with chloroform as eluent to obtain a yellow solid (98 mg, 97%).  $^1\text{H}$  NMR:  $\delta$  4.31 (d,  $J$  = 5.1 Hz, 2 H,  $\text{OCH}_2$ ), 4.27 (br. s, 2 H, Fc), 4.21 (s, 7 H, Fc), 1.25 (br. s, 1 H, OH).

**3-(3-Pentyloxy)phthalonitrile (68).**<sup>43</sup> A mixture of **53** (0.43 g, 2.5 mmol), 3-pentanol (**67**) (0.45 g, 5.0 mmol), and  $\text{K}_2\text{CO}_3$  (1.03 g, 10.0 mmol) in DMF (5 mL) was stirred at 60°C overnight, then poured into water (50 mL). The mixture was extracted with diethyl ether (3 x 30 mL) and the combined extracts were dried over anhydrous  $\text{Na}_2\text{SO}_4$  and evaporated using a rotatory evaporator. The crude product was purified by column chromatography with ethyl acetate and hexane (1 : 1) as eluent to afford a white solid (410 mg, 77%).  $^1\text{H}$  NMR:  $\delta$  7.60 (dd,  $J$  = 7.7, 8.6 Hz, 1 H, ArH), 7.30 (d,  $J$  = 7.7 Hz, 1 H, ArH), 7.20 (d,  $J$  = 8.8 Hz, 1 H, ArH), 4.30 (quintet,  $J$  = 5.8 Hz, 1 H, OCH), 1.81-1.61 (m, 4 H,  $\text{CH}_2$ ), 1.01-0.91 (m, 6 H,  $\text{CH}_3$ ).

**1,8,15,22-Tetrakis(3-pentyloxy)phthalocyanine (69).**<sup>43</sup> A suspension of lithium (15 mg, 2.14 mmol) in *n*-octanol (5 mL) was stirred at 150°C until the solution became clear. The homogenous solution was cooled to 60°C, then dinitrile **68** (100 mg, 0.47 mmol) was added. The temperature was increased to 70°C where

the mixture was stirred for 4 h. Glacial acetic acid (4 mL) was then added and the mixture was kept at this temperature for 15 min before being poured into a mixture of methanol and water (1 : 1, 50 mL). The precipitate formed was filtered and subjected to column chromatography with  $\text{CHCl}_3/\text{THF}$  (10 : 1) as eluent to give a green powder (30 mg, 30%).  $^1\text{H}$  NMR:  $\delta$  9.06 (d,  $J = 6.0$  Hz, 4 H, ArH), 8.12 (dd,  $J = 6.0, 9.0$  Hz, 4 H, ArH), 7.52 (d,  $J = 9.0$  Hz, 4 H, ArH), 4.92 (quintet,  $J = 6.0$  Hz, 4 H, CH), 2.47-2.29 (m, 8 H,  $\text{CH}_2$ ), 2.27-2.18 (m, 8 H,  $\text{CH}_2$ ), 1.38 (t,  $J = 6.0$  Hz, 24 H,  $\text{CH}_3$ ).

**1,8,15,22-Tetrakis(3-pentyloxy)phthalocyaninatozinc(II) (70).**<sup>43</sup> A mixture of **69** (100 mg, 0.12 mmol) and  $\text{Zn}(\text{OAc})_2 \cdot 2\text{H}_2\text{O}$  (26 mg, 0.12 mmol) in DMF (3 mL) was heated to 150°C for 4 h. The volatiles were removed under reduced pressure to give a deep green residue which was subjected to chromatography using  $\text{CHCl}_3$  as eluent (96 mg, 90%).  $^1\text{H}$  NMR:  $\delta$  8.30 (br. s, 4 H, ArH), 7.98 (dd,  $J = 7.5, 7.8$  Hz, 4 H, ArH), 7.52 (d,  $J = 7.8$  Hz, 4 H, ArH), 4.81 (br. s, 4 H, CH), 2.30-2.25 (m, 8 H,  $\text{CH}_2$ ), 2.17-2.12 (m, 8 H,  $\text{CH}_2$ ), 1.32-1.25 (m, 24 H,  $\text{CH}_3$ ).

### 3.4 Synthesis of Ferrocenyl Tetrapyrrole Derivatives with Ethynyl Linkers



**(1-Chloro-2-formyl)vinylferrocene (71).**<sup>57</sup> A solution of **49** (5.7 g, 25 mmol) in DMF (20 mL) was added dropwise into the Vilsmeier reagent, prepared from POCl<sub>3</sub> (5 mL) and DMF (20 mL) at r.t., under vigorous stirring at 0°C. The resulting mixture was stirred at this temperature for 2 h, then at r.t. for a further 1 h. A 30% aqueous NaOAc solution (150 mL) was added dropwise and the mixture was stirred at r.t. overnight. The red precipitate was filtered and purified by column chromatography with ethyl acetate and hexane (1 : 3) as eluent to afford a red solid (6.2 g, 91%). <sup>1</sup>H NMR: δ 10.07 (d, *J* = 3.0 Hz, 1 H, CHO), 6.39 (d, *J* = 3.0 Hz, 1 H, C=CH), 4.76 (br. s, 2 H, Fc), 4.57 (br. s, 2 H, Fc), 4.25 (s, 5 H, Fc).

**Ferrocenylethyne (72).**<sup>57</sup> To a solution of **71** (476 mg, 1.73 mmol) in refluxing dioxane (15 mL) was added an aqueous NaOH solution (0.5 M, 10 mL). After addition, the mixture was stirred for a further 5 min, then poured into ice water (50 mL). Conc. HCl was added to acidify the solution until the pH paper turned pale red. Then, the solution was extracted with diethyl ether (3 x 100 mL). The combined ether solution was dried with anhydrous MgSO<sub>4</sub> and then evaporated under reduced pressure. The resulting brown residue was purified by column chromatography with hexanes as eluent to afford an orange-yellow solid (305 mg, 88%). <sup>1</sup>H NMR: δ 4.47 (br. s, 2 H, Fc), 4.22 (br. s, 2 H, Fc), 4.20 (s, 5 H, Fc), 2.73 (s, 1 H, C≡CH). <sup>13</sup>C {<sup>1</sup>H} NMR: δ 73.5, 71.7, 70.0, 69.8, 69.4, 68.7. MS (EI): *m/z*



210 ( $M^+$ ).

**5,6-Dichloro-1,3-isobenzofurandione (74).** A mixture of 4,5-dichlorophthalic acid (**73**) (30 g, 0.127 mol) and acetic anhydride (50 mL) was stirred at 140°C for 5 h, and then cooled to r.t. to give white crystals which were filtered, washed with hexanes, and dried in vacuo (24.9 g, 90%); mp 183-185°C (lit.<sup>58</sup> 184-186°C).

**5,6-Dichloro-1*H*-isoindole-1,3(2*H*)-dione (75).** A mixture of **74** (22 g) and  $HCONH_2$  (30 mL) was refluxed for 3 h. The resulting mixture was cooled to r.t. and then filtered. The white crystals collected were washed with water and dried in vacuo (20.8 g, 96%); mp 191-193°C (lit.<sup>58</sup> 193-195°C).

**4,5-Dichloro-1,2-benzenedicarboxamide (76).** A solution of **75** in an aqueous  $NH_4OH$  solution (25%, 300 mL) was stirred at r.t. for 24 h. Then, a 33% aqueous  $NH_4OH$  solution (100 mL) was added. The mixture was stirred for a further 24 h. The precipitate was filtered, washed with water, and dried in vacuo (16.5 g, 71%); mp 243-245°C (lit.<sup>58</sup> 245-247°C).

**1,2-Dichloro-4,5-dicyanobenzene (77).** To a solution of  $SOCl_2$  (70 mL) in DMF (100 mL) was added **76** in an ice bath. The mixture was stirred at this temperature for 5 h, then at r.t. overnight. Ice water (100 mL) was then added dropwise, and the product was filtered, washed with water, and dried in vacuo (12.1 g, 74%); mp 182-184°C (lit.<sup>58</sup> 182-184°C).

**1,2-Dibromo-4,5-dimethylbenzene (79).** To a mixture of *o*-xylene (78) (46 mL, 0.35 mol) and iodine (0.2 g) was added bromide (40 mL, 1.28 mol) dropwise over 2 h at 0°C. The resulting viscous mixture was left at r.t. overnight. Then, diethyl ether (150 mL) was poured to dissolve the mixture. The solution was then washed with 2 N NaOH (3 x 50 mL) and saturated brine (2 x 50 mL). The ether layer was collected and dried with anhydrous MgSO<sub>4</sub> which was then filtered. A pale yellow solid was obtained after removing the solvent which was recrystallized in methanol to give white crystals (50.3 g, 50%); mp 86–88°C (lit.<sup>59</sup> 86–88°C).

**1,2-Dibromo-4,5-bis(dibromomethyl)benzene (80).** A mixture of 79 (8.0 g, 30 mmol), dibenzoyl peroxide (0.32 g, 1.3 mmol) and *N*-bromosuccinimide (11 g, 60 mmol) in CCl<sub>4</sub> (150 mL) was refluxed for 5 h. Then, a second portion of *N*-bromosuccinimide (11 g, 60 mmol) was added. The mixture was continued to reflux for a further 12 h, then a third portion of *N*-bromosuccinimide (11 g, 60 mmol) was added. The suspension was refluxed for a further 7 h, then cooled to r.t. The mixture was filtered and the filtrate was collected and evaporated to give a yellow solid which was then dissolved in hot chloroform and precipitated with hexanes to afford a pale yellow powder (10.5 g, 61%); mp 126–128°C (lit.<sup>59</sup> 128–129°C).

**2,3-Dibromo-6,7-dicyanonaphthalene (81).** A mixture of 80 (10 g, 18 mmol), fumaronitrile (1.5 g, 19 mmol), and anhydrous sodium iodide (20 g, 130 mmol) in



DMF (70 mL) was heated to 75°C for 7 h. The dark brown mixture was cooled to r.t. and slowly poured into water (300 mL) with stirring. Sodium pyrosulfite was then added to the mixture until the color was changed to pale yellow. The pale yellow precipitate was collected by suction filtration, washed with hot ethyl acetate, and dried in vacuo (2.7 g, 45%); mp 246-248°C (lit.<sup>59</sup> 248-249°C).

**4,5-Bis(2-ferrocenylethynyl)phthalonitrile (82).** A mixture of **72** (426 mg, 2.03 mmol), **77** (100 mg, 0.51 mmol), Pd(PPh<sub>3</sub>)<sub>2</sub>Cl<sub>2</sub> (20 mg) and CuI (2.8 mg) in Et<sub>3</sub>N (10 mL) was heated at 90°C overnight. The red solid was filtered and washed with hexanes, and purified by column chromatography with CHCl<sub>3</sub> and hexanes (4 : 1) as eluent to afford a deep red solid (210 mg, 76%, mp 219-222°C). <sup>1</sup>H NMR: δ 7.83 (s, 2 H, ArH), 4.62 (br. s, 4 H, Fc), 4.40 (br. s, 4 H, Fc), 4.28 (s, 10 H, Fc). <sup>13</sup>C {<sup>1</sup>H} NMR: δ 135.8, 130.8, 115.1, 112.9, 101.1, 82.9, 72.1, 70.4, 70.1, 62.9. IR (KBr): ν = 2203s cm<sup>-1</sup> (C≡N). HRMS (LSI): *m/z* calcd for C<sub>32</sub>H<sub>20</sub><sup>56</sup>Fe<sub>2</sub>N<sub>2</sub> (M<sup>+</sup>) 544.0325, found 544.0329. Anal. Calcd for C<sub>32</sub>H<sub>20</sub>Fe<sub>2</sub>N<sub>2</sub>: C, 70.58; H, 3.71; N, 5.15. Found: C, 70.38; H, 3.56; N, 4.98.

**2,3,9,10,16,17,23,24-Octakis(2-ferrocenylethynyl)phthalocyaninatozinc(II)**

**(83).** Self-cyclization method: A mixture of **82** (200 mg, 0.37 mmol) and Zn(OAc)<sub>2</sub>·2H<sub>2</sub>O (33 mg, 0.15 mmol) in *n*-pentanol (10 mL) was heated to 90°C, and then a few drops of DBU was added. The red solution was then heated to 150°C

overnight. The resulting dark green solution was poured into 100 mL methanol and water (1 : 1) and the precipitate was filtered and washed extensively with methanol, hexanes and acetone using a Soxhlet extraction apparatus. The product was then dissolved in THF and precipitated by adding methanol to give a green solid (66 mg, 32%). Mixed cyclization method: A mixture of **82** (484 mg, 0.89 mmol), **84** (46.7 mg, 0.06 mmol), and  $\text{Zn}(\text{OAc})_2 \cdot 2\text{H}_2\text{O}$  (64.8 mg, 0.30 mmol) in *n*-pentanol (30 mL) was heated to 90°C and then a few drops of DBU was added. The red solution was then heated to 150°C overnight. The volatiles were removed and the residue was purified by column chromatography with  $\text{CHCl}_3$  and THF (9 : 1) as eluent. Two green bands were developed containing **85** (trace amount) and **83** (8 mg, 2%) which were collected, evaporated, and dried in vacuo. Compound **83**: UV-Vis (THF) [ $\lambda_{\text{max}}$  nm (log  $\epsilon$ )]: 377 (5.42), 662 (5.03), 705 (sh), 736 (5.70). IR (KBr):  $\nu = 2200\text{s cm}^{-1}$  ( $\text{C}\equiv\text{N}$ ). MS (MALDI-TOF): an isotopic cluster peaking at  $m/z$  2242.6 ( $\text{M}^+$ ). Compound **85**: MS (MALDI-TOF): an isotopic cluster peaking at  $m/z$  2485.5 ( $\text{M}^+$ ).

**6,7-Bis(2-ferrocenylethynyl)naphthalonitrile (86).** A mixture of **72** (375 mg, 1.79 mmol), **81** (150 mg, 0.45 mmol),  $\text{Pd}(\text{PPh}_3)_2\text{Cl}_2$  (20 mg) and  $\text{CuI}$  (2.8 mg) in  $\text{Et}_3\text{N}$  (10 mL) was heated at 90°C overnight. The resulting brown solid was filtered and washed with hexanes and a small amount of  $\text{CHCl}_3$  to afford an orange solid. The crude product could also be prepared by chromatography using  $\text{CHCl}_3$  as eluent



(143 mg, 54%).  $^1\text{H}$  NMR:  $\delta$  8.22 (s, 2 H, ArH), 8.05 (s, 2 H, ArH), 4.67 (br. s, 4 H, Fc), 4.40 (br. s, 4 H, Fc), 4.32 (s, 10 H, Fc). IR (KBr):  $\nu = 2203\text{ s cm}^{-1}$  ( $\text{C}\equiv\text{N}$ ). HRMS (LSI):  $m/z$  calcd for  $\text{C}_{36}\text{H}_{22}^{56}\text{Fe}_2\text{N}_2$  ( $\text{M}^+$ ) 594.0482, found 594.0428.

**4,5,16,17,28,29,40,41-Octakis(2-ferrocenylethynyl)naphthalocyaninato-**

**zinc(II) (87).** Self-cyclization method: A mixture of **86** (200 mg, 0.34 mmol) and  $\text{Zn}(\text{OAc})_2 \cdot 2\text{H}_2\text{O}$  (12 mg, 0.05 mmol) in *n*-pentanol (10 mL) was heated to  $90^\circ\text{C}$ , and a few drops of DBU was added. The orange solution was then heated to  $150^\circ\text{C}$  overnight to give a dark brown solution which was poured into 100 mL methanol and water (1 : 1). The precipitate formed was filtered and washed with methanol, hexanes and acetone using a Soxhlet extraction apparatus. The product was then dissolved in THF and precipitated with MeOH to give a brown solid which was dried in vacuo (63 mg, 31%). Mixed cyclization method: A mixture of **86** (426 mg, 0.72 mmol), **84** (38 mg, 0.05 mmol), and  $\text{Zn}(\text{OAc})_2 \cdot 2\text{H}_2\text{O}$  (53 mg, 0.24 mmol) in *n*-pentanol (30 mL) was heated to  $90^\circ\text{C}$ , and then a few drops of DBU was added. The orange solution was then heated to  $150^\circ\text{C}$  overnight. The volatiles were removed under reduced pressure and the residue was purified by column chromatography with  $\text{CHCl}_3$  and THF (9 : 1) as eluent. Two bands were developed containing **88** (21 mg, 17%) and **87** (22 mg, 6%) which were collected, evaporated, and dried in vacuo. Compound **87**: UV-Vis (THF) [ $\lambda_{\text{max}}$  nm (log  $\epsilon$ ): 369 (5.54), 486 (4.93), 705 (5.16),

756 (5.22), 792 (5.91). IR (KBr):  $\nu = 2200\text{s cm}^{-1}$  (C $\equiv$ N). MS (MALDI-TOF): an isotopic cluster peaking at  $m/z$  2442.0 ( $M^+$ ). Compound 88: UV-Vis (THF) [ $\lambda_{\text{max}}$  nm (log  $\epsilon$ ): 364 (5.48), 484 (4.74), 679 (5.11), 733 (5.30), 763 (5.86). IR (KBr):  $\nu = 2204\text{s cm}^{-1}$  (C $\equiv$ N). MS (MALDI-TOF): an isotopic cluster peaking at  $m/z$  2634.8 ( $M^+$ ).

**[5,15-Bis(ferrocenylethynyl)-10,20-diphenylporphyrinato]nickel(II) (90).** A mixture of **72** (375 mg, 1.79 mmol), (5,15-Dibromo-10,20-diphenylporphyrinato)nickel(II) (**89**) (150 mg, 0.45 mmol), Pd(PPh<sub>3</sub>)<sub>2</sub>Cl<sub>2</sub> (20 mg) and CuI (2.8 mg) in THF (8 mL) and Et<sub>3</sub>N (2 mL) was stirred at r.t. overnight. The solvent was then removed under reduced pressure and the residue was subjected to chromatography using hexanes as eluent to develop an orange band. The column was then eluted with CHCl<sub>3</sub> to develop a green band which was collected and evaporated. The green solid was redissolved in CHCl<sub>3</sub> and then precipitated by adding methanol (277 mg, 66%). <sup>1</sup>H NMR:  $\delta$  9.46 (d,  $J = 4.5$  Hz, 4 H, py-H), 8.72 (d,  $J = 4.7$  Hz, 4 H, py-H), 8.00 (br. s, 5 H, ArH), 7.71 (br. s, 5 H, ArH), 4.89 (br. s, 4 H, Fc), 4.44 (br. s, 14 H, Fc). UV-Vis (THF) [ $\lambda_{\text{max}}$  nm (log  $\epsilon$ ): 433 (5.59), 564 (4.40), 624 (4.80). IR (KBr):  $\nu = 2199\text{s cm}^{-1}$  (C $\equiv$ N). HRMS (LSI):  $m/z$  calcd for C<sub>32</sub>H<sub>20</sub><sup>56</sup>Fe<sub>2</sub>N<sub>2</sub> ( $M^+$ ) 934.0992, found 934.0960.

## 4. REFERENCES

- (1) *Phthalocyanines – Properties and Applications*; Leznoff, C. C., Lever, A. B. P., Eds.; VCH: New York, 1989, Vol. 1; 1993, Vol. 2; 1993, Vol. 3; 1996, Vol. 4.
- (2) Buchler, J. W.; Ng, D. K. P. In *Handbook of Porphyrins and Related Macrocycles: Biomaterials for Materials Scientists, Chemists, and Physicists*; Kadish, K. M., Smith, K., Guillard, R. Eds.; Academic Press: San Diego, 1999; ch. 20.
- (3) Horton, H. R.; Moran, L. A.; Ochs, R. S.; Rawn, J. D.; Scrimgeour, K. G. *Principles of Biochemistry*; Prentice Hall: New Jersey, 1993, chs. 14 and 16.
- (4) Mortimer, R. J. *Chem. Soc. Rev.* **1997**, 26, 147.
- (5) (a) Gould, R. D. *Coord. Chem. Rev.* **1996**, 156, 237. (b) Hanack, M.; Subramanian, L. R. In *Handbook of Organic Conductive Molecules and Polymers*; Nalwa, H. S. Ed.; Wiley: Chichester, 1997; Vol. 1, pp. 687-726.
- (6) Snow, A. W.; Barger, W. R.; Klusty, M.; Wohltjen, H.; Jarvis, N. L. *Langmuir* **1986**, 2, 513.
- (7) (a) Iliev, V.; Ileva, A. *J. Mol. Catal. A.: Chem.* **1995**, 103, 147 and references therein. (b) Spikes, D. J. *Photochem. Photobiol.* **1986**, 43, 691. (c) Vacus, J.; Simon, J. *Adv. Mater.* **1995**, 7, 797. (d) Dhami, S.; Phillips, D. J. *Photochem.*



- Photobiol. A: Chem.* **1996**, *100*, 77. (e) Howe, L.; Zhang, J. Z. *J. Phys. Chem. A* **1997**, *101*, 3207. (f) Schelly, Z. A.; Harward, D. J.; Hemmes, P.; Eyring, E. M. *J. Phys. Chem.* **1970**, *74*, 3040. (g) Yang, Y.-C.; Ward, J. R.; Seiders, R. P. *Inorg. Chem.* **1985**, *24*, 1765.
- (8) Lever, A. B. P.; Milaeva, E. R.; Speier, G. In *Phthalocyanines: Properties and Applications*; Leznoff, C. C., Lever, A. B. P. Eds.; VCH: New York, 1996; Vol. 4, pp. 351-353.
- (9) Lexa, D.; Reix, M. *J. Chim. Phys.* **1974**, *71*, 511.
- (10) Lever, A. B. P.; Minor, P. C. *Inorg. Chem.* **1981**, *20*, 4015.
- (11) Shannon, R. D.; Prewitt, C. T. *Acta Crystal.* **1965**, *A7*, 27.
- (12) (a) Giraudeau, A.; Louati, A.; Gross, M.; Andre, J. J.; Simon, J.; Su, C. H.; Kadish, K. M. *J. Am. Chem. Soc.* **1983**, *105*, 2917. (b) Clack, D. W.; Hush, N. S.; Woolsey, I. S. *Inorg. Chim. Acta* **1976**, *19*, 129. (c) Homborg, H.; Murray, K. S. Z. *Anorg. Allg. Chem.* **1984**, *517*, 149. (d) Giraudeau, A.; Fau, F.-R. F.; Bard, A. J. *J. Am. Chem. Soc.* **1980**, *102*, 5137. (e) Lever, A. B. P.; Wilshire, J. P. *Can. J. Chem.* **1976**, *54*, 2514. (f) Wolberg, A.; Mannasson, J. *J. Am. Chem. Soc.* **1970**, *92*, 2982. (g) Campbell, R. H.; Heath, G. A.; Hefter, G. T.; McQueen, C. S. *J. Chem. Soc., Chem. Commun.* **1983**, 1123.
- (13) (a) Hariprasad G.; Dahal, S. Maiya, B. G. *J. Chem. Soc., Dalton Trans.* **1996**,



3429. (b) Kadish, K. M.; Autret, M.; Ou, Z.; Tagliatesta, P.; Boschi, T.; Fares, V. *Inorg. Chem.* **1997**, *36*, 204. (c) Bonfantini, E. E.; Burrell, A. K.; Officer, D. L.; Reid, D. C. W. *Inorg. Chem.* **1997**, *36*, 6270. (d) Kadish, K. M.; Sazou, D.; Maiya, G. B.; Han, B. C.; Liu, Y. M.; Saoiabi, A.; Ferhat, M.; Guillard, R. *Inorg. Chem.* **1989**, *28*, 2542.
- (14) Chang, D.; Malinski, T.; Ulman, A.; Kadish, K. M. *Inorg. Chem.* **1984**, *23*, 817.
- (15) (a) Chow, H.-F.; Mong, T. K.-K.; Nongrum, M. F.; Wan, C.-W. *Tetrahedron* **1998**, *54*, 8543 and references therein. (b) Uno, M.; Dixneuf, P. H. *Angew. Chem. Int. Ed. Engl.* **1998**, *37*, 1714.
- (16) (a) Steiger, B.; Anson, F. C. *Inorg. Chem.* **1994**, *33*, 5767. (b) Bard, A. J. *Nature* **1995**, *374*, 13.
- (17) (a) Schmidt, E. S.; Calderwood, T. S.; Bruice, T. C. *Inorg. Chem.* **1986**, *25*, 3718. (b) Beer, P. D.; Kurek, S. S. *J. Organomet. Chem.* **1989**, *366*, C6. (c) Wagner, R. W.; Brown, P. A.; Johnson, T. E.; Lindsey, J. S. *J. Chem. Soc., Chem. Commun.* **1991**, 1463. (d) Giasson, R.; Lee, E. J.; Zhao, X.; Wrighton, M. S. *J. Phys. Chem.* **1993**, *97*, 2596 and references therein. (e) Uosaki, K.; Kondo, T.; Zhang, X.-Q.; Yanagida, M. *J. Am. Chem. Soc.* **1997**, *119*, 8367. (f) Thornton, N. B.; Wojtowicz, H.; Netzel, T.; Dixon, D. W. *J. Phys. Chem.* **1998**, *102*, 2101.
- (18) Chidsey, C. E. D. *Science* **1991**, *251*, 919.

- (19) Lambert, C.; Noll, G. *Angew. Chem. Int. Ed. Engl.* **1998**, *37*, 2107.
- (20) Barlow, S.; O'Hare, D. *Chem. Rev.* **1997**, *97*, 637.
- (21) (a) Bartik, T.; Bartik, B.; Brady, M.; Dembinski, R.; Gladysz, J. A. *Angew. Chem. Int. Ed. Engl.* **1996**, *35*, 414. (b) Bunz, U. H. F. *Angew. Chem. Int. Ed. Engl.* **1996**, *35*, 969. (c) Dagani, R. *Chem Eng. News* January 22, 1996, 22.
- (22) Narvor, N. L.; Toupet, L.; Lapinte, C. *J. Am. Chem. Soc.* **1995**, *117*, 7129.
- (23) Ribou, A.-C.; Launay, J.-P.; Sachtleben, M. L.; Li, H.; Spangler, C. W. *Inorg. Chem.* **1996**, *35*, 3735.
- (24) Cuadrado, I.; Casado, C. M.; Alonso, B.; Moran, M.; Losada, J.; Belsky, V. *J. Am. Chem. Soc.* **1997**, *119*, 7613.
- (25) Cuadrado, I.; Moran, M.; Casado, C. M.; Alonso, B.; Lobete, F.; Garcia, B.; Ibisate, M.; Losada, J. *Organometallics* **1996**, *15*, 5278.
- (26) Fillaut, J.-L.; Astruc, D. *J. Chem. Soc., Chem. Commun.* **1993**, 1320.
- (27) Fillaut, J.-L.; Linares, J.; Astruc, D. *Angew. Chem. Int. Ed. Engl.* **1994**, *33*, 2460.
- (28) Moulines, F.; Djakovitch, L.; Boese, R.; Gloaguen, B.; Thiel, W.; Fillaut, J.-L.; Delville, M.-H.; Astruc, D. *Angew. Chem. Int. Ed. Engl.* **1993**, *32*, 1075.
- (29) Wollmann, R. G.; Hendrickson, D. N. *Inorg. Chem.* **1977**, *12*, 3079.
- (30) Boyd, P. D. W.; Burrell, A. K.; Campbell, W. M.; Cocks, P. A.; Gordon, K. C.; Jameson, G. B.; Officer, D. L.; Zhao, Z. *Chem. Commun.* **1999**, 637.

- (31) Kadish, K. M.; Xu, Q. Y.; Barbe, J.-M. *Inorg. Chem.* **1987**, *26*, 2566.
- (32) (a) Beer, P. D.; Drew, M. G. B.; Hesek, D.; Jagessar, R. *J. Chem. Soc., Chem. Commun.* **1995**, 1187. (b) Beer, P. D.; Drew, M. G. B.; Jagessar, R. *J. Chem. Soc., Dalton Trans.* **1997**, 881.
- (33) (a) Collman, J.P.; Gague, R. R.; Reed, C. A.; Halbert, T. R.; Lang, H.; Robinson, W. T. *J. Am. Chem. Soc.* **1975**, *97*, 1429. (b) Sorrell, T. N. *Inorg. Synth.* **1980**, *20*, 163.
- (34) (a) Baumann, T. F.; Sibert, J. W.; Olmstead, M. M.; Barrett, A. G. M.; Hoffmam, B. M. *J. Am. Chem. Soc.* **1994**, *116*, 2639. (b) Baumann, T. F.; Nasir, M. S.; Sibert, J. W.; White, A. J. P.; Olmstead, M. M.; Williams, D. J.; Barrett, A. G. M.; Hoffmam, B. M. *J. Am. Chem. Soc.* **1996**, *118*, 10479.
- (35) Jin, Z.; Nolan, K.; McArthur, C. R.; Lever, A. B. P.; Leznoff, C. C. *J. Organomet. Chem.* **1994**, *468*, 205.
- (36) Silver, J.; Sosa-Sanchez, J. L.; Frampton, C. S. *Inorg. Chem.* **1998**, *37*, 411.
- (37) Dabak, S.; Bekaroglu, O. *New J. Chem.* **1997**, *21*, 267.
- (38) Cook, M. J.; Cooke, G.; Jafari-Fini, A. *J. Chem. Soc., Chem. Commun.* **1995**, 1715.
- (39) Gonzalez, A.; Vazquez, P.; Torres, T. *Tetrahedron Lett.* **1999**, *40*, 3263.
- (40) Poon, K.-W.; Yan, Y.; Li, X.-Y.; Ng, D. K. P. *Organometallic*, in press.



- (41) (a) Rinehart, K. L. Jr.; Curby, R. J. Jr.; Sokol, P. E. *J. Am. Chem. Soc.* **1957**, *79*, 3420. (b) Nataro, C.; Cleaver, W. M.; Landry, C. C.; Allen, C. W. *Polyhedron* **1999**, *18*, 1471.
- (42) (a) Leznoff, C. C.; Hu, M.; McArthur, C. R.; Qin, Y.; VanLier, J. E. *Can. J. Chem.* **1994**, *72*, 1990. (b) Leznoff, C. C.; Hu, M.; Nolan, K. J. M. *Chem. Commun.* **1996**, 1245.
- (43) (a) Kasuga, K.; Kawashima, M.; Asano, K.; Sugimori, T.; Abe, K.; Kikkawa, T.; Fujiwara, T. *Chem. Lett.* **1996**, 867. (b) Kasuga, K.; Asano, K.; Lin, L.; Sugimori, T.; Handa, M.; Abe, K.; Kikkawa, T.; Fujiwara, T. *Bull. Chem. Soc. Jpn.* **1997**, *70*, 1859.
- (44) Rager, C.; Schmid, G.; Hanack, M. *Chem. Eur. J.* **1999**, *5*, 280.
- (45) (a) Benkeser, R. A.; Goggin, D.; Schroll, G. *J. Am. Chem. Soc.* **1954**, *76*, 4025. (b) Katada, T.; Nishida, M.; Kato, S.; Mizuta, M. *J. Organomet. Chem.* **1977**, *129*, 189.
- (46) Lee, C. C.; Chen, S. C.; Sutherland, R. G. *Can. J. Chem.* **1975**, *53*, 232.
- (47) Eberhardt, W.; Hanack, M. *Synthesis* **1997**, 95.
- (48) Combs, C. S.; Ashmore, C. I.; Bridges, A. F.; Swanson, C. R.; Stephens, W. D. *J. Org. Chem.* **1969**, *34*, 1511.
- (49) Kaneko, Y.; Arai, T.; Tokumaru, K.; Matsunaga, D.; Sakuragi, H. *Chem. Lett.*

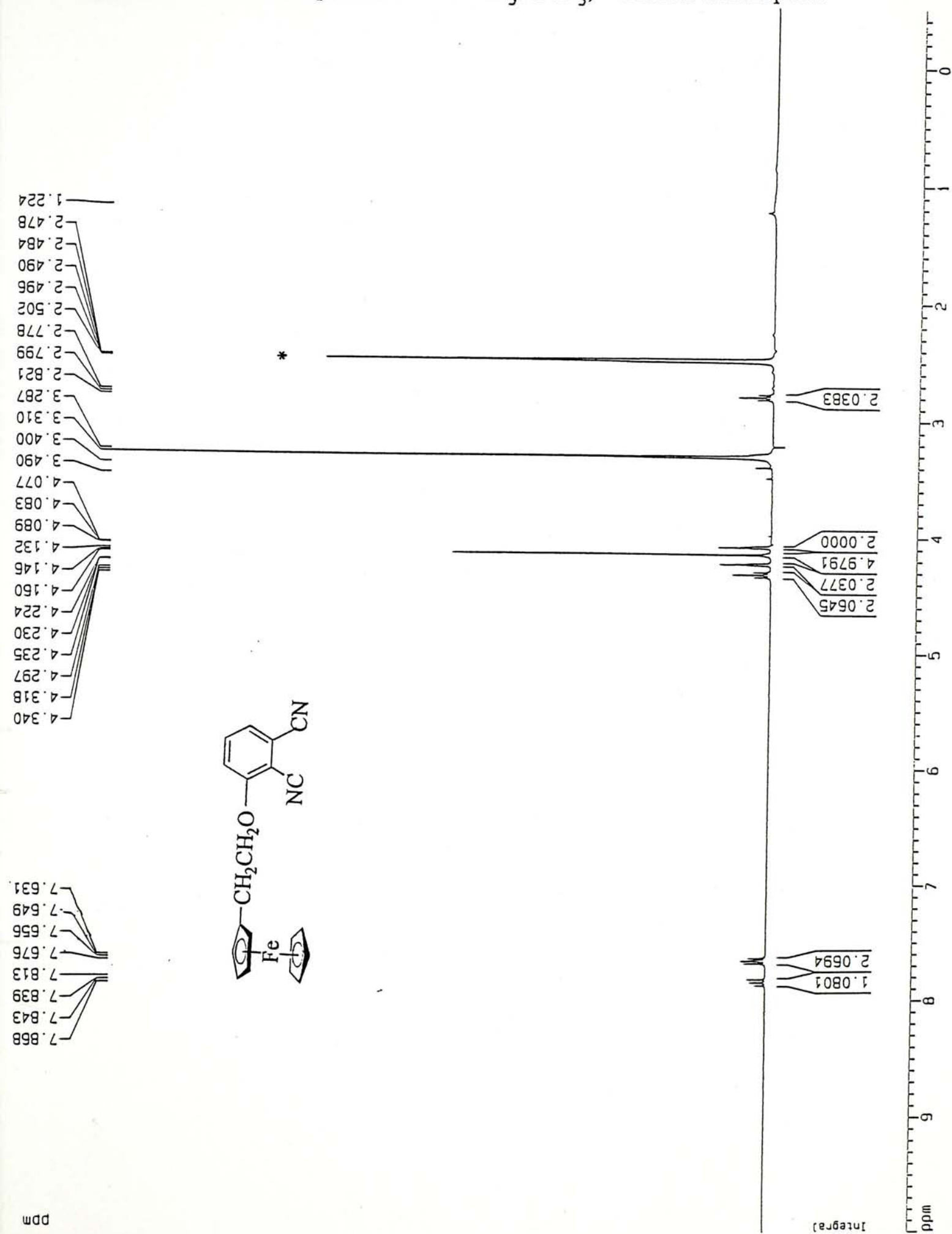


1996, 345.

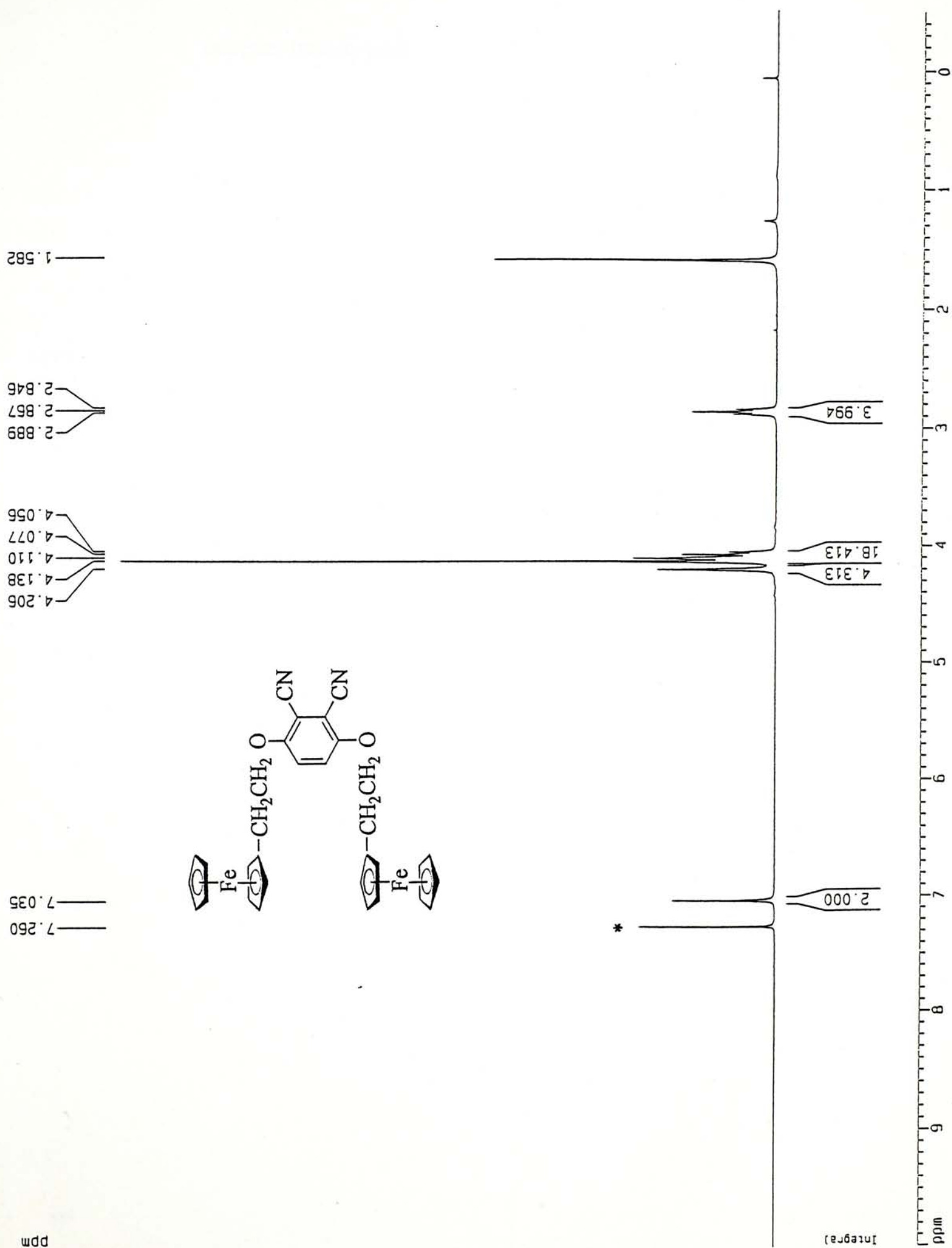
- (50) Yoon, M.; Cheon, Y.; Kim, D. *Photochem. Photobiol.* **1993**, 58, 31.
- (51) Bartak, D. E.; Houser, K. J.; Rudy, B. C.; Hawley, M. D. *J. Am. Chem. Soc.* **1972**, 94, 7526.
- (52) The potential of  $\text{Ag-Ag}^+$  in MeCN was taken as +0.31 V vs. the saturated calomel electrode (SCE) as determined for this system previously using ferrocene as an internal standard. Wong, Y.-L.; Ma, J.-F.; Law, W.-F.; Yan, Y.; Wong, W.-T.; Zhang, Z.-Y.; Mak, T. C. W.; Ng, D. K. P. *Eur. J. Inorg. Chem.* **1999**, 313.
- (53) Lever, A. B. P.; Milaeva, E. R.; Speier, G. In *Phthalocyanines: Properties and Applications*; Leznoff, C. C., Lever, A. B. P. Eds.; VCH: New York, 1993; Vol. 3, pp. 1-69.
- (54) Rehm, D.; Weller, A. *Isr. J. Chem.* **1970**, 8, 259.
- (55) Kavarnos, G. J. *Fundamentals of Photoinduced Electron Transfer*, VCH: New York, 1993; p. 43.
- (56) Sohn, Y. S.; Hendrickson, D. N.; Gray, H. B. *J. Am. Chem. Soc.* **1971**, 93, 3603.
- (57) Rosenblum, M.; Brawn, N.; Papenmeier, J.; Applebaum, M. *J. Organometal. Chem.* **1966**, 6, 173.
- (58) Wohrle, D.; Eskes, M.; Shigehara, K.; Yamada, A. *Synthesis* **1992**, 194.
- (59) Koval'shev, E. I.; Puchnova, V. A.; Luk'yanets, E. A. *Zh. Org. Khim.* **1971**, 7, 369.

- (60) (a) Brandsma, L.; Vasilevsky, S. F.; Verkruijsse, H. D. In *Applications of Transition Metal Catalysts in Organic Synthesis*; Springer: Berlin, 1998, ch. 10.
- (b) *Metal-catalyzed Cross-coupling Reactions*; Diederich, F., Stang, P. J. Eds.; Wiley-VCH: Weinheim, 1998, ch. 5. (c) Terekhov, D. S.; Nolan, K. J. M.; McArthur, C.R.; Leznoff, C. C. *J. Org. Chem.* **1996**, *61*, 3034.
- (61) Ng, A. C. H.; Li, X.-Y.; Ng, D. K. P. *Macromolecules*, in press.
- (62) Stillman, M. J.; Thomson, A. J. *J. Chem. Soc., Faraday Trans.* **1974**, *70*, 790.
- (63) (a) Yeung, Y.-O.; Liu, R. C. W.; Law, W.-F.; Lau, P.-L.; Jiang, J.; Ng, D. K. P. *Tetrahedron* **1997**, *53*, 9087. (b) Ng, D. K. P.; Yeung, Y.-O.; Chan, W. K.; Yu, S.-C. *Tetrahedron Lett.* **1997**, *38*, 6701.
- (64) Hu, M.; Brasseur, N.; Yildiz, S. Z.; Lier, J. E. V.; Leznoff, C. C. *J. Med. Chem.* **1998**, *41*, 1789.
- (65) Arnold, D. P.; Bott, R. C.; Eldridge, H.; Elms, F. M.; Smith, G.; Zojaji, M. *Aust. J. Chem.* **1997**, *50*, 495.

Appendix A-1  $^1\text{H}$  NMR spectrum of **54** in  $\text{CD}_3\text{SOCD}_3$ ; \* indicates solvent peak.

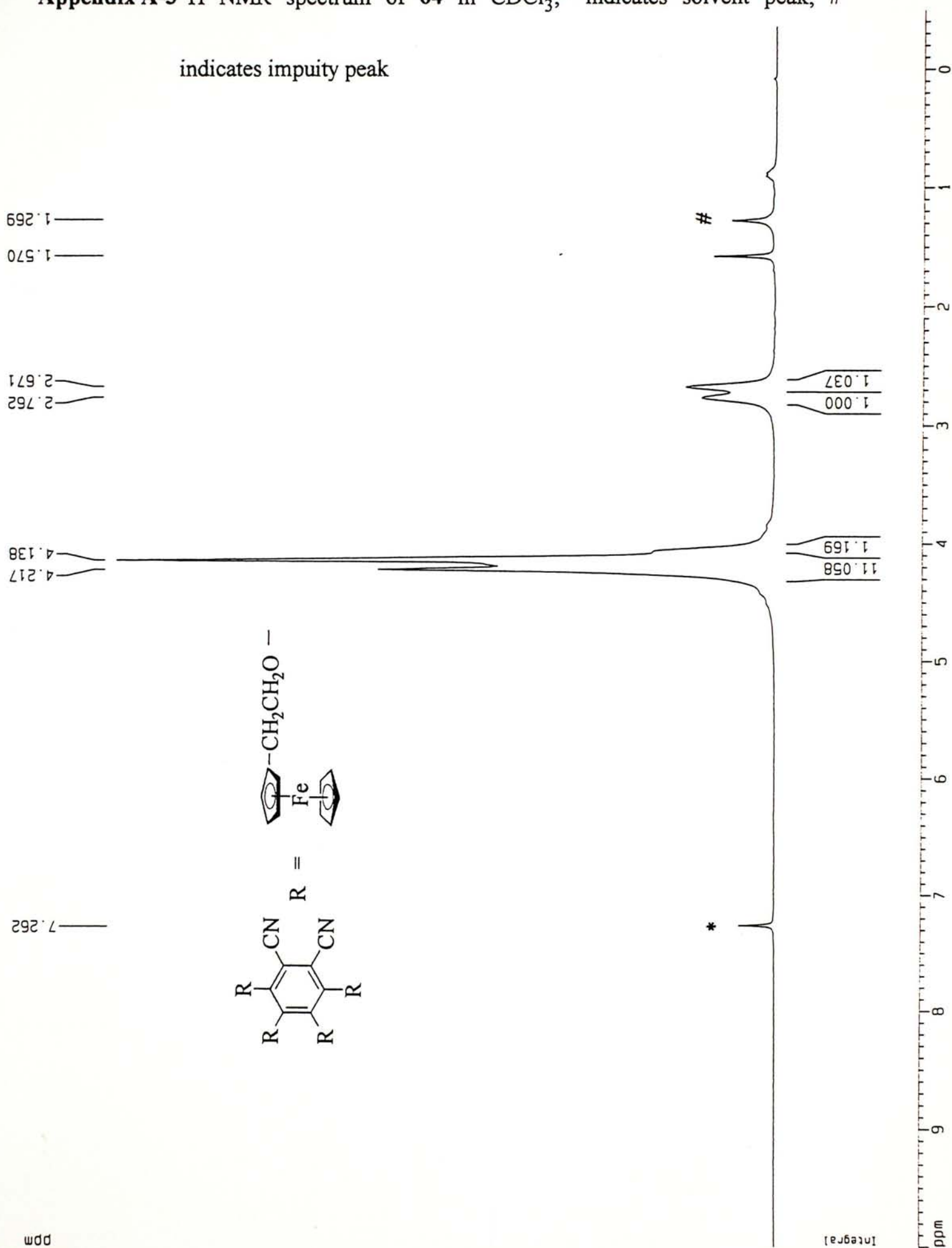


Appendix A-2  $^1\text{H}$  NMR spectrum of 61 in  $\text{CDCl}_3$ ; \* indicates solvent peak.

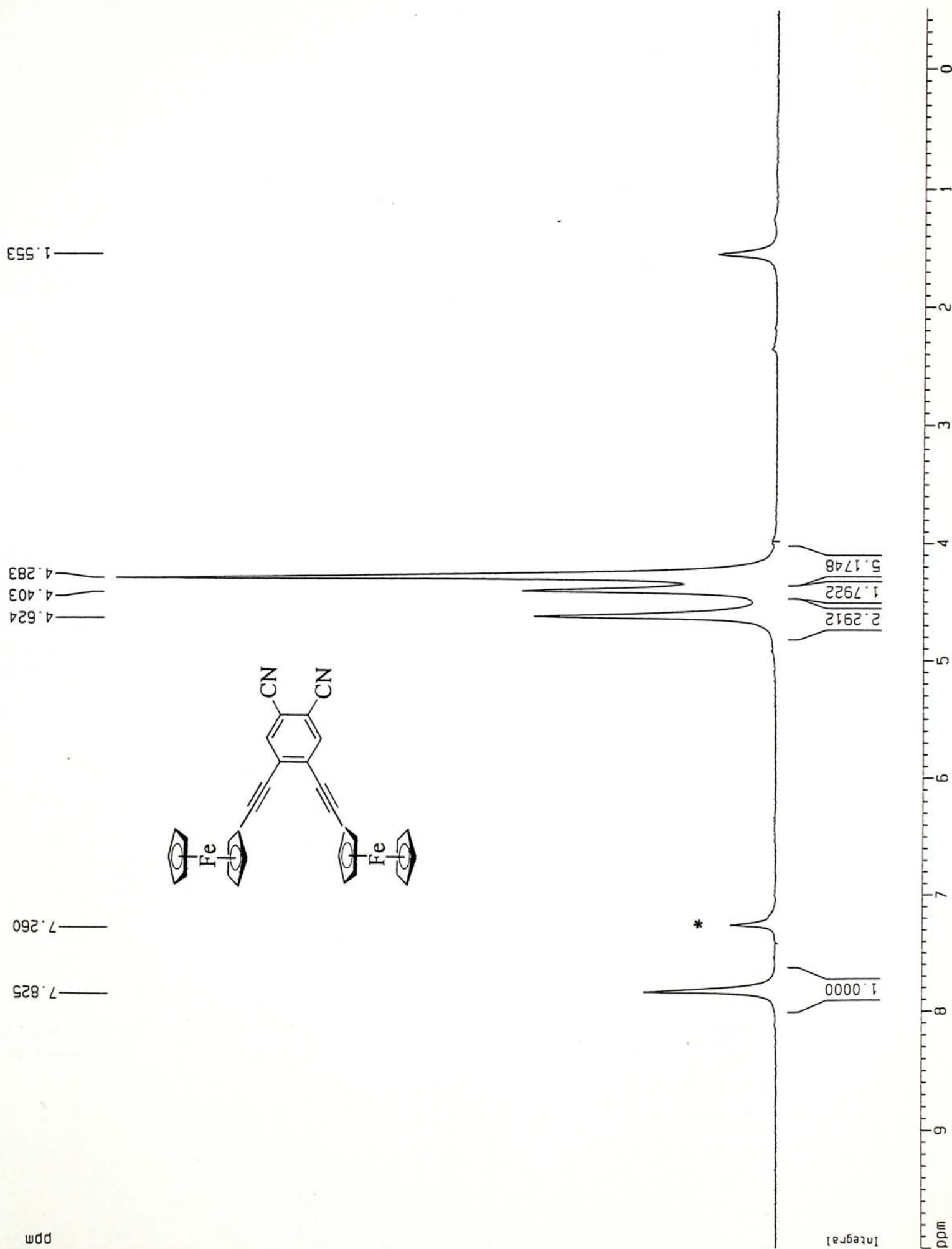




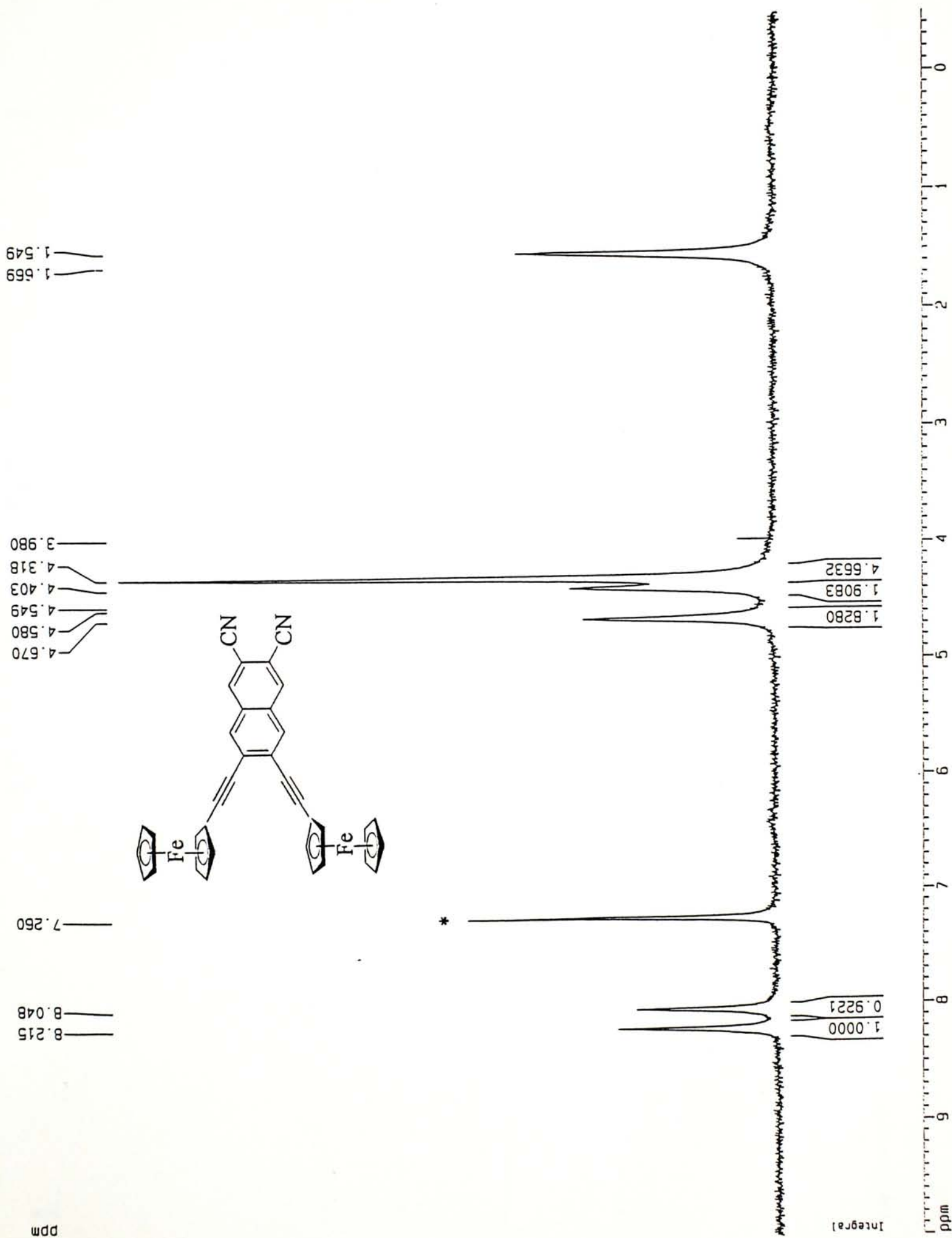
Appendix A-3  $^1\text{H}$  NMR spectrum of 64 in  $\text{CDCl}_3$ ; \* indicates solvent peak; #



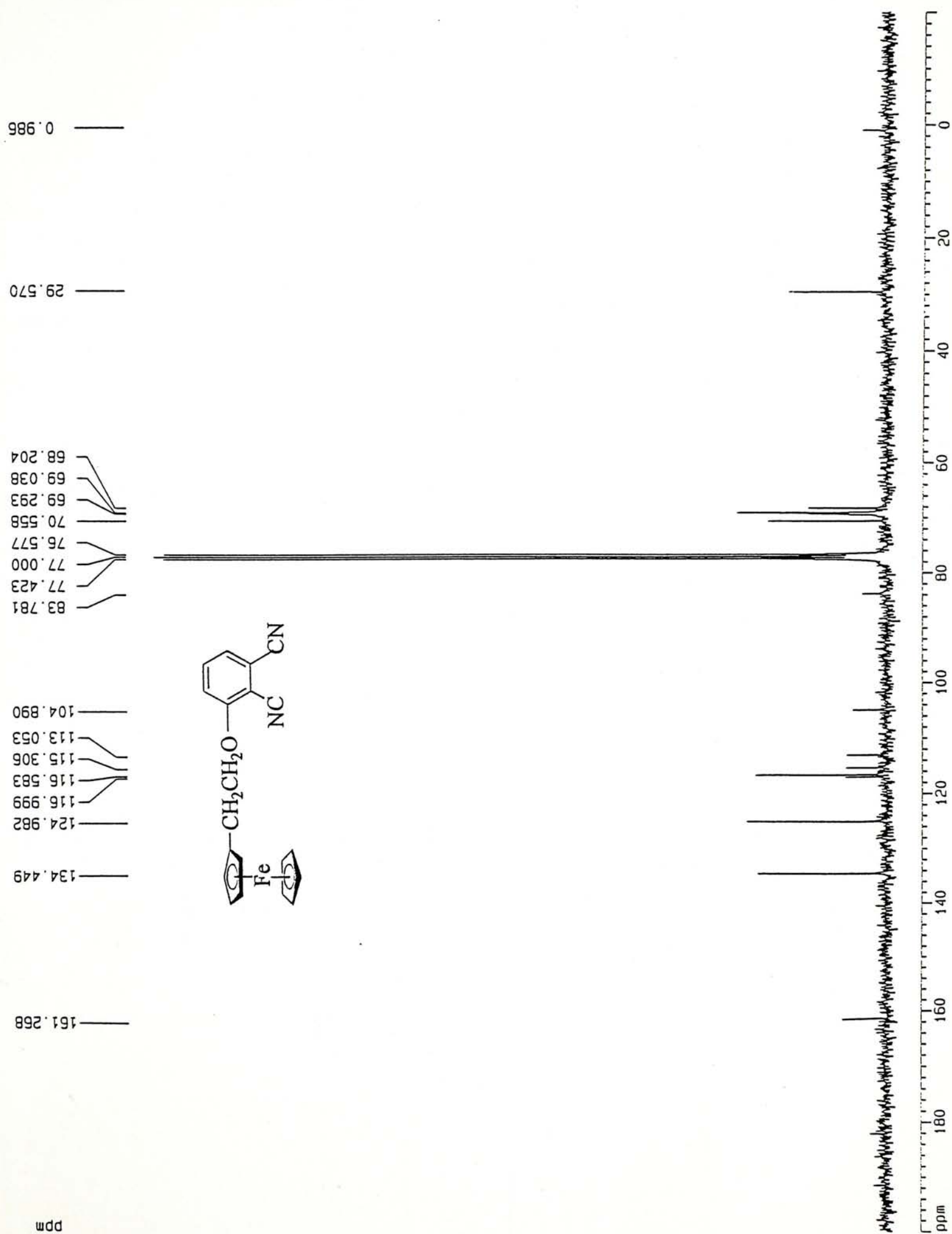
Appendix A-4  $^1\text{H}$  NMR spectrum of **82** in  $\text{CDCl}_3$ ; \* indicates solvent peak.



Appendix A-5  $^1\text{H}$  NMR spectrum of **86** in  $\text{CDCl}_3$ ; \* indicates solvent peak.

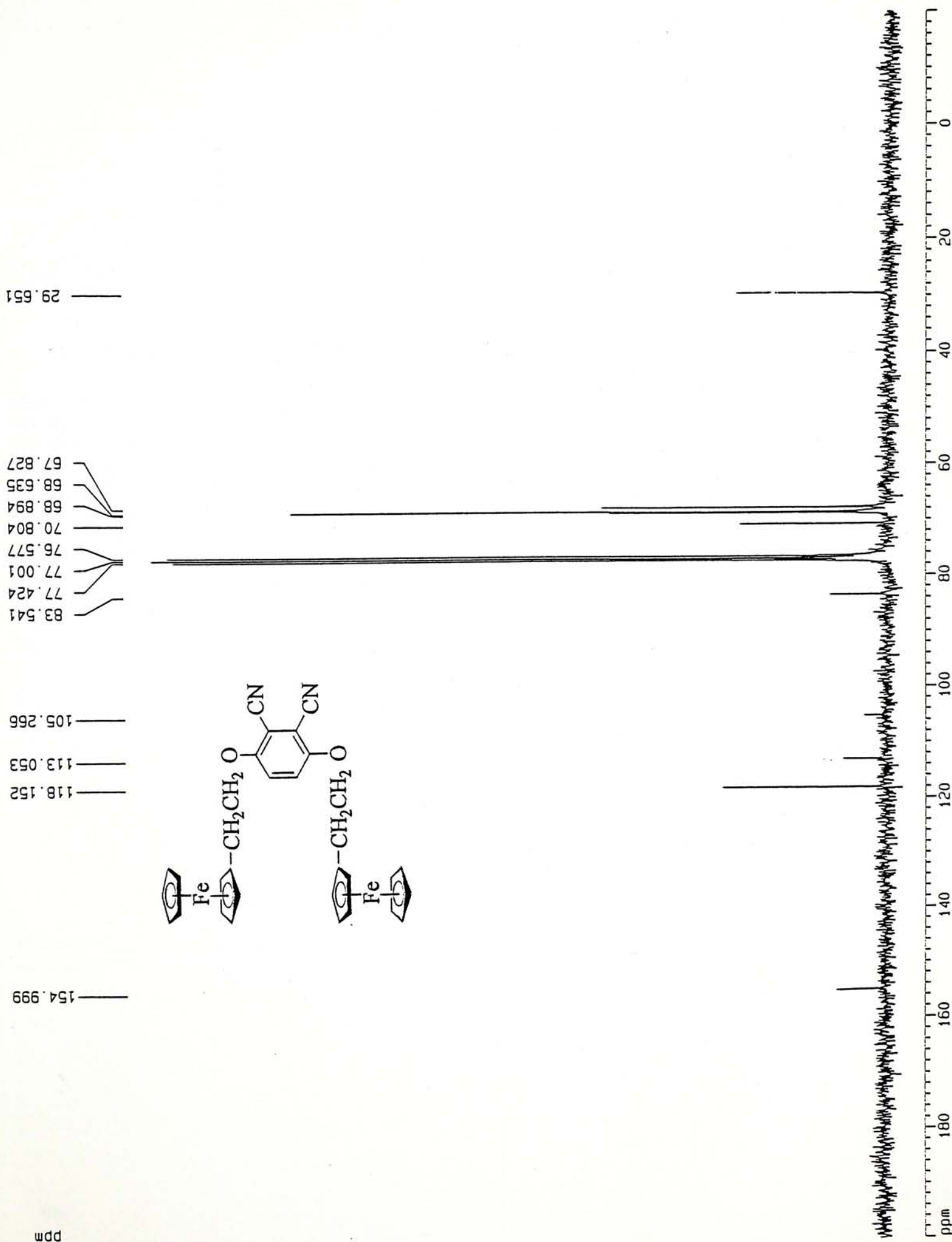


Appendix B-1  $^{13}\text{C}$   $\{^1\text{H}\}$  NMR spectrum of **54** in  $\text{CDCl}_3$ .

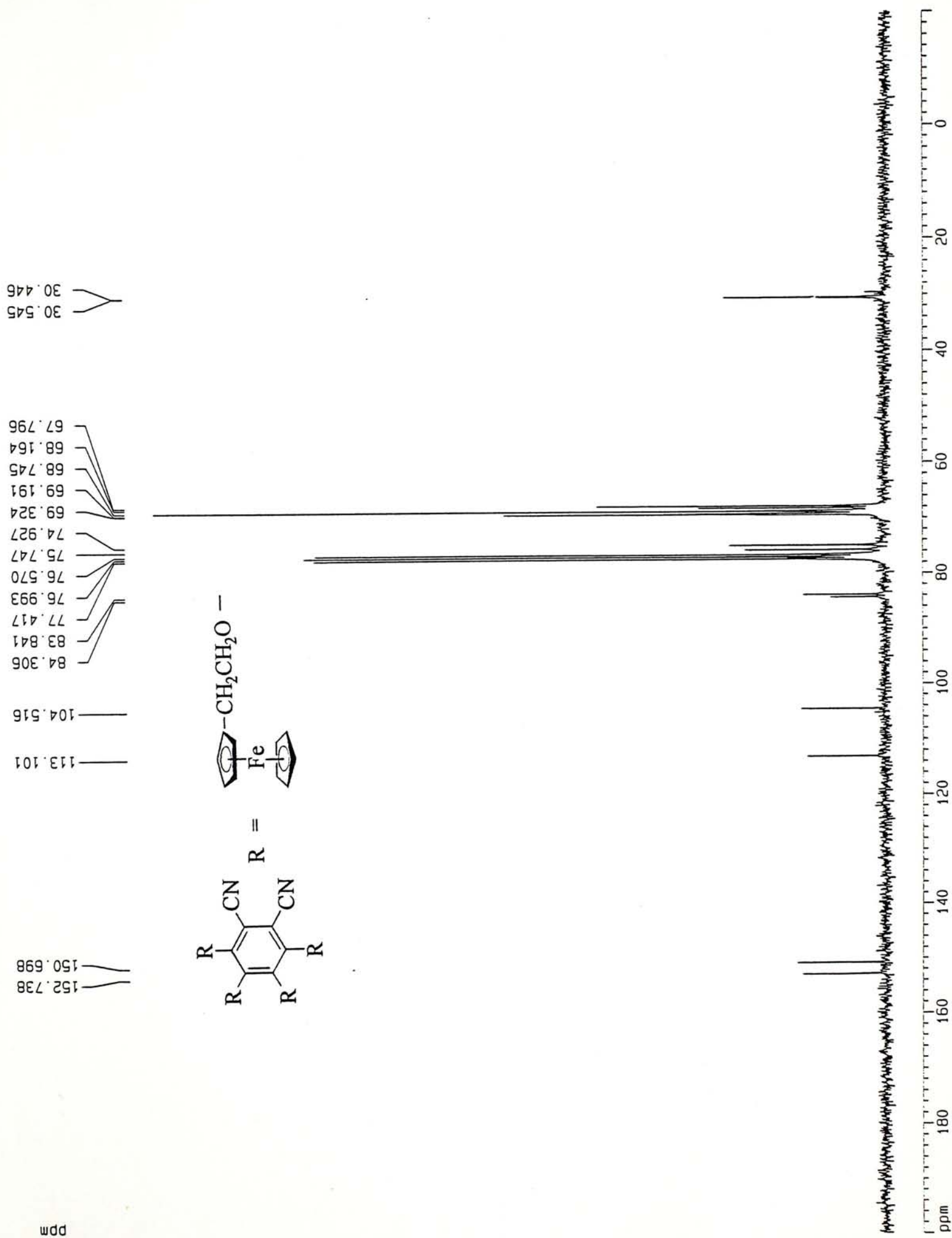




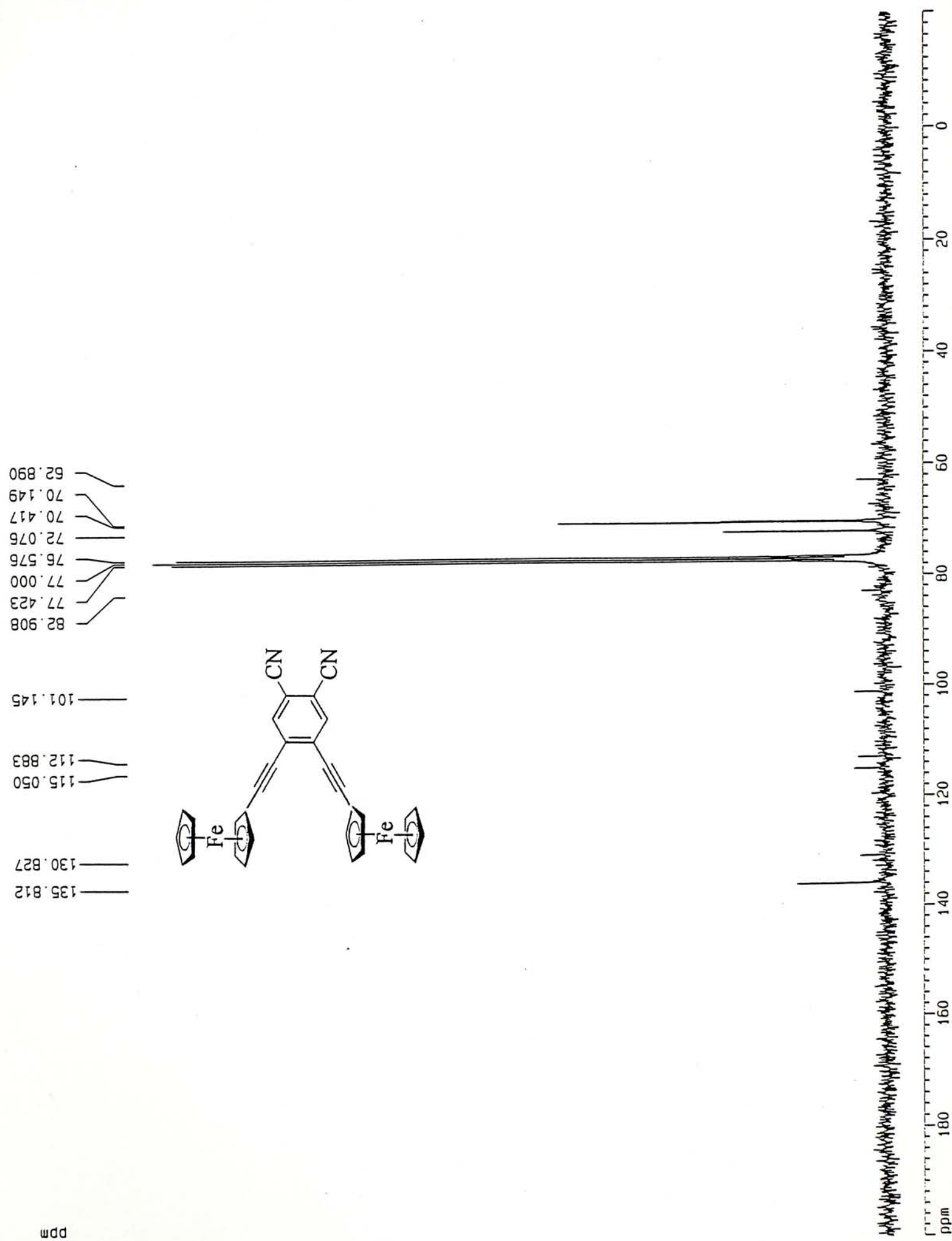
Appendix B-2  $^{13}\text{C}$   $\{^1\text{H}\}$  NMR spectrum of 61 in  $\text{CDCl}_3$ .



Appendix B-3  $^{13}\text{C}$   $\{^1\text{H}\}$  NMR spectrum of 64 in  $\text{CDCl}_3$ .



Appendix B-4  $^{13}\text{C}$   $\{^1\text{H}\}$  NMR spectrum of 82 in  $\text{CDCl}_3$ .







CUHK Libraries



003723678